REPUBLIQUE DU CAMEROUN

****

Paix-Travail-Patrie

****

****

DEPARTMENT OF CIVIL ENGINEERING

DEPARTEMENT DE GENIE CIVIL

****

REPUBLIC OF CAMEROON

****

Peace-Work-Fatherland

****

****

DEPARTMENT OF CIVIL, ARCHITECTURAL AND ENVIRONMENTAL ENGINEERING

****

COMPARATIVE ANALYSIS OF PREDICTED AND MEASURED SETTLEMENTS OF AN EMBANKMENT ON SOFT SOIL ALONG THE FOUMBOT-BAMENDJING-GALIM ROAD

A thesis submitted in partial fulfilment of the requirement for the degree of Master of Engineering (Meng) in civil engineering

Curriculum: ***Geotechnical Engineering***

Presented by:

DONGMO NGUIMGO DUCHELLE

Student number: **16TP21228**

Supervised by:

Pr. Simonetta COLA

Academic year

2020/2021

DEDICATION

I dedicate my work

To

My parents DONGMO GASTON

AND

NGUIMGO PASCALINE

In gratitude for their inconditional love and the support that they bring to me for the achievement of my studies and my accomplishment as an engineer

ACKNOWLEDGEMENTS

I would like to thank above all the Almighty God for his grace, protection, motivation and his breath without which I wouldn't have achieved this work and for the blessings he gave to me throughout my training in school and the period during which I carried out this work. My special thanks to:

- The President of the jury for the honour given to me by accepting to chair this thesis defence;
- The examiner for accepting to examine my work and making some suggestions;
- My supervisor **Pr. Simonetta COLA** for her patient guidance, advices, availability and constant encouragements throughout this work;
- The Director of the National Advanced School of Publics Works (NASPW), **Pr. NKENG George ELAMBO** for his academic and administrative support during our five years in his school;
- **Pr. Carmelo MAJORANA** of University of Padua in Italy for his contribution to realize the cooperation Cameroon-Italy;
- The Head of the Department of Civil Engineering at the ENSTP, **Pr. MBESSA Michel** for all his help and advices;
- **Eng. MBO Franky Serein**, for his time he dedicated during this research, his availability and follow up;
- **All the teaching and administrative staff** of the university of Padua and the ENSTP for the quality of their teaching and permanent accompaniment;
- All my classmates and friends of the 7th batch for their support and for been a source of motivation;
- All my family for support, love and attention they have for me;
- All those people who, from near or far have given me their help in carrying out this work.

LIST OF SYMBOLS AND ABREVIATIONS

List of abbreviations

PK	Kilometric Point
FEM	Finite Element Model
OCR	Over Consolidation Ratio
CPT	Cone Penetrometer Test
SS	Soft Soil
SSC	Soft Soil Creep
FOS	Factor of safety
HS	Hardening soil
X	Axe
L	Left

List of symbols

c	Effective cohesion of the soil
c_u or s_u	Undrained shear strength of the soil
ϕ'	Internal frictional angle
E	Young modulus / Elastic modulus
E_{oed}	Oedometric modulus
E_{50}	Secant stiffness
E_{ur}	Unloading/reloading stiffness
e_0	Initial void ratio
C_c	Compression index
C_s	Swelling index
C_α	Secondary consolidation index
C_v	Coefficient of consolidation
σ_p	Pre-consolidation pressure

K_0	At rest coefficient
k_h	Horizontal permeability
k_v	Vertical permeability
m_v	Volume compressibility
S_t	Total settlement
υ	Poisson's ratio
γ_{dry}	Dry unit weight
γ_{sat}	Saturated unit weight
λ^*	Modified compression index
κ^*	Modified swelling index
μ^*	Modified secondary compression index

ABSTRACT

The main objective of this study is to show that it is possible to predict the total settlement of an embankment and estimate the duration of soil consolidation using a numerical model. To do this, a study of a 6 m high embankment on soft ground previously instrumentalized by settlement plates present in the Foumbot-Bamendjing-Galim road project between the PK 12 + 650 and the PK 12 + 950 was carried out. After a literature review on the behaviour of embankments constructed on soft soils and on the settlement determination methods, a presentation of the project and a physical description of the site was done. The site visit made it possible to acquire the necessary data in order to numerically model and analyse the behaviour of the soils and thus predict settlements over time and determine the time required for the end of consolidation by using various numerical material models, such as the Soft Soil model, the Soft Soil Creep model and the Hardening Soil model implemented inside the finite element software PLAXIS. The numerical results were compared to those being measured in situ and allowed to determine which numerical model better simulated the reality. For the case study here presented, it emerged that the model which have the best corresponding with reality was the Soft Soil Creep because it takes into account the creep of the soil. The predicted settlement was 35.45 cm at the level of the central axis of the embankment at the original ground level and 24.47 cm on the left side of the embankment, reached at 255.4 days from the construction start: these values are fairly close to those observed in the field, notably 32.7 cm at the axis and 27.2 cm on the left side, thus demonstrating that it is possible by making an adequate choice of input values, to predict the behaviour of an embankment on soft soils by a numerical analysis. An analysis was also done on the pore pressure prediction and the safety factor and it was seen that their prediction plays an important role in the prediction of soil behaviour.

Keys words: Soft soil, Embankment, Settlement, Settlement plates, Numerical analysis.

RESUME

L'objectif principal de cette étude est de montrer qu'il est possible de prédire le tassement total d'un remblai et d'estimer la durée de consolidation du sol en utilisant un modèle numérique. A cet effet, une étude du comportement d'un remblai de 6 m de hauteur sur sol compressible préalablement instrumentalisé par des massifs de tassement présent dans le projet routier Foumbot-Bamendjing-Galim entre le PK 12 + 650 et le PK 12 + 950 a été effectuée. Après une revue littéraire sur le comportement remblais construits sur sols compressibles et sur les méthodes de détermination des tassements, une présentation du projet et une description physique du site a été faite. La visite du site a permis d'acquérir les données nécessaires afin de pouvoir modéliser numériquement et analyser le comportement des sols et prédire ainsi le tassement dans le temps et déterminer le temps nécessaire à la fin de la consolidation en utilisant divers modèles de comportement numériques des sols tels que le modèle « Soft Soil », le modèle « Soft Soil Creep » et le modèle « Hardening Soil » exécutés dans le logiciel des éléments finis PLAXIS. Les résultats obtenus suite à cette modélisation numérique ont été comparés à ceux mesurés in situ et ont permis de déterminer le modèle numérique qui simule le mieux la réalité. Pour le cas d'étude ici présenté, il ressort que le modèle qui correspond le mieux à la réalité était le modèle « Soft Soil Creep » car ce dernier prend en compte le fluage du sol. Le tassement prédit à l'axe du remblai au niveau du sol d'origine était de 35.45 cm et de 24.47 cm sur le côté gauche atteints 255.4 jours après le début de la construction : ces valeurs étant assez proches de celles observées sur le terrain, notamment, 32.7 cm à l'axe et 27.2 cm sur le côté gauche, démontrant ainsi qu'il est possible en faisant un choix adéquat des valeurs d'entrée, de prédire le comportement d'un remblai par une analyse numérique. Une analyse a été également faite sur la prédiction de la pression interstitielle et le facteur de sécurité ayant démontré que leur prédiction joue un rôle important dans la prédiction du comportement d'un sol.

Mots clés : Sol mou, Remblai, Tassement, Massif de tassement, Analyse numérique

LIST OF FIGURES

Figure 1.1: Peat (Burton, 2005)........ 3
Figure 1.2: Mud (Shutterstock)........ 4
Figure 1.3 : Atterberg limits........ 7
Figure 1.4 : Method for vertical stress distribution from Holtz and Kovacs (1981)........ 11
Figure 1.5: Vertical stress increment under a half embankment load........ 11
Figure 1.6: Vertical stress increase due to an embankment........ 12
Figure 1.7 : vertical stress due to a flexible strip load (Das 2006)........ 13
Figure 1.8: Translational slide (Collin et al., 2005)........ 14
Figure 1.9: Schematic of lateral squeeze (Samtani and Nowatzki, 2006)........ 15
Figure 1.10 : Effect of water content on strength of clay........ 16
Figure 1.11: Settlement components (Das, 1994)........ 17
Figure 1.12 : Geometry, loads and finite element meshes........ 20
Figure 1.13: The Mohr-Coulomb yield surface in principal stress space (PLAXIS manual, 2008)........ 21
Figure 1.14: Representation of total yield contour of the Soft Soil model in principal stress space (PLAXIS manual, 2008)........ 23
Figure 1.15: Logarithmic relation between volumetric strain and mean stress (PLAXIS manual, 2008)........ 25
Figure 1.16: Void ratio versus effective stress for both normally and over consolidated clay from oedometer test........ 26
Figure 1.17: Consolidation and creep behaviour in standard oedometer test (PLAXIS manual, 2008)........ 27
Figure 1.18: Yield surface of the Modified Cam-Clay model in p'-q plane........ 30
Figure 1.19 : Three plots of settlement data from consolidation........ 32
Figure 1.20 : Compression curve in semi log scale........ 32
Figure 1.21 : Secondary compression........ 33
Figure 1.22: Schematic of the rod extensometer........ 34
Figure 1.23: Schematic of the magnetic extensometer........ 35
Figure 1.24: Typical digital hydrostatic profile gauge installation in embankment........ 36

Figure 1.25: Hydraulic settlement cell 37
Figure 1.26: **(a)** Inclinometer probe (Geokon Inc 2007) and **(b)** Inclinometer Casing 38
Figure 1.27: Vibrating wire piezometer 39
Figure 2.1: PLAXIS Input interface 43
Figure 2.2: PLAXIS Calculations interface 46
Figure 2.3: PLAXIS Output interface 48
Figure 2.4: PLAXIS Curves interface 49
Figure 2.5: Settlement plate 50
Figure 3.1: Presentation of the West region of Cameroon 54
Figure 3.2: Physical location of the Bagangté-Foumbot-Bamendjing-Galim road (Project document) 54
Figure 3.3: Geotechnical laboratory of the site 58
Figure 3.4: Quarry from the section 2 (Foumbot - Bamendjing - Galim) of the project PK 21+250 m 58
Figure 3.5: Area of study (PK 12+650 – PK 12+950) 58
Figure 3.6: Plan view of the study area (Project document) 59
Figure 3.7: Typical transverse profile at PK 12+650 (Project documents) 60
Figure 3.8: CPT test at PK 12+900 m 61
Figure 3.9: 64
Figure 3.10: Site plan of the settlement plates (Project document) 65
Figure 3.11: Principle of setting up a settlement plate 66
Figure 3.12: Settlement curves of masse 21 and 22 (phase 1, phase 2 and phase 3 being each stage of construction) 69
Figure 3.13: Meshing system of the embankment (PLAXIS V20) 71
Figure 3.14: Points location in FEM analysis (PLAXIS V20) 71
Figure 3.15: Stratigraphy of foundation and embankment soil (PLAXIS V20) 72
Figure 3.16: Calculation steps of the embankment (PLAXIS V20) 72
Figure 3.17: Deformed mesh with Soft Soil model (PLAXIS V20) 73
Figure 3.18: Shading of the vertical displacement with Soft soil model (PLAXIS V20) 74
Figure 3.19: Settlement versus time at point X and L with Soft Soil Creep model (PLAXIS V20) 74

Figure 3.20: Deformed mesh with Soft Soil Creep model 75

Figure 3.21: Shading of the vertical displacement with Soft soil Creep model (PLAXIS V20) 75

Figure 3.22: Settlement versus time at point X and L with Soft Soil Creep model (PLAXIS) 76

Figure 3.23: Deformed mesh with Hardening Soil model (PLAXIS V20) 76

Figure 3.24: Shading of the vertical displacement with Hardening Soil model (PLAXIS V20) 77

Figure 3.25: Settlement versus time at point X and L with Hardening Soil model (PLAXIS) 77

Figure 3.26: Distribution of excess pore pressures at the end of consolidation predicted using the SS model 78

Figure 3.27: Simulated excess pore pressures as a function of time at points X and L using the SS model 78

Figure 3.28: Distribution of excess pore pressures at the end of consolidation predicted using the SSC model 79

Figure 3.29: Simulated excess pore pressures as a function of time at points X and L using the SS model 79

Figure 3.30: Distribution of excess pore pressures at the end of consolidation predicted using the HS model 80

Figure 3.31: Simulated excess pore pressures as a function of time at points X and L using the HS model 80

Figure 3.32: Measured and predicted settlements on the axis of the embankment with different models 81

Figure 3.33: Measured and predicted settlements on the axis of the embankment with different models with logarithmic scale 82

Figure 3.34: Measured and predicted settlements on the left side of the embankment with different models 82

Figure 3.35: Measured and predicted settlements on the left side of the embankment with different models with logarithmic scale 83

Figure 3.36: Predicted excess pore pressure versus time at point X 86

Figure 3.37: Predicted excess pore pressure versus time at point L 86

Figure 3.38: Variation of Safety factors Vs time for the different models 87

LIST OF TABLES

Table 2.1: Parameters to be find for the study 41
Table 3.1: Soil Stratigraphy (Project Documents) 61
Table 3.2: Foundation soil parameters (Project Documents) 62
Table 3.3: Foundation soil parameters (Project Documents) 63
Table 3.4: Location of the installed plates (Project document) 65
Table 3.5: Settlement records of masse 21 (Project document) 68
Table 3.6: Settlement records of masse 22 (Project document) 68
Table 3.7: Other data obtained from the embankment instrumentation with settlement plates (Project document) 69
Table 3.8: Measured and predicted values of total settlement after the 168 days 83

TABLE OF CONTENTS

ACKNOWLEDGEMENTS i

LIST OF SYMBOLS AND ABREVIATIONS iii

ABSTRACT v

RESUME vi

LIST OF FIGURES vii

LIST OF TABLES xi

TABLE OF CONTENTS xii

GENERAL INTRODUCTION 1

Chapter 1 : LITERATURE REVIEW 2

1.1. Soils 2

1.1.1. Soils formation 2

1.1.2. Types of soils 3

1.1.3. Properties of soft soils 6

1.2. Embankments 9

1.2.1. Definition and use 10

1.2.2. Increment of stress in soil due to embankment loading 10

1.2.3. Behaviour of an embankment on soft soils 13

1.3. Settlement 16

1.3.1. Definition 16

1.3.2. Components of settlement 17

1.3.3. Settlement prediction 18

1.3.4. Settlement calculation 30

1.3.5. Settlement monitoring and record 34

Chapter 2 : METHODOLOGY 40

2.1. General recognition of the site 40

2.2. Visit of the site 40

2.3. Data acquisition 41

2.3.1. Geometric data 41

2.3.2. Geotechnical data 41

2.4. Numerical analysis in the Software PLAXIS (2D V20) 42

2.4.1. Input program 42

2.4.2. PLAXIS calculation program 45

2.4.3. PLAXIS output program 48

2.4.4. PLAXIS curve program 48

2.5. Instrumentation of embankments by settlement masse method 49

2.5.1. Method description 49

2.5.2. Location of installed plates 50

2.5.3. Settlement recording methodology 51

2.5.4. Presentation of result 52

Chapter 3 : RESULTS AND INTERPRETATION 53

3.1. General presentation of the site 53

3.1.1. Physical parameters 53

3.1.2. Socioeconomic parameters 56

3.2. Physical description of the site 57

3.3. Data presentation 59

3.3.1. Geometrical data 59

3.3.2. Geotechnical data 60

3.3.3. Settlement plates parameters 63

3.4. Results from the settlement plates records 67

3.4.1. Topographic data of the PK 12+900 m 67

3.4.2. Other data obtained.. 69

3.5. PLAXIS simulation results 70

3.5.1. Modelling procedure... 70

3.5.2. Presentation of the results obtained 72

3.6. Interpretation of the results obtained 80

3.6.1. Settlements.. 81

3.6.2. Consolidation end time 84

3.6.3. Pore pressures 85

3.6.3. Factor of safety 87

GENERAL CONCLUSION 89

REFERENCES.. 91

APPENDIX 94

GENERAL INTRODUCTION

The development of a country depends on the well-being of its population one of the key elements of this well-being being the ability of each other to move from one point to another in a minimum of comfort. It is in this momentum that the project entitled « *Travaux de construction des routes de désenclavement du bassin agricole de l'Ouest* » was born in order to facilitate trade between the regions.

When talking about road project, one of the challenges encountered in the field is the presence of very soft soils, known to be soils with a very low bearing capacity and a high susceptibility to settle. The study of settlements is of paramount importance for the life of the project, so it is important to find methods to be able to predict them and better understand them in order to optimize construction times and costs.

The general objective of this work is to find a numerical method to predict the settlements and the duration of consolidation o an embankment located from PK 12 + 650 to PK 12 + 900 of the project by comparing the settlement values obtained thanks to numerical simulation to those obtained by in-situ measurements.

To do this, this study will be divided into three main chapters. Chapter one will deal in the general characteristics of soft soils, the behaviour of embankment on soft soil, settlement evaluation by observational method, by calculation, by numerical modelling and lastly the instrumentation of embankments in order to measure settlements. Chapter 2 will present the methodology used to carry out this study notably the numerical method of prediction and the embankment instrumentation with settlement plates. Finally, chapter 3 will conclude this work by presenting on the one hand the results of this study through a general presentation of the project and a physical description of the site, followed by the geometric and geotechnical data useful for the development of this work. And on the other hand, the results obtained from the instrumentation by the settlement plates and those obtained from the numerical simulation with PLAXIS software with different which will then be interpreted in order to carry out a comparative analysis between the two.

Chapter 1 : LITERATURE REVIEW

Introduction

Soft soil occurs in many parts of the world and their specific properties require significant attention for analysis, design and maintenance of geotechnical constructions that they will support. Constructions located on soft soils are more challenging to withstand due to their low stabilizing properties and the presence of loose space between its constituent particles.

In the case of the construction of an embankment on soft soils, the engineering task are to ensure its stability against possible failure mechanisms and to control the soft soil deformation or settlement.

Several methods are used to predict ground settlement such as observational method and numerical methods, and also to calculate and measure it. This chapter will deal first with soil through its formation, types, physical and geotechnical properties. Then, will follow a discuss about embankments and their behaviour on soft soils. After, a discuss about the process of settlement and at the end the different materials models that exist to simulate the behaviour of soil materials.

1.1. Soils

Soils are materials that are derived from the weathering of rocks (Budhu, 2011). There are many types of soils, but in the case of this work, a particular interest will be placed on soft soils. To learn more about the notion of soft soils, a presentation of their formation process, the types and their properties will be done.

1.1.1. Soils formation

Soil formation begins with the physical and chemical breakdown of rocks, caused by atmospheric agents. Considering their modes of formation, there are three main types of soil: transported soils, residual soils and organic soils (Murthy, 2002).

1.1.1.1. Transported soil

Transported soils are soils composed by weathering products which were transported and deposited in a different location. The agents of transportation being gravity, wind, water and glaciers. The composition of these soils depends on the environment under which they were transported and is often different from the parent rock (Craig, 2004).

1.1.1.2. Residual soil

Residual soil is formed from weathering of parent rock at the present location. Residual soils They are derived from rock, but the original rock texture has been completely destroyed. Generally residual soils contain a wide range of particle sizes, shapes and composition (Craig, 2004).

1.1.1.3. Organic soil

Organic sedimentary rocks are formed from organic materials such as plants, bones, and shells. Organic soils contain a significant proportion of dispersed vegetable matter which usually produces a distinctive odour and often a dark brown, dark grey or bluish grey colour (Craig, 2004).

1.1.2. Types of soils

Soft soils are defined as soils with large fractions of fine particles such as silty and clayey soils, which have high moisture content, peat foundation and loose sand deposits, located near or under the water table (Kamon and Bergado, 1991). There are four main types of soil.

1.1.2.1. Peat

Peat is an accumulation of partially decayed vegetation or organic matter. According to Joseph E. Bowles (1997), peat is not a soil but rather an organic deposit of rotting wood from trees, plants, and mosses.

Figure 1.1: Peat (Burton, 2005)

Peat soils are usually dark brown or black in colour, very spongy and can be describe as fibrous, pseudo-fibrous or amorphous (Craig, 2004). They have a high-water table (the management of water is very difficult on peat soils), small surface of particles and a very light structure.

These soils are geotechnically problematic as the shown high compressibility and low shear strength, and high-water content. Peat is subjected to local sinking and development of local failure. It is also subjected to very large primary and long-term settlement under an even moderate increase in load. There are also some difficulties in accessing the sites, a large variation in material properties coupled with difficulty in sampling. There is also some possibility of chemical and biological changes in these materials with time (Kazemian et al. 2011).

1.1.2.2. Mud

Mud is clay and silt mixed with water into a viscous fluid (Budhu, 2011). The soft muddy soil is considered that unconsolidated soft fine-grained soils or very fine soil is deposited and formed in a standing or slow flowing water environment by physical, chemistry and biological effects, which belongs to modern recent sediments. The soft muddy soil, which is different from general soil, mainly consists of clay (Wang et al., 2018).

Figure 1.2: Mud (Shutterstock)

1.1.2.3. Silts

Silt is a solid, dust-like sediment that water, ice, and wind transport and deposit. Silt is made up of rock and mineral particles sized between clay and sand which exhibit little or no strength when dried. Silts easily crumble, and water migrates to the surface on application of pressure.

Silts and clays are of particular interest in foundation engineering because they tend to be most troublesome in terms of strength and settlements. Silts and rock flour in the particle range of 0.074mm down to about 0.001mm are inert by-products of rock weathering. They may be organic silts if contaminated with organic materials or inorganic otherwise. Most silt deposits, however, are contaminated with clay minerals so that they have cohesion (Joseph E. Bowles et al. 1997).

1.1.2.4. Clays

The term clay is commonly used to describe any cohesive soil deposit with sufficient clay minerals present that drying produces shrinkage with the formation of cracks or fissures such that block slippage can occur. Clays feel smooth, greasy, and sticky to the touch when wet, but are very hard and strong when dry. They have a very good water holding capacity, a large surface of soil particles and a heavy structure

The clay mineral has a high affinity for water, and individual particles may absorb 100^{+} times the particle volume. The presence or absence (during drying) of water can produce very large volume and strength changes. Clay particles also have very strong interparticle attractive forces, which account in part for the very high strength of a dry lump (or a clay brick). Water absorption and interparticle attraction collectively give the activity and cohesion to clay (and to soils containing clay minerals) (Joseph E. Bowles, 1997).

The three principal identified clay minerals can be characterized in terms of activity and plasticity.

a) Montmorillonite (or smectite)

Montmorillonite exhibits a high degree of swell potential; water can easily enter between the layers in montmorillonite, causing swelling. It has a structure similar to illite, but the layers are held together by weak van der Waals forces.

Montmorillonite belongs to the smectite clay family. It is an aluminium smectite with a small amount of Al^{3+}replaced by Mg^{2+}.

b) Illite

Illite has no to moderate swell potential. Illite consists of repeated layers of one alumina sheet sandwiched by two silicate sheets. The layers, each of thickness 0.96 nm, are held together by potassium ions.

Illite has a basic structure consisting of a sheet of gibbsite between and combined with two sheets of silica.

c) Kaolinite

Kaolinite exhibits almost none swell potential and consists of a structure based on a single sheet of silica combined with a single sheet of gibbsite. There is very limited isomorphous substitution. The combined silica–gibbsite sheets are held together relatively strongly by hydrogen bonding.

Kaolinite has a structure that consists of one silica sheet and one alumina sheet bonded together into a layer about 0.72 nm thick and stacked repeatedly. The layers are held together by hydrogen bonds. Tightly stacked layers result from numerous hydrogen bonds. Kaolinite is common in clays in humid tropical regions.

1.1.3. Properties of soft soils

Soft soils occur in many parts of the world. Their specific properties require significant attention for analysis, design and maintenance of geotechnical structures founded on them.

1.1.3.1. Physical properties

Physical properties are obtained by visual inspection, in-situ tests and laboratory tests.

a) Soil texture

The term texture refers to the degree of fineness and uniformity of a soil. It is described by such expressions as floury, smooth, gritty, or sharp, in accordance with the sensation produced by rubbing the soil between the fingers.

b) Soil structure

Structure may refer to the geometrical arrangement of soil particles with respect to each other. It may also refer to features acquired after deposition

c) Soil porosity and void ratio

The porosity n is the ratio of the volume of voids to the total volume of the soil aggregate. The term volume of voids refers to that portion of the volume of the soil not occupied by mineral grains.

The void ratio *e* is the ratio of the volume of voids to the volume of the solid substance.

$$n = \frac{V_v}{V} \quad (1.1)$$

$$e = \frac{V_v}{V_s} = \frac{V_v}{V - V_v} = \frac{n}{1-n} \quad (1.2)$$

With V_v the total volume of voids, V_s the total solid volume and V the total volume.

1.1.3.2. Geotechnical properties

a) Specific gravity and particle density

The density of the soil aggregate is defined as the mass of the aggregate (soil plus water) per unit of volume. It depends on the density of the solid constituents, the porosity of the aggregate, and the degree of saturation.

The specific gravity of a material is the ratio of the weight or mass of a volume of the material to the weight or mass of an equal volume of water. In soil mechanics the most important specific gravity is that of the actual soil grains and is given the symbol *Gs* (Smith, 2014)

b) Consistency limits

The term consistency refers to the degree of adhesion between the soil particles and to the resistance offered against forces that tend to deform or rupture the soil aggregate. The consistency of clays and other cohesive soils is usually described as soil, medium, stiff or hard.

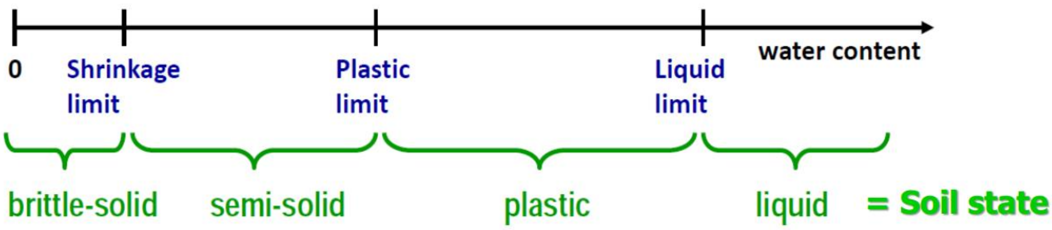

Figure 1.3 : Atterberg limits

The consistency of a fine-grained soil is largely influenced by the water content of the soil. The consistency of soil can change by increasing or decreasing the water content. the water contents that correspond to the boundaries between the states of consistency are called the Atterberg limits (figure 1.3).

i) Liquid limit (LL)

The Liquid Limit (LL) is the water content corresponding to the boundary water content at which a soil changes from a viscous liquid to a plastic state.

ii) Plastic limit (PL)

The plastic limit PL is defined as the water content at which a soil thread with 3.2 mm diameter just crumbles when it is rolled out on a plate.

iii) Shrinkage limit (SL)

The Shrinkage Limit or lower limit of volume change is the water content at which a further reduction in water does not cause a decrease in the volume of the soil mass.

iv) Plasticity index (PI)

For describing the range of water content over which a soil is plastic:

$$PI = LL - PL \quad (1.3)$$

v) Liquidity index (LI)

It gives an idea of relatively consistency of a cohesive soil in natural state

$$LI = \frac{w - PL}{PI} \quad (1.4)$$

vi) With *w* the water content Activity index (A)

Skempton (1953) observed that *PI* of a soil increase linearly with the % of clay fraction *CF* (<0.002mm).

The type of the clay soils gives different lines with slope also called activity index:

$$A = PI/CF \quad (1.5)$$

c) Particle size

Particle size plays a dominant role in distinguishing soil types. Commonly used names of soil such as gravel, sand, silt, and clay are based on their grain sizes. The boundary particle sizes are slightly different depending on the standards.

To identify grain size characteristics of soils, a grain size distribution curve is developed. When a relatively large percentage passing through a No. 200 sieve (e.g., more than 10% as a guideline) is obtained from the sieve analysis, a hydrometer analysis is conducted.

d) Permeability

The key physical property that governs the flow of water in soils is permeability, also called hydraulic conductivity

The presence or absence of water in soil can have a considerable effect on soil strength and the duration of settlements. In estimating the time for settlements to take place, or for water flow studies, permeability is the property of interest. Permeability may be defined as the facility for water flow through a soil mass. It is quantified as a coefficient k (Joseph E. Bowles, 1997) in units of flow (ms^{-1}).

The coefficient of permeability depends primarily on the average size of the pores, which in turn is related to the distribution of particle sizes, particle shape and soil structure. The coefficient of permeability also varies with temperature, upon which the viscosity of the water depends. If the value of *k* measured at 20°C is taken as 100% then the values at 10°C and 0°C are 77 and 56%, respectively (Craig, 2004).

The coefficient of permeability can be determined using laboratory methods (constant-head permeability test for coarse soils and falling head test for fine soils) or field tests (well pumping test and Borehole tests).

1.2. Embankments

Embankments have been constructed for more than 3000 years (Dirt Connections, 2020). They serve an essential purpose and can be either man-made or naturally-formed.

1.2.1. Definition and use

An embankment refers to a volume of earthen material that is placed and compacted for the purpose of raising the grade of a roadway (or railway) above the level of the existing surrounding ground surface. The grade line of the road may be raised due to some reasons as:

- Keeping subgrade above ground water table
- Preventing damage of pavement from the surface and capillarity water
- To maintain the designed vertical alignment of the road

Embankment may vary significantly in size. Its design consideration includes filling height, the material used, settlement consideration and stability analysis.

Embankments are constructed of materials that usually consist of soil, but may also include aggregate, rock, or crushed paving materials.

Normally, the coarse materials are placed at or near the bottom or base of the embankment in order to provide a firm foundation for the embankment and also facilitate drainage and prevent saturation. The top portion of an embankment usually is constructed of relatively high quality, well-compacted subgrade material that is capable of supporting the overlying pavement layers and imposed wheel loadings without deflection or undesirable movements.

1.2.2. Increment of stress in soil due to embankment loading

The distribution of stresses in the soil must be known for a good estimation of the displacement caused by the applied load on supporting soil. The following methods can be used to estimate the stress distribution of the soil for the applied load.

1.2.2.1. The approximate 2:1 method

An approximate stress distribution assumes that the total applied load on the soil surface is distributed over an area of the same size as the surface loaded area, but increases by an amount equal to the depth below the surface (Figure 1.4)

The equation used to calculate the stress increment is given by:

$$\Delta\sigma_z = \frac{\sigma_0 BL}{(B+z)(L+z)} \quad (1.6)$$

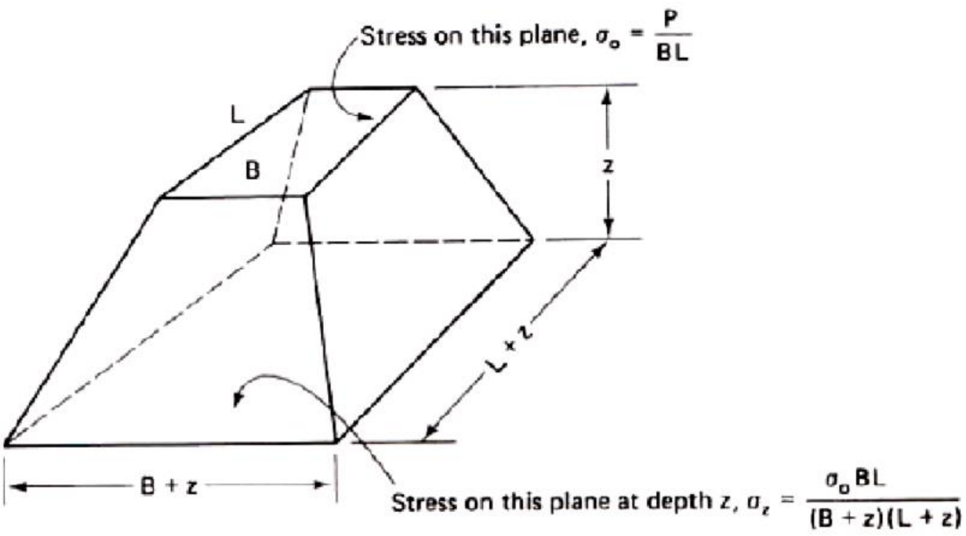

Figure 1.4 : Method for vertical stress distribution from Holtz and Kovacs (1981)

The 2:1 method underestimates the vertical stress and can causes errors on the unsafe side.

1.2.2.2. The Osterberg method

The Osterberg method (Figure 1.5) is use to estimate the stress increment at the centre of each soil layer.

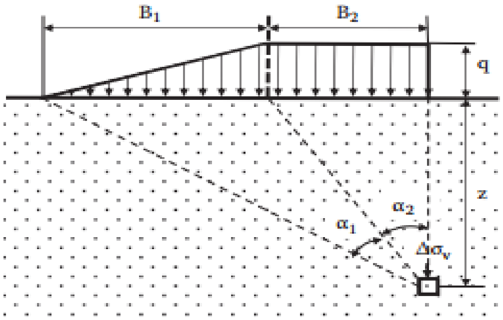

Figure 1.5: Vertical stress increment under a half embankment load

Embankment cause an increase of stress in soil (figure 1.6) shows a half section of an embankment load. The integrated solution is given by:

$$\Delta\sigma_v = \frac{q}{\pi}\left[\frac{B_1+B_2}{B_1}(\alpha_1+\alpha_2) - \frac{B_2}{B_1}\alpha_2\right] = qI_5 \quad (1.7)$$

$$I_5 = \frac{1}{\pi}\left[\frac{B_1+B_2}{B_1}(\alpha_1+\alpha_2) - \frac{B_2}{B_1}\alpha_2\right] = qI_5 \quad (1.8)$$

$$\alpha_1 = tan^{-1}\left(\frac{B_1+B_2}{z}\right) - tan^{-1}\left(\frac{B_2}{z}\right) \quad (1.9)$$

$$\alpha_2 = tan^{-1}\left(\frac{B_2}{z}\right) \quad (1.10)$$

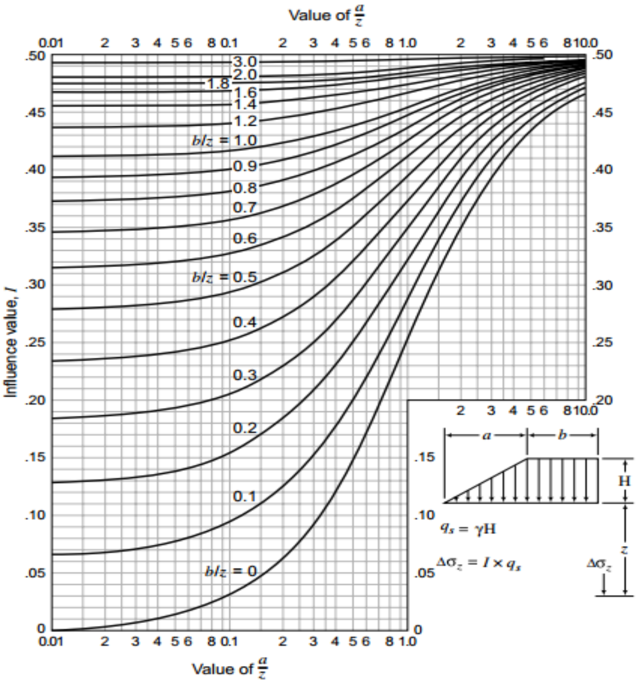

Figure 1.6: Vertical stress increase due to an embankment

1.2.2.3. The modified Boussinesq method

The use of the Boussinesq method requires some assumptions:

- The soil is homogeneous and isotropic
- The soil mass is semi-infinite
- The soil may not be elastic but obey Hooke's law
- The soil is weightless and unstressed before application of the load
- The load is applied at the ground surface

The Equation bellow gives the vertical stress caused by a vertical strip load (finite width and infinite length) (Figure 1.7), which is derived from the Boussinesq (1883) solution of stresses produced at any point.

$$\Delta\sigma_z = \left\{tan^{-1}\left[\frac{z}{x-(B/2)}\right] - tan^{-1}\left[\frac{z}{x+\left(\frac{B}{2}\right)}\right] - \frac{Bz\left[x^2-z^2-\left(\frac{B}{4}\right)\right]}{\left[x^2+z^2-\left(\frac{B^2}{4}\right)\right]+B^2z^2}\right\} \quad (1.11)$$

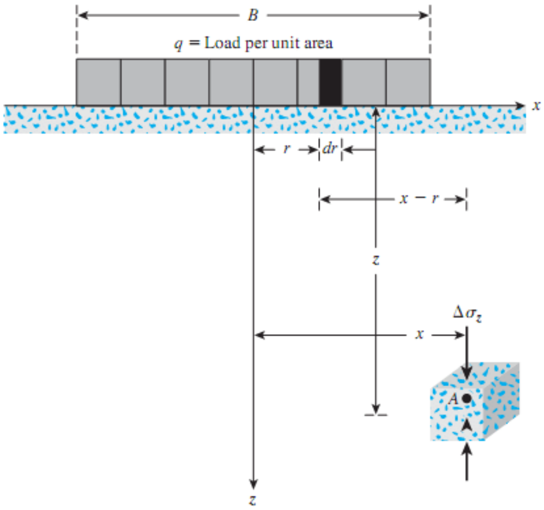

Figure 1.7 : vertical stress due to a flexible strip load (Das 2006)

1.2.3. Behaviour of an embankment on soft soils

Embankments constructed on soft soils tend to spread laterally because of horizontal earth pressures acting within the embankment. These earth pressures cause horizontal shear stresses at the base of the embankment that must be resisted by the foundation soil.

The failure of an embankment on soft soil happens at an undrained condition within a short period after the embankment construction.

1.2.3.1. Instability

The mechanisms of failure may dictate the required analysis method to be used to determine stability. They may be controlled by the composition of the embankment structures (types of soils, layer geometry, etc.) and from its use (road embankments, river embankments, dams, etc.). The different failure mechanisms are:

- **Erosion:** erosion is basically the displacement of soil from one area to another. On embankments, erosion is caused primarily by water, especially by heavy rainfall. Rain that falls onto the exposed ground dislodges soil particles which are the carried away down the slope by the flowing water.

- **Slide:** Slides are downward slope movements that occur along definite slip or sliding surfaces. Slides may be translational, rotational, or a composite of rotation and translation. Translational slides are typically shallow and linear in nature.

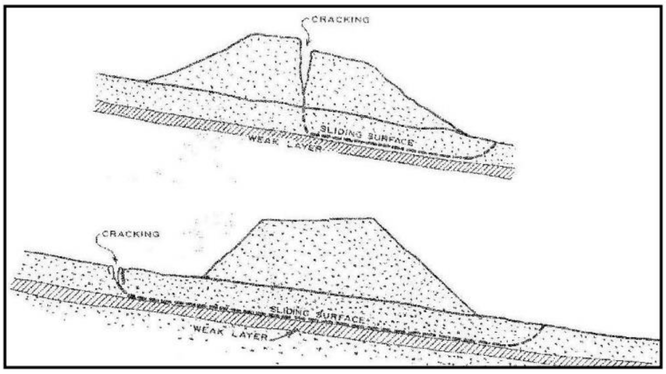

Figure 1.8: Translational slide (Collin et al., 2005)

Rotational slides are slides that form an arc along the shearing surface. This is the most common type of failure analysed. In soft, relatively homogenous Clay-Like materials, the rotational slide forms a deep-seated arc, while in Sand-Like materials the rotational slide failure surface tends to be relatively shallow.

Compound slides are a composite of translational and rotational slides. Compound slides can have 2 general forms: retrogressive and progressive. Retrogressive compound slides continue to cut into the existing slope. After initial failure, the new slope that is formed is unstable and fails, developing another new unstable slope face that fails. Progressive slides occur when an existing slope surface is loaded with either new fill or debris from a slope failure, resulting in failure of the slope toward the toe.

- **Spread:** Spread was originally defined by Terzaghi and Peck in 1948 to describe sudden movements of water bearing seams of Sand-like materials overlain by homogeneous Clay-Like soils or fills. Spreads occur on very gentle slopes (< 5 percent) or flat terrain. Spreads can occur in Sand-like soils (liquefaction) or in Clay-like soils (quick clays) that are externally loaded.

1.2.3.2. Settlement

Settlements are caused by an increase in the overburden stress. Settlement of an embankment can occur for many reasons such as:

- compaction when embankment foundation consists of compressible soil with high moisture content
- Due to inadequate of filled layers during construction operation

Some actions can be taken to eliminate the problems due to the developing of settlement during (if they take too time) and after construction operation:

- By increasing the rate of consolidation of foundation soil by providing sand drain;
- By properly compacting the earth layers during construction operation;
- If the specified compaction is not achieved by the soft area, the material shall be removed and replaced by approved material, compacted to the specification.

1.2.3.3. Lateral squeeze

Lateral squeeze is a phenomenon that occurs when a soft Clay-Like soil deforms and displaces when subjected to embankment loadings and is primarily a concern at the end bents where the deep foundations may be installed through thick layers of soft Clay-Like soils.

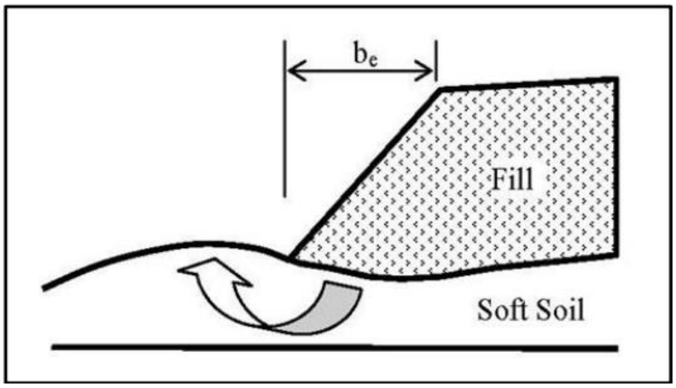

Figure 1.9: Schematic of lateral squeeze (Samtani and Nowatzki, 2006)

1.2.3.4. Water drainage

Routine seasonal fluctuations in the ground water table do not usually influence either the amount of water in the pore spaces between soil grains or the cohesion. certain clay minerals do react to the presence of water and cause volume changes of the clay mass. An increase in absorbed moisture is a major factor in the decrease in strength of cohesive soils as shown schematically in (Figure 1.10). Water absorbed by clay minerals causes increased water contents that decrease the cohesion of clayey soils.

When placed on clay or silt, embankments create excess pore water. Provided the applied loads do not cause the undrained shear strength of the clay or silt to be exceeded, as the excess pore water pressure dissipates consolidation occurs, and the shear strength of the clay or silt increases with time. For this reason, the factor of safety increases with time under the load of the fill.

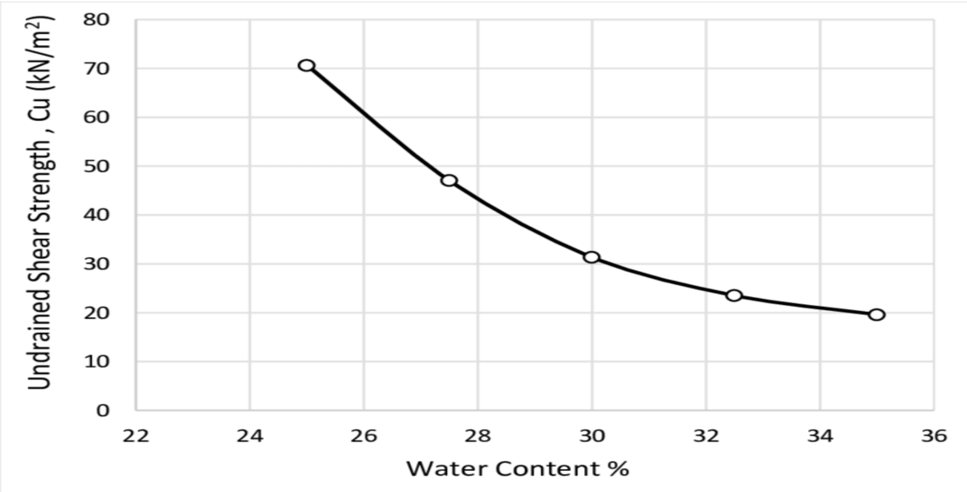

Figure 1.10 : Effect of water content on strength of clay

1.3. Settlement

Civil engineers must design some soil constructions which must be safe and serviceable. For that, those constructions must not be submitting to large deformation such as settlement which is due to compressibility characteristics of soil submit to an external load producing an amount of volume change of the soil. For a better conduct of this work, the meaning of the phenomenon of settlement will be see in detail.

1.3.1. Definition

When a soil is loaded by any new load condition (a foundation, fill, embankment, etc.), settlements always occur. They may be insignificant or large enough to require special construction procedures. Settlement is the vertical statistical accumulation of particle rolling, sliding, and slipping into the void spaces together with some particle crushing (or fracturing) at the contact points.

1.3.2. Components of settlement

Settlement can be subdivided based on time-dependence response into three separate components: immediate settlement S_i (initial), primary settlement S_c(consolidation) and secondary settlement S_s(creep).

$$S_t = S_i + S_c + S_s \quad \dots\dots\dots\dots\dots\dots \quad (1.12)$$

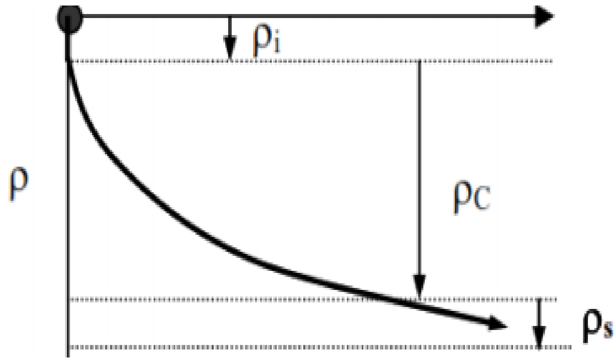

Figure 1.11: Settlement components (Das, 1994)

1.3.2.1. Immediate settlements

Immediate settlements are the settlement which occurred directly after the application of a load, without a change in moisture content. They take place when the load is applied. For soft soils, the immediate settlements are generally very small comparing to the consolidation settlement. They can be easily quantify using the elastic formula and depends on the rate of embankment construction.

1.3.2.2. Primary consolidation settlement

Primary consolidation is the change in volume of a fine-grained soil caused by the expulsion of water from the voids and the transfer of stress from the excess porewater pressure to the soil particles (Budhu, 2011). It is a time dependent and take months to years to develop. The analysis of this kind of settlements are used to all saturated, fine grained soils when the particles displacement and void reduction can produce a temporary excess pore pressure. For these soils one estimate both settlement and how long time it will take for most of the settlement to occur.

1.3.2.3. Secondary compression settlement

Secondary compression or creep is the change in volume of a fine-grained soil caused by the adjustment of the soil fabric (internal structure) after primary consolidation has been completed (Budhu, 2011). It is the slow compression of soil that occurs under constant effective stress after the excess pore pressures in the soil dissipated. It is considered to start from the time when the primary consolidation settlement was completed and continue over a long period of time under constant loading. It occurs at constant effective stress with volume change due to rearrangement of particles.

1.3.3. Settlement prediction

Prediction of settlement is very important during engineering construction. For this reason, some methods to predict the settlement of a structure before construction will be presented.

1.3.3.1. Methods based on observation

The use of analytical solution of consolidation equation for settlement prediction is not always effective because some conditions are sometimes quite uncertain in practical engineering problems (initial distribution of pore water pressure, drain length, final vertical strain of soil, coefficient of consolidation, etc.). For this reason, some observational settlement prediction has been proposed.

a) **Asaoka's method**

Its philosophy is based on "observational procedure». The theory is derived from 1D consolidation equation. The settlement *S(t)* at time *t* can be calculated as follow:

$$S(t) = \frac{\beta_0}{1-\beta_1} - \left(\frac{\beta_0}{1-\beta_1} - S_0\right)\beta_1^t \quad (1.13)$$

Where S_0 is the settlement at the initial time.

One should first determine the value of S_0 which will influence the result. However, the selection of its value will depend on the designer and can cause the deviation of settlement calculation.

b) **Hyperbolic method**

The Hyperbolic method proposed by tan et al. (1991) has its origin in the rectangular hyperbolic fitting method. According to this method, the final settlement δ_f can be calculated by the following equation:

$$\delta_f = \frac{\alpha_i}{s_i} = \frac{\delta_{60}}{0.6} = \frac{\delta_{90}}{0.9} \quad (1.14)$$

Where α_i and s_i are the slope of linear segment in hyperbolic plot of Terzaghi theory and hyperbolic plot of field settlement respectively.

The limitation of this method is also the determination of the initial time point because the method is based on the initial slope of the settlement.

c) **Settlement potential method**

It is method proposed by Janbu (1991) based in the time resistance concept. It can be used for interpreting creep parameters. The settlement potential is given by:

$$S = \frac{H}{r_s} \qquad (1.15)$$

With H the thickness of the layer and r_s the creep number.

However, limitations still exist in these methods because the initial time point is necessary to be determine first and the difference of the initial time point determination can significantly influence the accuracy of the settlement prediction.

1.3.3.2. Numerical methods

During the last decades, many impressive developments have been made in the numerical methods applied to engineering fields including geotechnical engineering. Many numerical methods exist as limit theorems, limit equilibrium method, inverse analysis but one of the most is the emergence of Finite Element Method (FEM) for solutions of problems.

The basic idea of FEM is to divide the body into finite elements, often just called elements, connected by nodes, and obtain an approximate solution as shown in Figure 1.12. This is called the finite element mesh and the process of making the mesh is called mesh generation. The FEM provides a systematic methodology by which the solution, can be determined by a computer program. For linear problems, the solution is determined by solving a system of linear equations; the number of unknowns is equal to the number of nodes. To obtain a reasonably accurate solution, thousands of nodes are usually needed, so computers are essential for solving these equations. Generally, the accuracy of the solution improves as the number of elements (and nodes) increases, but the computer time, and hence the cost, also increases.

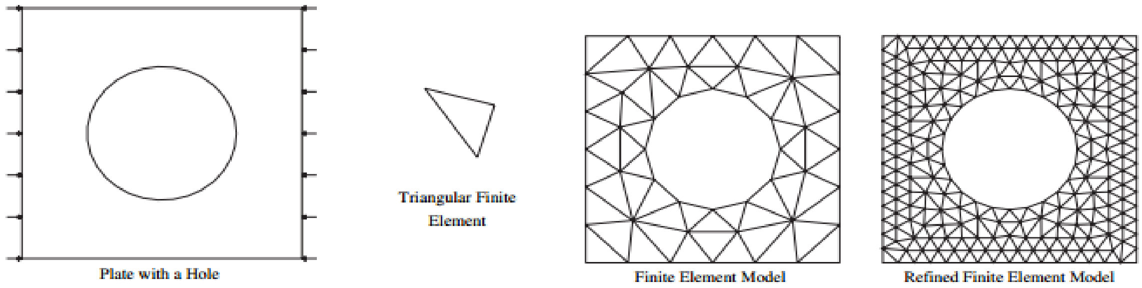

Figure 1.12 : Geometry, loads and finite element meshes.

This numerical method will help to do a numerical simulation of the geotechnical structures and study their behaviour and particularly their settlement over time.

One of the most used software in geotechnical engineering that performs FEM is PLAXIS which is a simulation software developed specifically for deformation analysis of soils and rock. PLAXIS supports various models to simulate soil and other continua and proposes different material models for modelling the soil.

Constitutive models form the basis of how the soil behaviour in a Finite Element Analysis can accurately be simulated. In time, the researches have proposed many materials models: here will be presented only the most important for the analysis of soft soil behaviour.

a) **Mohr Coulomb model**

This model is used as a first order approximation of soil or rock behaviour as for the embankment and the substitution material. For each layer one estimates a constant average stiffness or a stiffness that increases linearly with depth. The specification of this model and its yield criterion typically involves Coulomb's hypothesis which postulated a linear relationship between shear strength on a plane and the normal stress acting on it.

$$\tau = c - \sigma_n tan\varphi \quad \text{(1.16)}$$

Where τ is the shear strength, σ_n is the normal stress, φ is the angle of internal friction and c is the cohesion.

The mechanical behaviour of a material that is modelled with Mohr-Coulomb model includes features such as:

- Isotropic shear strength (peak and residual) that has cohesive frictional characteristic, and increases linearly with the level of stress/confinement;

- Tensile strength (by using a tension cut-off yield (function);
- Dilatation (increase in volume) or critical state (constant volume) at failure;
- Dependency of shear strength on Lode's angle.

Combining the Coulomb criterion with the Mohr circle representation of stress and considering the admissible states the Mohr-Coulomb failure criterion in terms of principal stresses can be expressed as:

$$F_s = \frac{1}{2}(\sigma_1 - \sigma_3) + \frac{1}{2}(\sigma_1 + \sigma_3)sin\varphi - ccos\varphi = 0 \quad \ldots\ldots\ldots\ldots\ldots\ldots\ldots\ldots\ldots \quad (1.17)$$

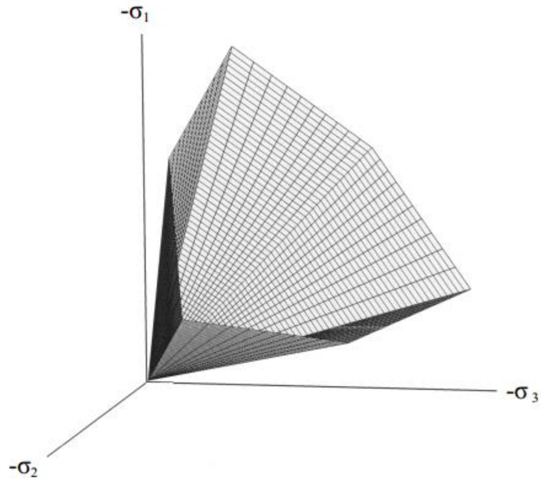

Figure 1.13: The Mohr-Coulomb yield surface in principal stress space (PLAXIS manual, 2008)

The full Mohr-Coulomb yield condition consists of six yield functions when formulated in terms of principal stresses (Smith & Griffith, 1982). These yield functions together represent a hexagonal cone in principal stress space as shown in Figure 1.13.

Two plastic model parameters appear in the yield functions: the friction angle φ and the cohesion c; a third one, the dilatancy ψ appears in the six plastic potential functions defined for the Mohr-Coulomb model and is required to model a positive plastic volumetric strain increments as actually observed for dense soil.

The model involves five parameters: Young's modulus (E) and Poisson's ratio (v) for soil elasticity, Friction angle (φ) and Cohesion (c) for soil plasticity, and dilatancy angle (ψ).

- **Limitations**

The linear elastic perfectly-plastic Mohr-Coulomb model includes only a limited number of features that soil behaviour shows in reality. Although the increase of stiffness with depth can be considered, the Mohr-Coulomb model does neither include stress-dependency nor stress path dependency nor strain dependency of stiffness or anisotropic stiffness. For undrained materials, this model may be used with the friction angle φ set to 0° and the cohesion c to c_u (s_u), to enable a direct control of undrained shear strength but it does not automatically include the increase of shear strength with consolidation.

b) Soft soil model

One can rely on Soft Soil model when dealing with near-normally-consolidated clays. It was inspired by the Modified Cam Clay model (Roscoe & Burland, 1968). It distinguishes between primary loading behaviour and unloading or reloading below pre-consolidation pressure.

The best performance of this model is obtained in primary compression, since unloading is modelled as elastic behaviour. It includes some features that are relevant for practical applications on soft soils:

- Realistic non-linear behaviour for compression and shear;
- Linear stress dependency of stiffness (logarithmic compression behaviour);
- Distinction between primary loading and unloading-reloading;
- Memory for pre-consolidation stress;
- Failure behaviour according to the Mohr-Coulomb criterion;
- Realistic pore pressure development in undrained loading of soft soils;
- Accurate prediction of undrained shear strength based on effective strength parameters.

The model uses an isotropic compression index and swelling index as model parameters, which can be related to compression index C_c and swelling (or recompression) index C_s (or C_r) obtained from one-dimensional compression tests. The Soft Soil model include two parameters to characterise its stiffness response in primary loading and unloading or reloading. These parameters can easily be obtained from standard lab tests: compression test or oedometer test. This test also provides the initial pre-consolidation pressure that is used to initialise the model's stress state.

For general states of stress, the plastic behaviour of soft soil model is defined by a total of six yield functions: three compression yield functions and three Mohr-Coulomb yield functions. The total yield contour in principal stress space resulting from these six yield functions is indicated in Figure 1.14.

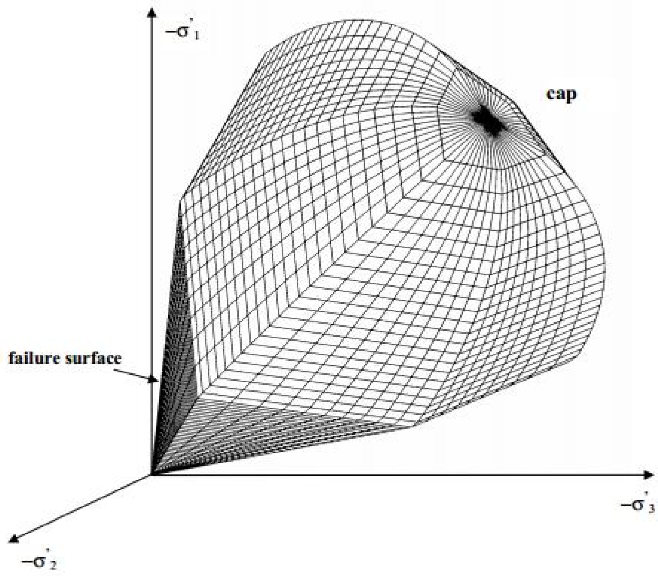

Figure 1.14: Representation of total yield contour of the Soft Soil model in principal stress space (PLAXIS manual, 2008)

The soft soil model includes two parameters to characterise its stiffness response in primary loading and unloading or reloading: The Modified compression index (λ*) and the Modified swelling index (κ*). Besides the compression parameters, the model has basically the same parameters as the simple Mohr-Coulomb model: The Effective cohesion (c), the Friction angle (φ) and the Dilatancy angle (ψ).

❖ **Limitations**

The utilisation of Soft Soil model should be limited to the situations that are dominated by compression. It is not recommended for use in excavation problems since the model hardly supersedes the Mohr-Coulomb model in unloading problems.

c) Soft soil creep model

Although the order and timing of construction stages or loading schemes are relevant for all non-linear elasto-plastic models, most soil models are time independent despite knowing that time can play an important role in soft soils. On the short term, soft soils behave undrained and generate pore pressures, while on the longer term these (excess) pore pressures dissipate, causing further settlement. After all excess pore pressures have dissipated, soft soils may continue to deform as a result of creep, which is often referred to as secondary compression. Creep is not include in Soft Soil model but the Soft Soil Creep model does. This model has been developed primarily for application to settlement problems of foundations, embankment, etc.

The Soft Soil Creep model does not only account for volumetric creep (time-dependent compression), it also accounts for deviatoric creep (time-dependent shear). Hence, the model may be used in several applications on soft soils where long-term time dependent behaviour is important (problems involving large primary compression) as embankments, slopes landfills.

This model has basically the same parameters as the Soft Soil model. The only extra parameter is the Creep index which can also be obtained from one-dimensional compression tests, when the applied stress is kept constant for a longer time.

Some basic characteristics of the Soft Soil Creep model are:

- Stress dependent stiffness;
- Distinction between primary loading and unloading-reloading;
- Secondary (time dependant) compression;
- Ageing of pre-consolidation stress;
- Failure behaviour according to the Mohr-Coulomb criterion.

The soft soil creep model has basically the same parameters as the soft soil model: The Modified compression index (λ*) and the Modified swelling index (κ*), the Effective cohesion (c), the Friction angle (φ) and the Dilatancy angle (ψ). The only extra parameter is the modified creep index (μ*) which can be obtain from one-dimensional compression tests, when the applied stress is kept constant for a longer time.

- **Cohesion (c'):** the cohesion has the dimension of stresses. A small effective cohesion may be used including a cohesion of zero. Entering a cohesion larger than zero may result in a state of over-consolidation depending on the magnitude of the cohesion and the initial stress state. It is not possible to specify undrained shear strength by means of high cohesion and friction angle of zero. Input of model parameters should always be based on effective values.

- **Friction angle (φ')** specified in degrees, the effective angle of internal friction represent the increase of shear strength with effective stress level.
- **Dilatancy angle (ψ):** the dilatancy can generally be neglected for the type of materials described by the Soft Soil Creep model.
- **Poisson's ratio (ν_{ur}):** it is the well-known pure elastic constant rather than the pseudo-elasticity constant as used in the linear elastic perfectly plastic model. Its value is in the range between 0.1 and 0.2 and the value 0.15 is automatically sets. It plays an important role in unloading problems rather than for loading of normally consolidated materials. Poisson's ratio should not be based on the normally consolidated k_0^{nc}-value, but on the ratio of the horizontal stress increment to the vertical stress increment in oedometer unloading and reloading test such that:

$$\frac{\nu_{ur}}{1-\nu_{ur}} = \frac{\Delta\sigma_{xx}}{\Delta\sigma_{yy}} \quad \text{(unloading and reloading)} \ldots\ldots\ldots\ldots \text{(1.18)}$$

- ***K_0^{nc}* -parameter:** the parameter M is automatically determined based on the coefficient of lateral earth pressure in normally consolidated condition. The value of M can be approximated by

$$M = 3.0 - 2.8K_0^{nc} \quad \ldots\ldots\ldots\ldots \text{(1.19)}$$

- **Modified swelling index (λ*), modified compression index (κ*) and modified creep index (μ*):** the parameters can be obtained from an isotropic compression test including isotropic unloading.

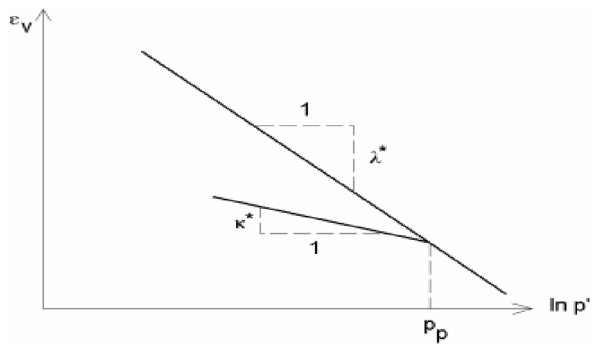

Figure 1.15: Logarithmic relation between volumetric strain and mean stress (PLAXIS manual, 2008)

The modified swelling index and the modified compression index can be obtained from an isotropic compression test including isotropic unloading. When plotting the logarithm of the mean stress as function of the volumetric strain for clay-type materials, the plot can be approximated by two straight lines (see Figure 1.15). The slope of the primary loading line gives the modified compression index.

There is a difference between the modified indices κ^* *and* λ^* and the original Cam-Clay parameters κ and λ. The latter parameters are defined in terms of the void ratio e instead of the volumetric strain ε_v.

Apart from the isotropic compression test, the parameters κ^* and λ^* can be obtained from the one-dimensional compression test. Here a relationship exists with the internationally recognized parameters for one-dimensional compression and recompression C_c and C_r.

Relationship to Cam-Clay parameters:

$$\lambda^* = \frac{\lambda}{1+e} \qquad \kappa^* = \frac{\kappa}{1+e} \quad \text{(1.20)}$$

Relationship to internationally normalized parameters

$$\lambda^* = \frac{C_c}{2.3(1+e)} \qquad \kappa^* = \frac{2C_r}{2.3(1+e)} \quad \text{(1.21)}$$

Where C_c is the compression index. The compression index (C_c) is the slope of the straight line on the e-log σ' plot, and is dimensionless (Figure 1.16). For any two points on the linear portion of the plot the equation for C_c may be written as:

$$C_c = -\frac{e_1 - e_0}{\log\left(\frac{\sigma'_1}{\sigma'_0}\right)} \quad \text{(1.22)}$$

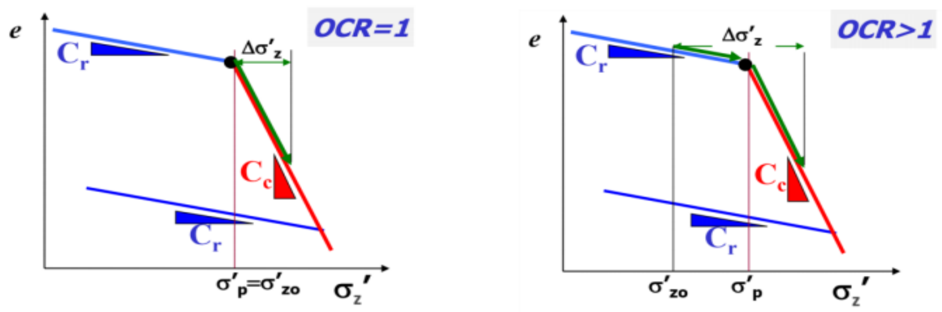

Figure 1.16: Void ratio versus effective stress for both normally and over consolidated clay from oedometer test

$\boldsymbol{C_r}$ is the recompression index. The equation of recompression Index C_r (Figure 1.16) is given by the following relation:

$$C_r = -\frac{e_2 - e_1}{\log\left(\frac{\sigma'_2}{\sigma'_1}\right)} \quad \text{(1.23)}$$

The parameter μ^* can be obtained by measuring the volumetric strain on the long term and plotting it against the logarithm of time (Figure 1.17).

$$\mu^* = \frac{C_\alpha}{2.3(1+e)} \quad \text{(1.24)}$$

$\boldsymbol{C_\alpha}$ is the secondary compression index.

This parameter is obtained by the creep curve. It is the plot of void ratio versus the logarithm of time from the experimental data. The secondary compression Index C_α may be written as:

$$C_\alpha = \frac{e_1 - e_p}{\log\left(\frac{t}{t_p}\right)} \quad \text{(1.25)}$$

Where (t_p, e_p) is the coordinate at the intersection of the tangents of the primary consolidation and secondary compression parts of the void ratio versus logarithm of time curve and (t, e_1) is the coordinate of any point on the secondary compression curve.

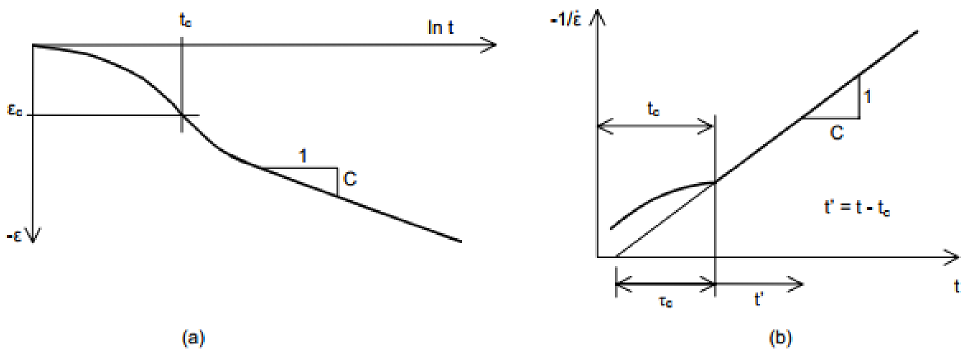

Figure 1.17: Consolidation and creep behaviour in standard oedometer test (PLAXIS manual, 2008)

❖ **Limitations**

All above limitations are also true for the Soft Soil Creep model. In addition, the Soft Soil Creep model overpredict the range of elastic soil behaviour. Care must also be taken with the generation of initial stresses for normally consolidated soils.

d) Hardening Soil model

The hardening Soil model is an advanced model for simulating the behaviour of behaviour of different types of soil, both soft soils and stiff soils. When subjected to primary deviatoric loading soil shows a decreasing stiffness and simultaneously irreversible plastic strains develop. Some basic characteristics of the model are:

- Stress dependency stiffness according to a power law;
- Plastic straining due to primary deviatoric loading;
- Plastic straining due to primary compression;
- Elastic unloading/reloading;
- Failure according to the Mohr-Coulomb failure criterion.

A basic feature of the present Hardening Soil model is the stress dependency of soil stiffness.

Some parameters of the present model coincide with those of the non-hardening Mohr-Coulomb: the (effective) cohesion (c), the (effective) angle of internal friction (φ) and the angle of dilatancy (ψ).

Other basic parameters for soil stiffness are:

- Secant stiffness in standard drained triaxial test (E_{50}^{ref});
- Tangent stiffness for primary loading (E_{oed}^{ref});
- Unloading/reloading stiffness (E_{ur}^{ref});
- Power for stress-level dependency of stiffness (m).

The advantage of the Hardening Soil model over the Mohr-Coulomb model is not only the use of a hyperbolic stress-strain curve instead of a bi-linear curve, but also the control of stress level dependency because while using Mohr-Coulomb model, the user has to select a fixed value of Young's modulus whereas for real soils this stiffness depends on the stress level.

Some alternative stiffness parameters can also be used when soft soils are considered. The stiffness parameters can be calculated from the compression index (C_c), swelling index (C_s) and the initial void ratio (e_{init}). The relationship between these parameters and the compression index is given by:

$$C_c = \frac{2.3(1+e_{init})p_{ref}}{E_{oed}^{ref}} \quad (1.26)$$

The relationship between the E_{ur}^{ref} and the swelling index is given by:

$$C_s \approx \frac{2.3(1+e_{init})(1+\nu_{ur})(1-2\nu_{ur})p_{ref}}{(1-\nu_{ur})E_{ur}^{ref}K_0} \quad (1.27)$$

Besides the model parameters mentioned above initial soil conditions such as pre-consolidation, play an essential role in most soil deformation problems.

- **Limitations**

The Hardening Soil model is an advanced model which despite being an advanced model, doesn't take into account a certain number of features of real soil behaviour as softening due to soil dilatancy and de-bonding effects. It is an isotropic hardening model so that it models neither hysteretic and cyclic loading nor cyclic mobility. Moreover, the model does not distinguish between large stiffness at small strains and reduced stiffness at engineering strain level.

e) Modified Cam-Clay model

The modified Cam-Clay is an incremental hardening/softening elastoplastic model based on Critical state theory and the basic assumption that there is a logarithmic relationship between the mean stress and the void ratio. Its features include a particular form of non-linear elasticity and a hardening/softening behaviour governed by volumetric plastic strain. This model describes three important aspects of soil behaviour, strength, compression or dilatancy (the volume change that occurs with shearing), and Critical State at which soil elements can experience unlimited distortion without any changes in stress or volume.

The modified Cam-Clay model may allow for extremely large shear stresses. This is particularly the case for stress paths that cross the critical state line. Furthermore, the modified Cam-Clay model may give softening behaviour for particular stress paths. Moreover, the modified Cam-Clay model cannot be used in combination with safety analysis by means of phi-c reduction. The use of the modified Cam-Clay model in practical applications is not recommended.

The yield function for modified Cam-Clay is:

$$F_c = q^2 + M^2 p(p + p_c) = 0 \quad (1.28)$$

In p-q space, the modified Cam -Clay yield surface plots as an elliptical curve (Figure 1.18). the parameter p_c (known as the yield stress or pre-consolidation pressure) controls the size of the yield surface. The parameter M is the slope of the critical state line in p-q space. A key characteristic of the critical state line is that it intersects the yield curve at the point at which the maximum value of q is attained.

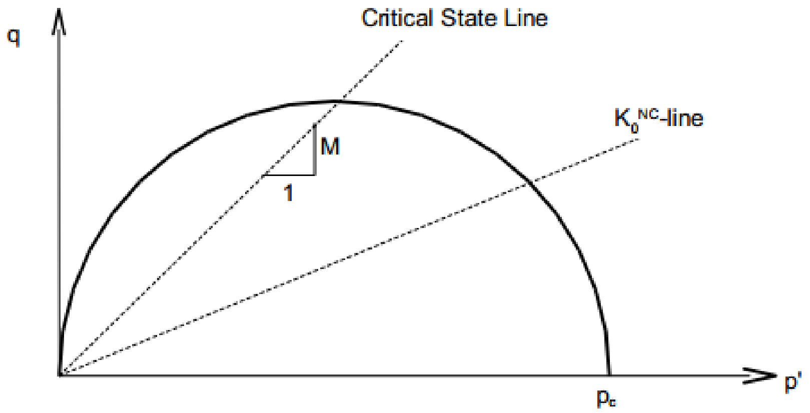

Figure 1.18: Yield surface of the Modified Cam-Clay model in p'-q plane

The modified Cam-Clay model is based on five parameters: the Poisson's ratio (μ_{ur}), the Cam-Clay swelling index (κ), the Cam-Clay compression index (λ), the Tangent to the critical state line (M) and the Initial void ratio (e_{init}).

1.3.4. Settlement calculation

The total settlement is the sum of its three components.

$$S_t = S_i + S_c + S_s \quad (1.29)$$

1.3.4.1. Immediate settlement

Immediate settlement takes place in a short time after the application of load and is due to elastic distortion of the soil. Compared to consolidation settlement, it is very small and often neglected unless the construction is very important.

These immediate settlements can be determined using the undrained elastic settlement at a corner of foundation from load of the embankment given by Ueshita and Meyerhof's equation (1968):

$$S_i = q\frac{BI}{E_u} \quad (1.30)$$

q: the applied load per unit area

B: width of the loaded area (taken at mid height of the embankment)

E_u: undrained elastic modulus

I: influence factor which is a function of H/B, L/B

H is the depth of the soft layer

L is the length of the structure and in case of road embankment it is taken as ∞

1.3.4.2. Primary consolidation settlement

a) Primary consolidation settlement parameters (Budhu, 2011)

The primary consolidation settlement of the soil can be expressed through the slopes of the curves in Figure 1.19. Two slopes for primary consolidation are going to be defined. One is called the compression index C_c, and is obtained from the plot of *e* versus logσ'_z (Figure 1.19b) as:

$$C_c = -\frac{e_2 - e_1}{\log\frac{(\sigma'_z)_2}{(\sigma'_z)_1}} \quad (1.31)$$

With 1 and 2 two arbitrary points on the normal consolidation line.

The other is the modulus volume compressibility m_v:

$$m_v = -\frac{(\varepsilon_z)_2 - (\varepsilon_z)_1}{(\sigma_z)_2 - (\sigma_z)_1} \quad (1.32)$$

where 1 and 2 are two arbitrary points on the normal consolidation line.

Similarly, the slope BC in Figure 1.19b can be defined as the recompression index C_r which can be express as:

$$C_r = -\frac{e_2 - e_1}{\log\frac{(\sigma'_z)_2}{(\sigma'_z)_1}} \quad (1.33)$$

where 1 and 2 are two arbitrary points on the unloading-reloading line.

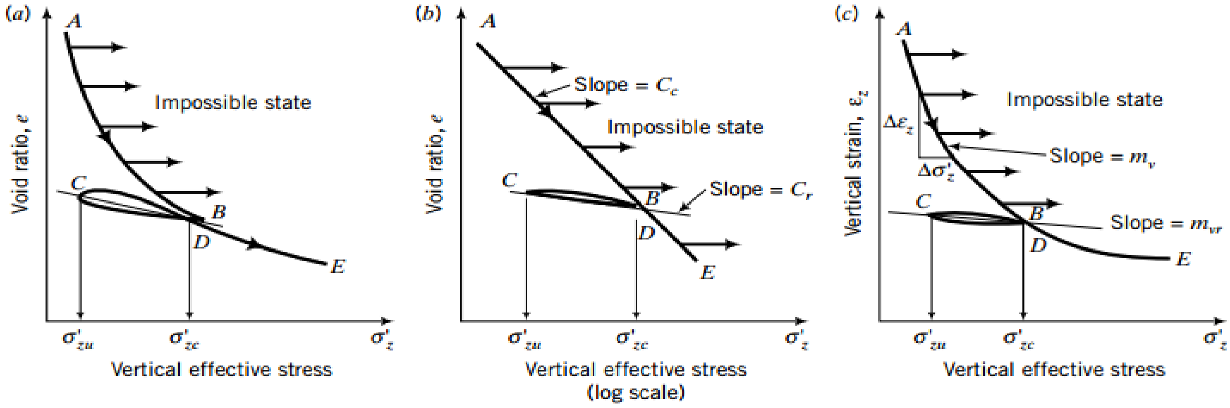

Figure 1.19 : Three plots of settlement data from consolidation.

From Hooke's law, it is known that constrained modulus is:

$$E_c' = \frac{\Delta\sigma_z'}{\Delta\varepsilon_z} = \frac{E'(1-\nu')}{(1+\nu')(1-2\nu')} = \frac{1}{m_v} \quad \text{(1.34)}$$

where the subscript *c* denotes constrained because the soil is constrained to settle only in one direction (one-dimensional consolidation), *E'* is Young modulus based on effective stresses, and *v'* is Poisson ratio.

The slopes C_c, C_r and *mv* are positive values to satisfy the sign convention of compression or recompression as positive.

b) Primary consolidation settlement calculation

The amount of primary consolidation settlement is computed using either the compression index C_c obtained from a plot of void ratio *e* versus log pressure or from a compression ratio C'_c obtained from a plot of strain ϵ versus log pressure. The void ratio or strain is computed based on initial sample conditions and the compression *ΔH* under the current load increment to D_{100}.

The Primary consolidation settlement depends of the *OCR* and the vertical stress increase $\Delta\sigma_z$

Over-consolidation ratio is: $OCR = \frac{\sigma_p'}{\sigma_{z0}'}$ .... (1.35)

- Over-consolidated soil: OCR > 1
- Normal consolidated soil: OCR = 1

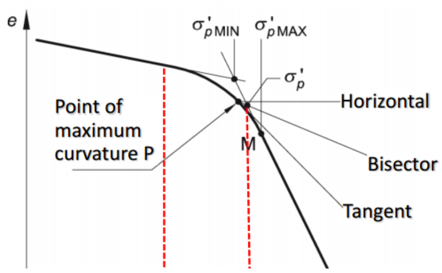

Figure 1.20 : Compression curve in semi log scale

- Under- consolidated soil: OCR < 1

To compute the primary settlement, one proceed as follow (Budhu 2011):

- If OCR = 1, the primary consolidation settlement is:

$$S_c = \frac{H_0}{1+e_0} C_c log \frac{\sigma'_{fin}}{\sigma'_{zo}} \quad \text{(1.36)}$$

- If OCR > 1 and $\sigma'_{fin} < \sigma'_{zc}$, the primary consolidation settlement is:

$$S_c = \frac{H_0}{1+e_0} C_r log \frac{\sigma'_{fin}}{\sigma'_{zo}} \quad \text{(1.37)}$$

- If OCR > 1 and $\sigma'_{fin} > \sigma'_{zc}$, the primary consolidation settlement is:

$$S_c = \frac{H_0}{1+e_0} [C_r log\ (OCR) + C_C log \frac{\sigma'_{fin}}{\sigma'_{zc}} \quad \text{(1.38)}$$

Where H_0 is the thickness of the soil layer.

1.3.4.3. Secondary compression settlement

Secondary compression, or creep, takes place under a constant vertical effective stress.

The secondary compression index is:

$$C_\alpha = \frac{(e_t - e_p)}{log\ (t/t_p} = \left|\frac{\Delta e}{log\ (t/t_p}\right| \qquad t > t_p \quad \text{(1.39)}$$

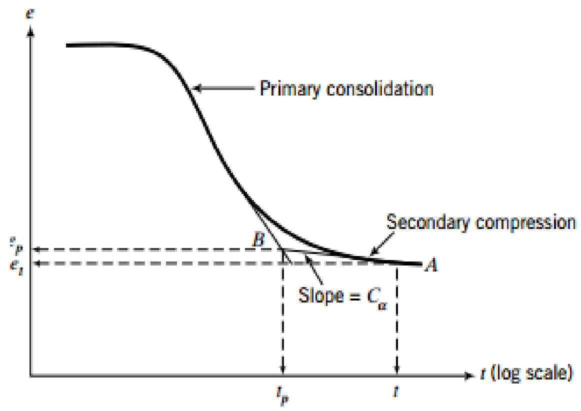

Figure 1.21 : Secondary compression

where (t_p, e_p) is the coordinate at the intersection of the tangents to the primary consolidation and secondary compression parts of the logarithm of time versus void ratio curve, and (t, e_t) is the coordinate of any point on the secondary compression curve, as shown in Figure 1.21.

The secondary consolidation settlement is:

$$\rho_{sc} = \frac{H_0}{1+e_p} C_\alpha log\left(\frac{t}{t_p}\right) \quad \text{(1.40)}$$

1.3.5. Settlement monitoring and record

Commonly, settlement is expected to continue after embankment construction. For this reason, some types of monitoring program should be provided. The type of monitoring will depend on the magnitude and time frame of the settlement. The principal parameters monitored during embankment construction are pore water pressure and displacements, both vertical and lateral. The monitoring of embankment settlement is normally done using one or more of the following well established methods.

1.3.5.1. Rod extensometer

The rod extensometer is a simple and accurate device for measuring movement (vertical settlements). The rods used are generally aluminium alloy tubes, typically 14 mm in diameter. Various lengths of rod can be coupled together as required. Settlement at various depths within a soil mass can also be determined by means of a multi-point extensometer.

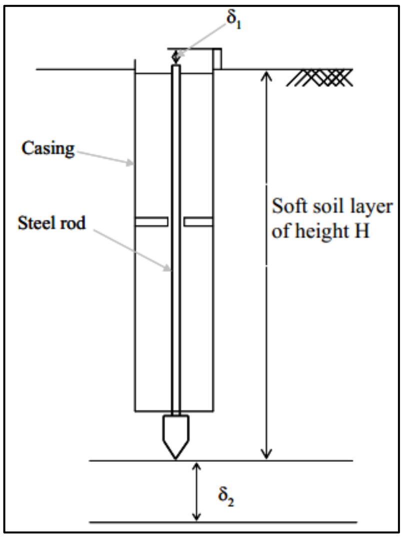

Figure 1.22: Schematic of the rod extensometer.

The devices measure the total settlement in the layer of height H (Figure 1.22).

When $\Delta\delta = \delta_1^{final} - \delta_1^{initial} < 0$ (-) the soft soil layer is settling.

When $\Delta\delta = \delta_1^{final} - \delta_1^{initial} > 0$ (+) the soft soil layer is expanding.

1.3.5.2. Magnetic extensometer

The magnetic extensometer system is designed to measure settlement or heave of the soft ground under the influence of loading or unloading due to the construction of embankments, fills and structures. The equipment consists of permanent ring magnets, axially magnetized, mounted in plastic holders which are supported at the required levels in the borehole by springs. The magnets, are inserted around a plastic guide tube placed down the centre of the borehole. The levels of the magnets are determined by lowering a sensor incorporating a reed switch down the central plastic tube. When the reed switch moves into the field of a magnet it snaps shut and activates an indicator light or buzzer. A steel tape attached to the sensor enables the level of the station to be obtained to an accuracy of 1–2 mm (Craig, 2004).

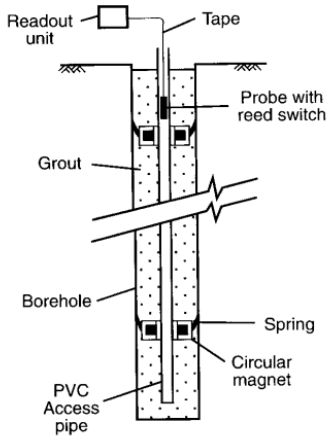

Figure 1.23: Schematic of the magnetic extensometer.

1.3.5.3. Settlement plates

Settlement plates are used to monitor settlement at the interface between native ground and the overlying fill. There are: surface settlement plates and depth settlement plates.

The surface settlement plate is a simple visual measuring device and normally consists of a flat plate on to which is welded a rod of sufficient length to ensure that the end extends above the surface once the settlement has taken place. The plate is positioned on the surface to be monitored, such as a construction layer, a geotextile layer or an original ground surface and as an added sophistication its rod can be sheathed in a duct to protect it during settlement of the overlying fill. These plates are then referenced back to fixed ground control points for consistency of monitoring.

A depth settlement plate is normally used where it is necessary to know the behaviour of a point below the settling embankment. To achieve this the settlement plate is fabricated as a short length of screw and screwed down into the soil to the depth required. Once in place, the screw is effectively locked in place within the soil mass and moves as the mass settles giving an indication of the settlement at the initial installed point. As with the surface settlement plates depth plates are referenced back to fixed ground control points for consistency of monitoring.

1.3.5.4. Pneumatic settlement cells:

These cells are generally placed at the interface between the embankment fill and native ground. A flexible tube is routed to a reservoir, which must be located away from the settlement area. The reservoir must be kept at a constant elevation. The precision of the cells is about 0.75 inches.

1.3.5.5. Sondex system

The Sondex System can be used for monitoring settlement at several points at depth. It consists of a series of ring attached to a flexible corrugated pipe. Measurements are lowering a probe through an inner access pipe to detect the position of the rings. Accurate measurement of settlement depends on the compatibility of the soil and grout (Geotechnical Design Manual, 2022). Therefore, if the grout mix has a higher strength than the surrounding soil, not all the settlement will be measured.

1.3.5.6. Hydrostatic profile gauge

A hydrostatic profile gauge is a device which can be used to measure the vertical displacement of structures such as road embankments and earth dams across the entire width of the structure.

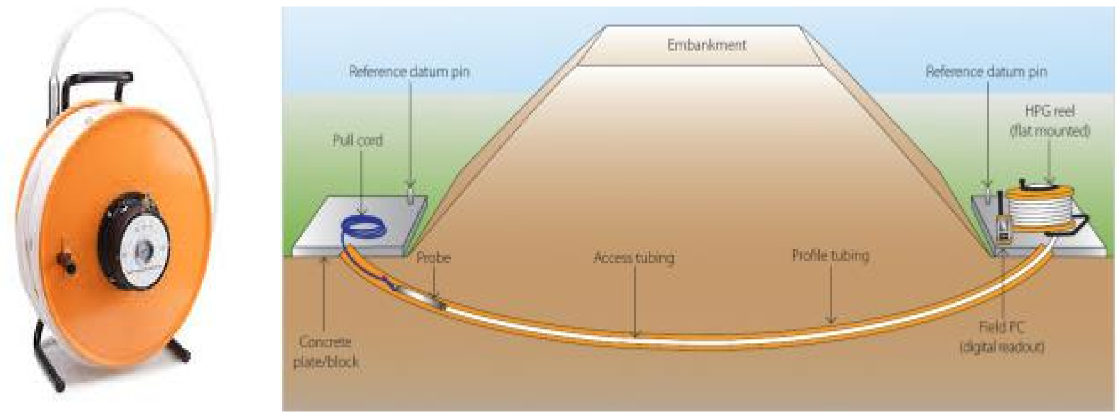

Figure 1.24: Typical digital hydrostatic profile gauge installation in embankment

For normal installation a 50mm diameter plastic tube is placed on the soil surface transverse to the road lone prior to the commencement of feeling operations. As the layers of fill are placed on the soil, and the embankment settles, a pressure transducer is pulled through the tube to measure its deflected shape under the embankment. The measurements obtained are then reduced to the contract level datum and presented as a cross section through the embankment for use in measurement and earthworks control purposes (Roadex Network, 2015).

The data from hydrostatic profile gauges can also have a secondary function that of quantifying the amount of fill material that has settle into the soil.

1.3.5.7. Hydraulic settlement cell

The settlement of embankments can be measured by means of steel plates with central holes which are threaded over a length of vertical plastic tubing and laid, at various levels, on the surface of the fill as it is placed. Hydraulic settlement gauges, which are used mainly in embankments, provide another means of determining vertical movement. In principle the hydraulic overflow settlement cell (Figure 1.25) consists of a U-tube with limbs of unequal height: water overflows from the lower limb when settlement occurs causing a fall in water level, equal to the settlement, in the higher limb (Craig, 2004).

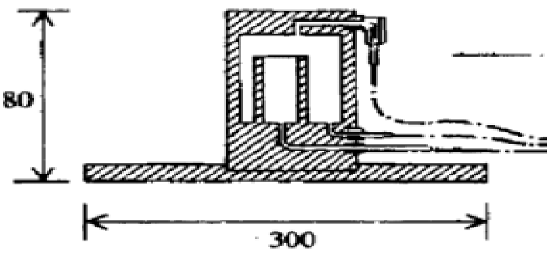

Figure 1.25: Hydraulic settlement cell

1.3.5.8. Inclinometer

Inclinometers are used to measure ground movement in unstable slopes and the lateral movement of ground around ongoing excavations. Inclinometers also monitor the stability of embankments, slurry walls, and the settlement of ground in fills, embankments, and beneath storage tanks.

The inclinometer casing has orthogonal grooves inside the casing (Figure 1.26b) designed to fit the wheels of a portable inclinometer probe (Figure 1.26a). This probe, suspended on the end of a cable connected to a readout device, is use to survey the inclination of the casing with respect to vertical (or horizontal), and in this way to detect any changes in inclination caused by ground movements.

However, inclinometer measurements of the lateral deformation of soil at the boundaries of embankments and storage facilities show that settlements resulting from lateral deformation are generally small compared with those resulting from compression if the factor of safety against undrained instability during construction or loading remains greater than about 1.4 (Terzaghi et al., 1996).

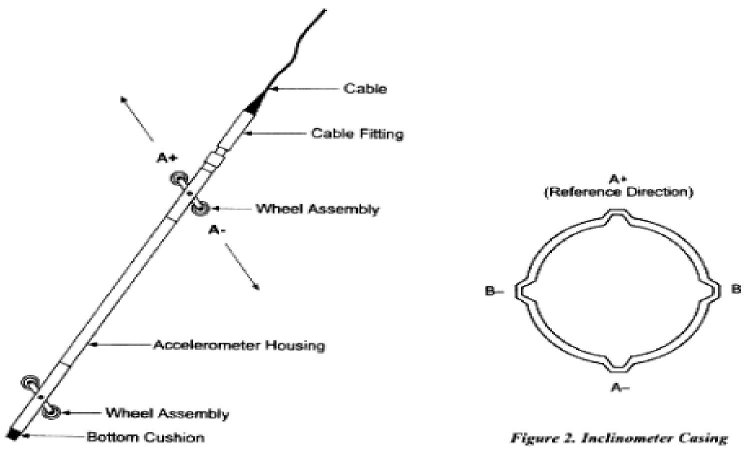

a) b)

Figure 1.26: (a) Inclinometer probe (Geokon Inc 2007) and **(b)** Inclinometer Casing

1.3.5.9. Piezometers

Piezometers are used to record the change in pore water pressure with time. A piezometer consists of porous stone at the tip that is connected to a plastic standpipe in the borehole and can be used for continuous monitoring of water pressure change at the tip section. The void in the borehole should be sealed by bentonite cement grout.

Three types of piezometers are commonly used to monitor embankment construction: open standpipe, pneumatic and vibrating wire.

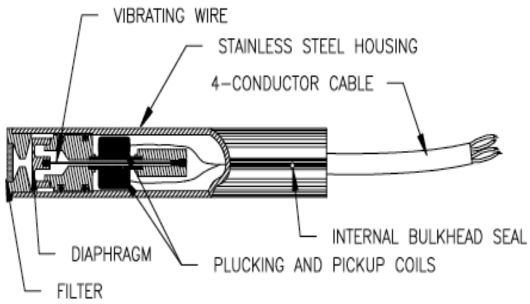

Figure 1.27: Vibrating wire piezometer

1.3.5.10. Topographic data

Surveys of the pre-construction condition of neighbouring structures should be conducted. Ordnance Survey maps provide information on, for example, the relief of the land, site accessibility, and the land forms present. A study of the sequence of maps for the same location produced at different periods in time, can reveal features which are now concealed and identify features which are experiencing change.

The instrumentation program should be developed with a consideration of the anticipated performance, risks and potential consequences. Parameters should be identified that are critical to project success and appropriate instrumentation selected. A key to successful use of instrumentation is to measure, plot and interpret the data in a timely manner to be able to take corrective measures, if needed (NHI-06-089, 2006).

Conclusion

This chapter was based on literature review and present in its first part an overview on soil, particularly soft soils, their formation, typologies and properties followed by concept of embankment and their behaviour when constructed on soft soils. It was also seen that the problem of settlement is one of the more relevant problem in soil construction and require a great attention. Settlement can be predicted, measured, calculated or measured. The next chapter will deal in the methodology of work to reach the objectives especially the prediction of settlement using numerical simulation.

Chapter 2 : METHODOLOGY

Introduction

As seen in the previous chapter, to quantify the amount of settlement of an embankment on soft soil, it is important to well know the properties of the soil in place, the behaviour of the embankment on the foundation soil, how to predict the settlement using observational and numerical methods and how to record the values of settlement using some instruments placed in the field. This pat will focus on the working methodology i.e. the steps of the research procedure that will enable to attain the main objective which is to compare the predicted and measured value of the settlement of an embankment constructed on soft soil along the Foumbot-Bamendjing-Galim road. This part will be divided into five parts. The first part will concern the general recognition of the site, followed by a descent on the site to observe the study area. Then, the necessary data to be collected (geometric and geotechnical data) will be presented. The fourth part will be about the numerical analysis method using the software PLAXIS and finally, the instrumentation of embankment using the settlement masse method will be presented in the last part.

2.1. General recognition of the site

In order to correctly find a solution to this thesis problem, many information has been sought about where the project is located and all the characteristics (physical and socioeconomic) of the zone concerned. The site general recognition is done through a documentary research. The essential objective is to know the geographical parameters of the site of the case study, the site location, the climatic conditions (temperature, precipitations of the area which are factors influencing the settlement process), the relief, the population, the hydrology and the economic activities of the site.

2.2. Visit of the site

After the documentary research, the site visit has been done by observing the study area. The observation of the site consists at taking pictures of it and asking questions, in order to have a better and wide set of information necessary to properly understand the problem. In fact, with the embankment already constructed, the available project reports were consulted and used, as well as documented or academic reports related to the study area for more information.

2.3. Data acquisition

The collection of geometric and geotechnical characteristics of road section from kilometric point (PK) 12+650 to PK 12+950 will permit to perform a two-dimensional modelling and analysis using analytical and numerical methods later described in this chapter.

2.3.1. Geometric data

The geometric data will be acquired from the company in charge of the supervision of the project. The data present the 2D plan drawings in which informations such as the length of the study area, the cross sections (longitudinal and transversal profiles) with information such as the slope and the embankment height and width were found. Also, the location of the installed plates for settlement recording was given.

2.3.2. Geotechnical data

The geotechnical data of the problem were gotten from the laboratory of the company in charge of the construction works of the project entitled *"Route de desenclavement du basin agricole de l'Ouest Lot 2 Bangangté Foumbot-Bamendjing-Galim"*. These data present the physical, mechanical and compressibility characteristics of the material forming the foundation and embankment soil. The identification of soil types and their different parameters was done through in-situ tests and laboratory tests.

Table 2.1: Parameters to be find for the study

PARAMETERS	SYMBOLS	PARAMETERS	SYMBOLS
Saturated soil unit weight	γ_{sat} (kN/m^3)	Poisson's ratio	ν
Dry soil unit weight	γ_d (kN/m^3)	Admissible stress	σ (kN/m^2)
Frictional angle	Φ'	Void ratio	e
Dilatancy angle	ψ	Compression index	C_c
Young modulus	E, E_u (kN/m^2)	Recompression index	C_r
Cohesion	c, c_u (kN/m^2)	Secondary compression index	C_α

Horizontal/Vertical permeability	k_h/k_v (m/day)	Coefficient of consolidation	C_v (m^2/s)

2.4. Numerical analysis in the Software PLAXIS (2D V20)

In the framework of the work, numerical analysis will be carried out namely to simulate and constate the state of settlement depending on the considered behaviour (material model) and then compare it to the one observed on the site to see if numerical analysis can be use to predict the behaviour of an embankment on soft soil.

The one-dimensional consolidation equation can be solved numerically by the Finite Element Method (FEM). The method has the advantage that any pattern of initial excess pore water pressure can be adopted and it is possible to consider problems in which the load is applied gradually over a period of time. The errors associated with the method are negligible and the solution is easily programmed for the computer (Craig, 2004).

The analytical analysis method using FEM is well implemented in the PLAXIS software which is a powerful and user-friendly finite-element (FE) package intended for 2D analysis of deformation and stability in geotechnical engineering and rock mechanics. The user interface consists of four sub-programs: input, calculation, output and curves. The presentation of this software will be done in the next part.

2.4.1. Input program

To carry out a finite element analysis using PLAXIS, a finite element model has to be created, the material defined and the boundary condition introduced. This is done in the input program of PLAXIS.

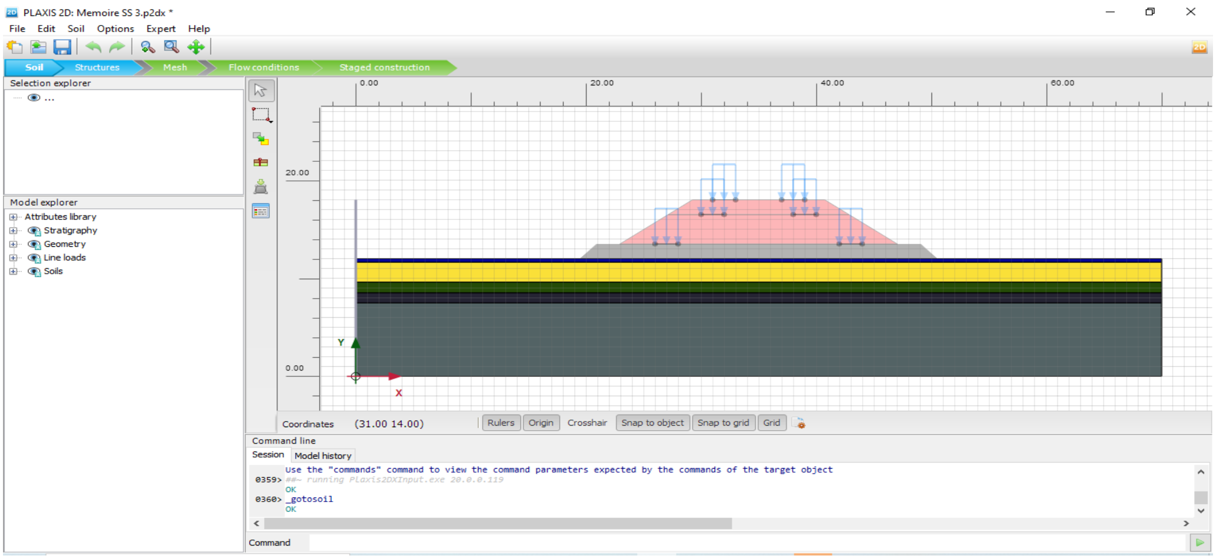

Figure 2.1: PLAXIS Input interface

In the Input program, the geometry is given by entering different soil layers, structural parts, and external loads etc. A choice between various available material models: Linear model, Mohr-Coulomb, Hardening Soil, Soft Soil, Soft Soil Creep and other advanced models is made at the input for each material. When the model is complete, a mesh is generated, the flow condition and the stages of construction are defined. Then, the Calculation program was running.

2.4.1.1. Ground modelling

A geometry model is a two-dimensional representation of the real three-dimensional problem and consists of three types of components which are points, lines and clusters. It should include a representative division of the soft soil and the embankment into distinct soil layers and loadings. The soil stratigraphy is defined in the soil mode using the borehole feature of the program. After the creation of the borehole, the soil layers are defined by entering the thickness of each layers and their properties (material properties) are assigned. Then, the water condition is defined.

2.4.1.2. Material properties

In order to simulate the behaviour of the soil, a suitable soil model and appropriate material parameters must be assigned to the geometry. In PLAXIS, soil properties are collected in material data sets and stored in a material database. There are four different types of material sets amongst which there are data sets for soil and interfaces, plates, geogrids, embedded beam rows and anchors. More explicitly, there are different material models proposed by PLAXIS for modelling the soil: the Mohr-Coulomb model, the Soft Soil model, the Soft Soil Creep model, the Hardening Soil model, etc. These models were presented in chapter one.

2.4.1.3. Hydraulic behaviour

In principle, all model parameters in PLAXIS are meant to represent the effective soil response i.e. the relation between the stresses and strains associated with the soil skeleton. An important feature of soil is the presence of pore water. Pore pressures significantly influence the soil response. To enable incorporation of the water-skeleton interaction in the soil response PLAXIS offers for each soil model a choice of three types of behaviour.

a) Drained behaviour

Using this setting no excess pore pressures are generated. This is the case for dry soils and full drainage due to high permeability and/or low rate of loading. This option may also be used to simulate long term soil behaviour without the need to model the precise history of undrained loading and consolidation.

b) Undrained behaviour

This setting is used for a full development of excess pore pressures. Flow of pore water can sometimes be neglected due to low permeability and/or high rate of loading. In undrained condition, no water movement takes place and undrained analysis is appropriate when permeability is low or rate of loading is high or when short term behaviour has to be assessed. Distinction is made between three different methods of modelling undrained soil behaviour:

- Undrained (A): it is an undrained effective stress analysis with effective stiffness as well as effective strength parameters. This method will not give a prediction of pore pressures and the analysis can be followed by a consolidation analysis.
- Undrained (B): it is an undrained effective stress analysis with effective stiffness parameters and undrained strength parameters. This method will give a prediction of pore pressures.
- Undrained (C): it is an undrained total stress analysis with all parameters undrained. This method will not give a prediction of pore pressures.

c) Non-porous behaviour

Using this setting neither initial nor excess pore pressures will be considered in clusters of this type. Applications may be found in the modelling of concrete or structural behaviour. Non-porous behaviour is often used in combination with the linear elastic model.

2.4.1.4. Modelling loads and structures

The geometry of the embankment, the applied loads and the boundary conditions are defined in the structure's mode.

2.4.1.5. Meshing

When the geometry model and the definition of all material data sets is complete, the finite element model (or mesh) can be generated. PLAXIS allows for a fully automatic mesh generation procedure in which the geometry is divided into elements of the basic element type and compatible structural elements, if applicable. The mesh generation takes full account of the position of points and lines in the geometry model, so that the exact position of layers, loads and structures is accounted for in the finite element mesh. In addition to the mesh generation itself, a transformation of input data (properties, boundary conditions, material sets, etc.) from the geometry model (points, lines and clusters) to the infinite element mesh (elements, nodes and stress points) is made.

2.4.1.6. Initial conditions

Once the geometry model has been created and meshing done, the finite element model is complete and before starting the calculations, the initial stress state and the initial configuration must be specified. In general, the initial conditions comprise the initial groundwater conditions, the initial geometry configuration and the initial effective stress state.

2.4.2. PLAXIS calculation program

After the generation of a finite element model, the actual finite element can be executed. Therefore, it is necessary to define which types of calculations are to be performed and which types of loadings or construction stages are to be activated during the calculation.

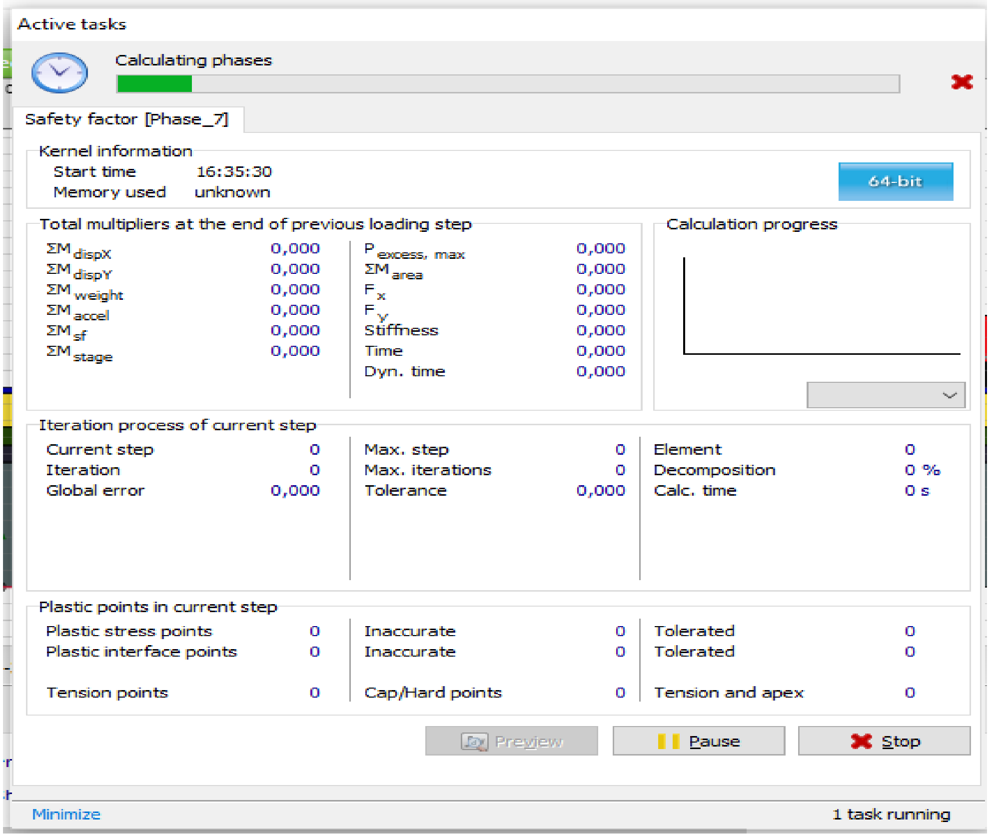

Figure 2.2: PLAXIS Calculations interface

2.4.2.1. Calculations types

PLAXIS allows for a different types of finite element calculations. The Calculations program considers only deformation analysis and distinguishes between:

- **Plastic calculation**: It is the one appropriate in most practical geotechnical application. Plastic calculation should be selected to carry out an elastic-plastic deformation analysis in which it is not necessary to take the decay of excess pore pressures with time into account. It does not take time effect into account, except when the soft soil creep model is used;
- **Consolidation analysis**: should be selected when it is necessary to analyse the development or dissipation of excess pore pressures in water-saturated clay-type soils as a function of time. PLAXIS allows for true elastic-plastic consolidation analyses. In general, a consolidation analysis without additional loading is performed after an undrained plastic calculation. It is also possible to apply loads during a consolidation analysis. However, it should be taken when a failure situation is approached, since the

iteration process may not converge in such situations. Varying time spans can be considered by choosing *Consolidation* and then enter the desired number of days. If full consolidation analysis is wanted, *Minimum Pore Pressure* should be selected, where all excess pore pressure is reduced.

- **Phi-c reduction (safety analysis):** can be executed by reducing strength parameters. A safety analysis can be performed after each individual calculation phase and thus for each construction stage to calculate the safety factor. However, the Phi-c reduction cannot be used as a starting condition for another calculation phase because it ends in a state of failure. When performing a safety analysis, no loads can be increased simultaneously and this type of calculation is considered as a special type of plastic calculation.

2.4.2.2. Loading types

After choosing the calculation type, the loading has to be specified. One can select one of the following types of loading:

- **Staged construction**: it is the most important type of loading input. In this PLAXIS feature it is possible to change the geometry and load configuration by deactivating or reactivating loads, volume clusters or structural objects as created in the geometry input. Staged construction enables an accurate and realistic simulation of various loading, construction and excavation processes. The option can be used to reassign material data sets or to change the water pressure distribution in the geometry. A staged construction analysis can be executed in a plastic calculation as well as a consolidation analysis.
- **Total multipliers type**: it represents the total level of the load in a particular calculation step or phase. It is used to specify the ultimate values of external loads.
- **Incremental multiplier type**: it represents the increment of load for an individual calculation step. It is selected when the external load is applied incrementally. Before entering a load increment, an increment of time can be entered. Increments of time are not relevant when using plastic calculation except when time dependent models are used.

Once the calculation has been completed, the result can be evaluated in the output program.

2.4.3. PLAXIS output program

The main output quantities of a finite element calculation are the displacements at the nodes and the stresses at the stress points. A large amount of data can be obtained from a finite element calculation such as stresses, pore pressures and displacements for soils, and displacement. The output program also permits to view the general project information including material data and calculation information.

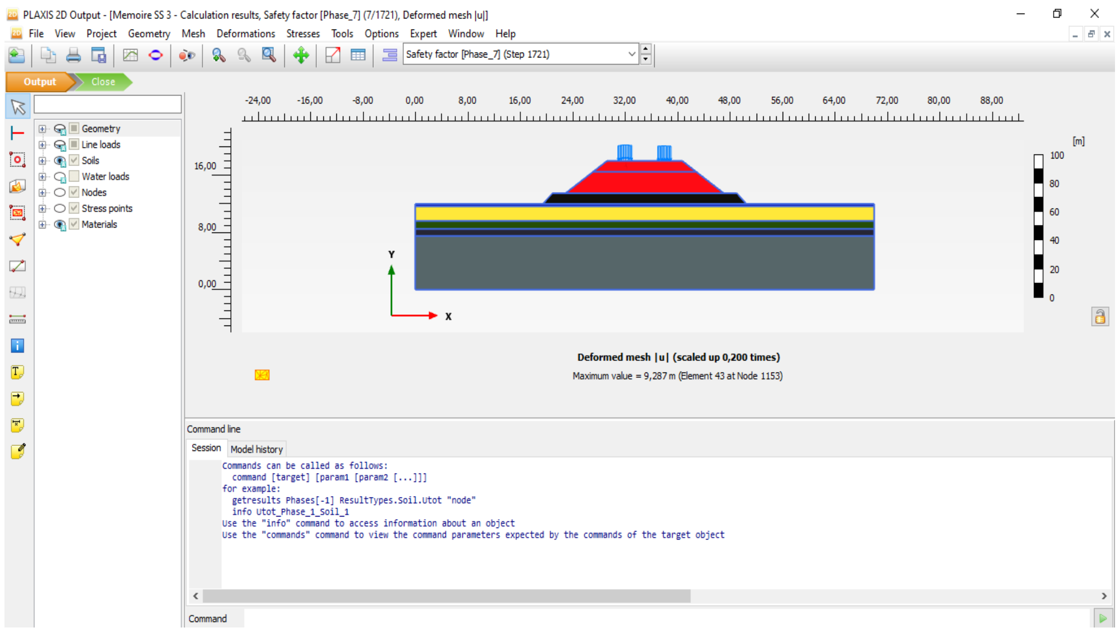

Figure 2.3: PLAXIS Output interface

Many results are available in the output program: connectivity plot, deformations (deformed mesh, total displacement, phase displacements, incremental displacements, velocities, accelerations…), stresses (effective stresses, total stresses, pore pressures, …), structures and interfaces.

2.4.4. PLAXIS curve program

The curve program is used to generate the stress paths, stress-strain diagrams and load displacement curves of pre-selected point in the geometry. These curves allow to visualise the variation of some quantities for various calculation and by this, the local and global behaviour of the soil can be observed.

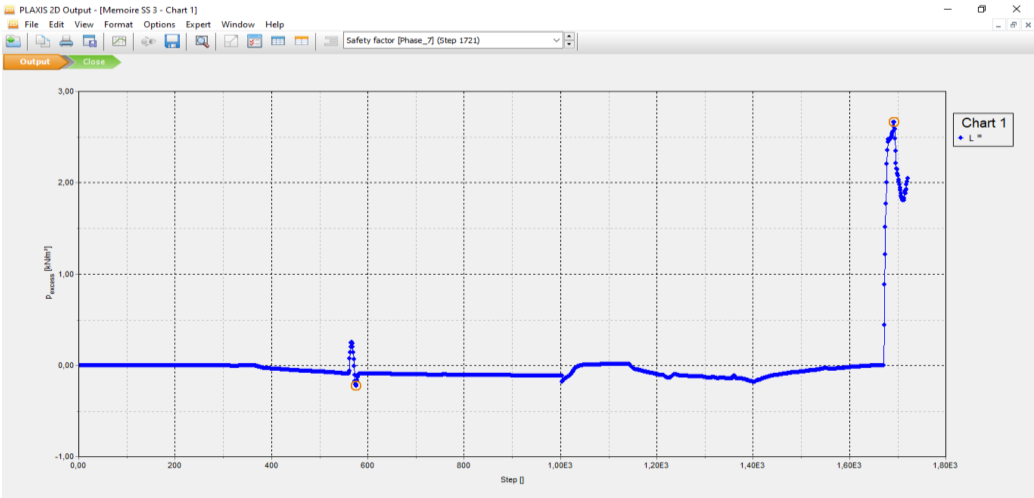

Figure 2.4: PLAXIS Curves interface

This facility allows for the generation of the load-displacement curves, force-displacement curves, stress-paths, strain-paths, stress-strain curves and time-related curves.

2.5. Instrumentation of embankments by settlement masse method

Earth materials generally compress an observable amount when load is applied. Soils in particular, when subject to load, may deflect, consolidate or densify. Fill materials and native soils may react immediately, slowly or very slowly to loadings depending on the type of material and the effect of water on the soil. The most common settlement monitoring system is the settlement plates. These instruments may be simply constructed and read. They are typically installed in areas where significant settlement is predicted.

2.5.1. Method description

The settlement plate is used to detect any settlement, subsidence and deformation of embankments, both during construction and in the management phase. Simplicity of installation and reading, reliability, accuracy of measurement and very low cost, make it extremely popular for geotechnical monitoring.

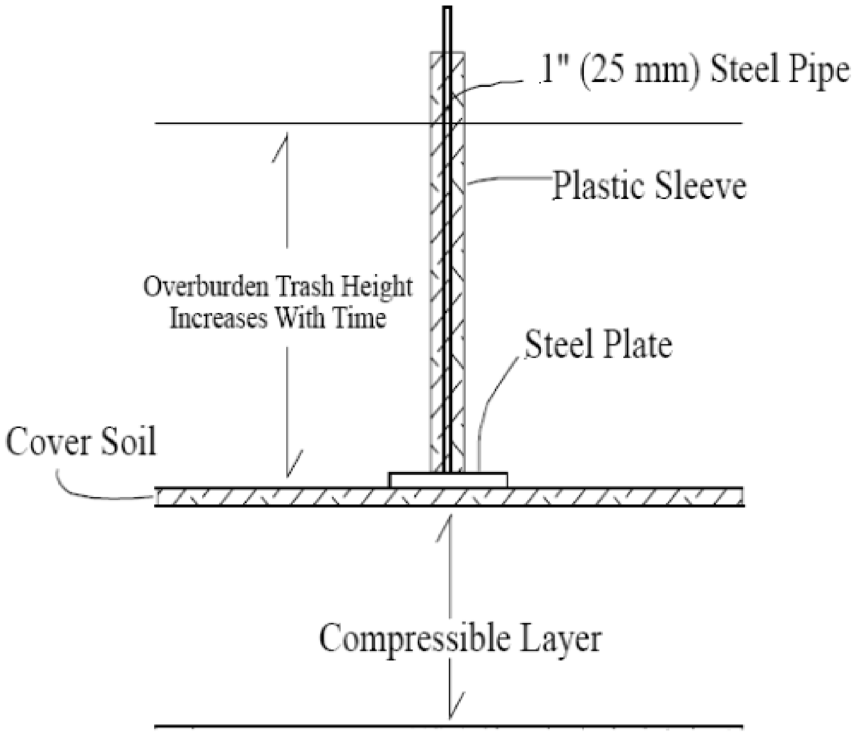

Figure 2.5: Settlement plate

A rigid rod is free to slide inside a tube or guide sheath. At the bottom, the rod has an integral plate which constitutes the rod anchor point in the ground. The upper end forms the measuring point. The anchor plate is galvanized steel (or concrete pad or polywood) which is connected to the measuring rod made of ¾" of galvanized pipes. The measuring rod is protected by a sheath made with corrugated tube, or with 2 galvanized pipes. To facilitate the formation of columns of various lengths, the system is divided into two groups namely: the bottom element constituted by the plate and the rod piece and the intermediate element consisting of a rod coupling with coupling friction tube of high-density polyethylene. As fill is placed over the settlement plate additional segments of pipe are added.

2.5.2. Location of installed plates

Settlement plates may be placed at any given elevation of interest. Typically, they are installed on the existing ground surface prior to the construction of embankment fill.

Settlement plates should be located such that construction traffic in the vicinity is minimized at all possible. Plate installations and riser pipes should be clearly and adequately marked to protect the riser pipes from impact or obliteration during fill placement, grading, and other construction activities that will be ongoing during the monitoring process. Note also that the bench-mark (or fixed reference elevation) used to survey the settlement plates must also remain intact through the monitoring process.

2.5.3. Settlement recording methodology

Settlement plates are frequently used where a “waiting period” for construction has been recommended. Waiting periods are a minimum specified time to allow consolidation settlement to occur, generally after fills over soft or compressible soils or large fills have been placed. Waiting periods are determined from predictions based on the geotechnical site investigation and associated testing and analysis.

Settlement plates should be installed prior to any addition of fill material. Ground elevation and the elevation of the settlement plate riser pipe should be established and recorded prior to placement of the fill material to establish a baseline reading. The plates should then be monitored regularly through the fill placement process and the following waiting period to determine the total soil movements, some of which occur during the fill placement process. It is important that the plates be surveyed immediately at the time of installation.

Settlement is determined by periodically measuring the elevation of the top of the reference rod. The elevation of the base platform elevation must be measured before the embankment construction begins. Subsequent readings should be taken periodically during the embankment construction. Stable benchmark should be used for a reference elevation datum and should be located away from a possible vertical movement or other disturbance.

The riser pipe should be surveyed to a fixed datum or bench mark well outside the embankment fill area. The height of fill should also be surveyed and recorded at each monitoring interval. It is important that original installation data and subsequent monitoring data be clearly recorded for each settlement plate installation. Added sections of riser pipe, and their lengths, should be clearly noted in the data log.

As settlements are relatively small, surveys should be conducted to the greatest accuracy reasonably obtainable under field conditions. It is essential that the settlement plates be surveyed as soon as they are placed.

During initial construction of the fill and any time there after when fill is being actively placed, the settlement plates should be read every two to three days. After the fill placement has been completed, the plates may generally be read weekly. When fill is being placed, the amount of fill (lift heights) should be recorded for use in settlement data interpretation.

Any extreme or unusual events should also be recorded, such as rainstorms, local flooding, or seismic activity (either natural or nearby blasting). If the plates are damaged and/or repaired or relocated, this should also be noted. It is preferred that the same surveyors read the settlement plates over the course of the monitoring period to reduce the opportunity for error.

2.5.4. Presentation of result

The recorded data helps to plot the graph of the settlement evolution during time and says if the consolidation is achieved or is still occurring. It enables to observe and determine the magnitude and rate of embankment settlement. Also, the determination of the time at which the necessary consolidation has taken place and the embankment may be released for additional lifts or fill or the next stages of construction can be determine on the basis of the data obtained from the settlement monitoring instrumentation.

Conclusion

The aim of this chapter was the presentation of the methodology that will be used for the comparative analysis to be done. The predicted amount of settlement will be obtained using the Finite Element Software PLAXIS with some materials model. Then, the measured values of settlement will come from the recording of settlement amount using the settlement plates placed in the fields before the construction of the embankment and recorded during a certain period of time. The next chapter will deal with the presentation of the results from the site visit, the data obtained, the numerical method to predict the settlement and he recorded values of settlement. At the end, the comparison between the predicted and measured values will be done and the results will be discussed.

Chapter 3 : RESULTS AND INTERPRETATION

Introduction

The prediction of settlement of an embankment on soft soils is a big challenge in engineering domain and find a way to achieve this will be a considerable progress. This chapter will present the results of the researches carried out during this study starting from the general presentation of the site and the project, a physical description of the site going through the location, climate, topography, geology, hydrology, hydrography, vegetation, the population and the economic activities carried out in the region. A presentation of the necessary data to continue the main goal of this work will be done followed by the showing of the results obtained from the field instrumentation with settlement plates. After this, the next part will be focused on the analysis with the FEM software PLAXIS V20 and finally the results from the field measurements will be compared with those obtained from the simulation.

3.1. General presentation of the site

This presentation will be done according to two aspects: the physical characteristics (geographical location, climate, topography, geology...) and the social and economic characteristics (population, agriculture).

3.1.1. Physical parameters

The physical parameters concern the geographical location of the project and the physical features characterizing the area.

3.1.1.1. Geographical location of the project

The project entitled *"Routes de désenclavement du basin agricole de l'Ouest "* is a social project designed with the objective to build the road to open up the western agricultural basin is to improve the level of road service in this large production basin. Concretely, this road will allow on the economic plan, to favour the exchanges in the West Region but also with the other regions, while facilitating the movement of the products of this region with strong agricultural potentialities. It is situated in the western region of Cameroon precisely in the eastern zone, lot 2 of this road project links over 107 km the towns of Bangangté-Foumbot-Bamendjing-Galim, subdivided into 2 sections as shown in the Figure 3.1 Section 1 extends over a length of 60 km from PK 0 to PK 60 and links the city of Bangangté, capital of Ndé division, and Foumbot city in the Noun division. Bangangté is connected to the capital city of the west region (Bafoussam) by the national road N°4 over about 50km, while the national road N°6 connects Foumbot to Bafoussam over 26.1km. As for section 2, it links over 47 km (from PK 0 to PK 47) the town of Foumbot to the towns of Bamendjing and Galim both located in the Bamboutos division.

Figure 3.1: Presentation of the West region of Cameroon

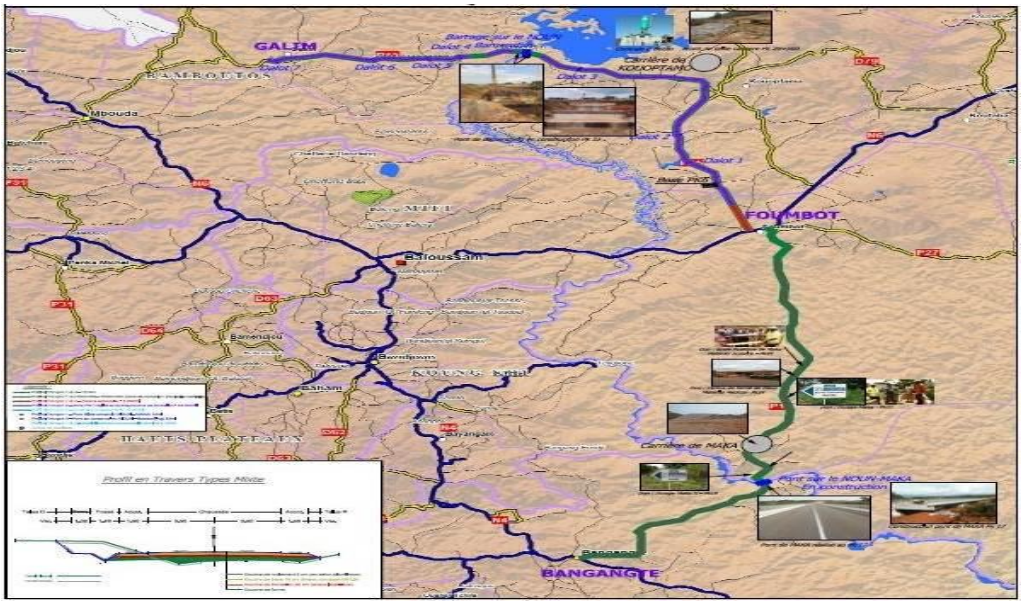

Figure 3.2: Physical location of the Bagangté-Foumbot-Bamendjing-Galim road (Project document)

In terms of geographical coordinates, the project extends in longitude from 10° 24' 00" to 10° 31' 38" East, and in latitude from 5° 41' 59" to 5° 08' 46" North.

3.1.1.2. Climate

The west region climate is in general equatorial of the Cameroon sub variety and has two main seasons: a dry season from October/November to March/April characterized by a strong evapotranspiration and a rainy season covering the rest of the year. Among the towns in the study area, the commune of Foumbot has the highest rainfall value, which varies between 2,500 and 5,000 mm of rain per year (IRAD, 2013). Temperatures oscillate around 21°C with maxima of 32°C and minima of 14°C. As for humidity, the study area has a high average relative humidity of 80% with peaks in August and September. The region is also subject to strong winds that change direction and strength according to the seasons

3.1.1.3. Topography

On the whole, the Western region of Cameroon presents a mountainous relief with altitudes ranging from 500 to more than 2500 m which extend along the Cameroonian fault. The highest peak in the region, standing at 2740 m, is part of the chain of the Bamboutos Mountains which are dormant volcanoes on the western side of the town of Mbouda, 22.4 km from Galim. The territory of the Foumbot municipality is made up in places of isolated mounds and residual hills of very low height, the western hillside of Mount Mbapit (2352m of altitude) is installed in this territory. In general, the hilly areas are excellent places for large livestock while the valleys and abundant plains are used for seasonal crops. The present relief forms are the result of a long and complex volcanic action that occurred in the area.

3.1.1.4. Geology

Most of the soils in the study area are the result of volcanic activity. In the plains of the commune of Foumbot, there are very porous and fertile black amorphous alluvial soils resulting from volcanic projections (pozzolana). These soils have an important agronomic value due to their high nitrogen, phosphorus and potassium content (PNDP, 2014). Due to their overexploitation and the difficulty of managing rain and wind erosion, this soil is becoming increasingly poor. There are also several other types of soil in the region, namely hydromorphic alluvial soils mainly in the lowlands, reddish lateritic soils remarkably present on the slopes of some peaks in the commune of Bangangté and sandy-clay soils in the marshy areas (PNDP, 2015).

3.1 1.5. Hydrology and hydrography

The territory of West Cameroon, due to its mountainous relief and the depth of the valleys, is watered by a dense hydrographic network made up of tortuous rivers with regular and seasonal regimes. These rivers, all part of the Atlantic basin, experience a high-water period during the rainy season and a low water period during the dry season. Among these rivers, the most important in the study area is the Noun River which is fed by smaller rivers such as the Kon, Ngam and Ndé and flowing from the central region around Bafoussam to the Bamendjing reservoir. This artificial lake is created by a dam on the river Noun, which contributes to the regulation of the Sanaga at Edéa in the Littoral region. Most of the lakes in the region are crater lakes formed as a result of the collapse of volcanoes. One example is Lake Baleng, northeast of Bafoussam, and the twin lakes of Foumbot.

3.1.1.6. Vegetation

The vegetation of the communes is characterized by the predominance of mixed woody (tree and shrub) and herbaceous plant formations. The woody cover is clear and dominated by savannahs with a variable local physiognomy. In addition to the so-called natural vegetation zones, the territory of the municipalities is dominated by agricultural zones covered by annual, semi-perennial and perennial crops.

3.1.2. Socioeconomic parameters

Socioeconomic characteristics are demography and economic activities.

3.1.2.1. Population

According to the last census of the population of Cameroon in 2005, the western region had about 1 720 047 inhabitants, making with respect to its surface area, one of the most densely populated regions with 124 inhabitants/km². As far as the Foumbot commune is concerned, its population is estimated at about 76 486 inhabitants with 38 891 women and 37 595 men. With a growth rate of 2.6%, this would give a population of 90 406 in 2012 PNDP, 2014). This population is essentially made up of Bamilékés, Bamouns, Banso'o and Mbororos who have migrated from the north in search of pasture for their cattle and have settled there permanently.

3.1.2 .2. Economic activities

a) Agriculture

Agriculture occupies an important place in the economic activity of the West Cameroon region in general and the commune of Foumbot in particular. This is due to the richness of the soil in nutrients and fertilizers. Thus, was encountered annual cultures dominated by maize, okra, watermelon, tomatoes; semi-perennial cultures such as plantains and perennial cultures such as coffee trees which are quite widespread in the commune.

b) Mining and quarrying

There are no real mining industries in the commune of Foumbot industries. It can be noted in this city the presence of a few unorganized operators of pozzolan or sand quarries. The exploitation of these quarries and the removal along the roadsides constitute an economic activity because of the financial income they provide to the populations who work in them, as well as the exploitation fees collected by the Council from operators in certain villages in the communes. Also, it provides building material for housing and public works. Given the rocky outcrops encountered in the municipalities, it can be noted with certainty that the potential of the stone quarries in the communes is still under-exploited. The same is true of the laterite deposits. This is an obstacle to the economic development of the area in view of the mass of jobs and income that their operations would provide for both the local population and the communal institution.

3.2. Physical description of the site

The first day of the visit was spent at the geotechnical laboratory where one were able to attend and participate in the development of some geotechnical tests, in particular: particle size analysis, determination of Atterberg limits, water content, specific weight, CBR and the modified proctor test.

A visit to the project site was carried out on the second day of arrival. Overall, the project is nearing completion but traffic remains low, probably due to work still in progress. The problem of upwelling by capillarity was observed in some areas along the project as at the ok 35. The presence of aggregates quarry exploited for the project was constate.

Figure 3.3: Geotechnical laboratory of the site

Figure 3.4: Quarry from the section 2 (Foumbot - Bamendjing - Galim) of the project PK 21+250 m

Figure 3.5: Area of study (PK 12+650 – PK 12+950)

For the study area was located from PK 12+650 m to PK 12+950 m of the project, where very compressible soils were found. A maximum height of 6 meters of road embankment were constructed in this section. This height of the embankment is chosen in such a way to respect the red line of the project with the initial level of the natural soil. So, the total settlement that will appear after the consolidation should be compensated by the embankment fill until the red line before the construction of the pavement.

3.3. Data presentation

They are the geometric and geotechnical parameters necessary to solve the problem raised by this study.

3.3.1. Geometrical data

The geometric data of the project concerns the longitudinal and transversal profiles of the study area.

The Figure 3.6 presents the layout involved by this work from PK 12+650 m to PK 12+950 m. The pavement has a width of seven meters and a thickness of forty centimetres.

The PK 12+900 is the chosen profile for this study because it presents a high road embankment of 6m and compressible soil with worse geotechnical properties. The Figure 3.7 presents the transversal profile of the embankment at this section. The embankment has a trapezoidal section with a maximum width at the base of 34 m and a top of 10 m. It rests on a soft soil of thickness of about 12 m.

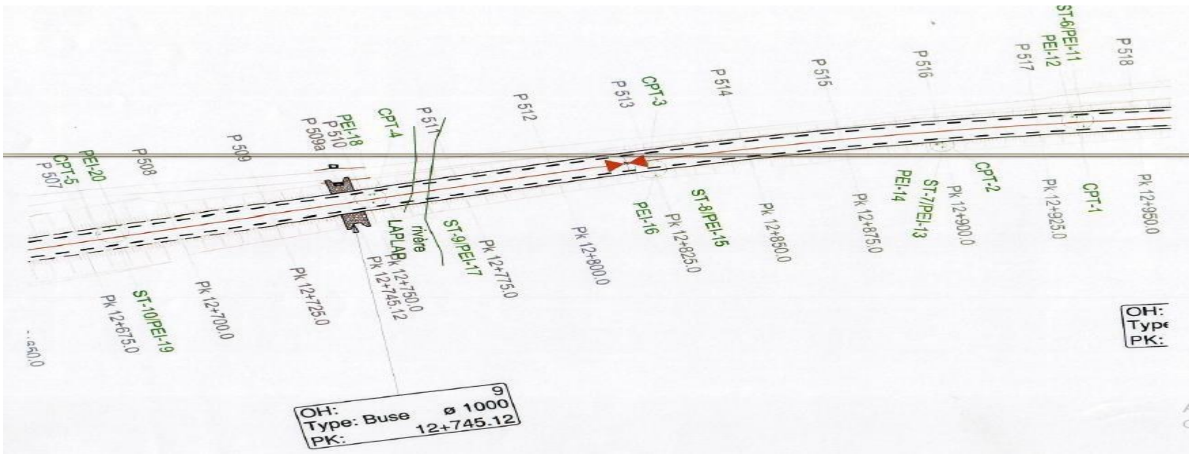

Figure 3.6: Plan view of the study area (Project document)

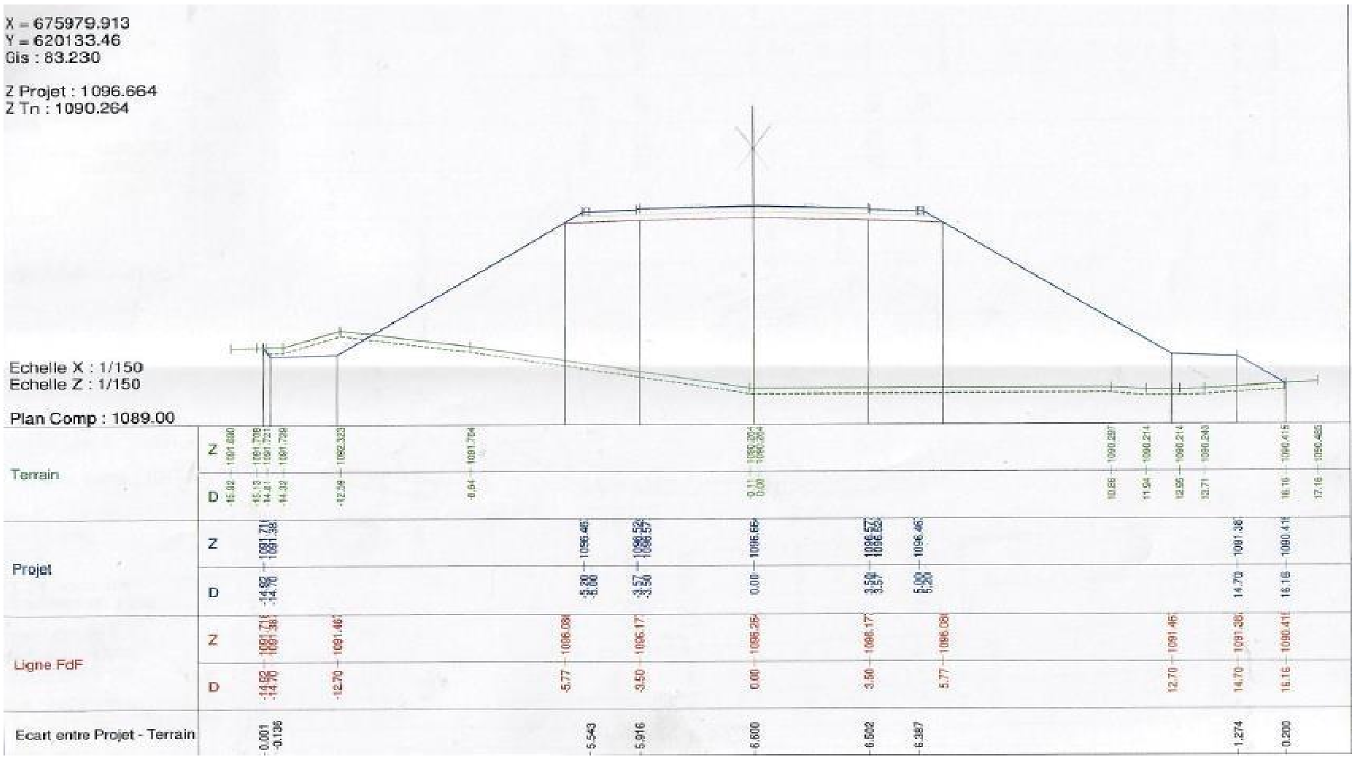

Figure 3.7: Typical transverse profile at PK 12+650 (Project documents)

3.3.2. Geotechnical data

As said before, the chosen profile chosen to do the comparative analysis is the PK 12+900 m because of its worse compressible properties. To predict the amount of settlement that will occur at this section, it is necessary to have the geotechnical data of the constituent's materials of the soft soil. In situ tests like the Cone Penetrometer Test (CPT) was used to define the soil stratigraphy and resistance while laboratory tests as Direct shear test, compressibility test, Atterberg limits tests, Oedometer test and Permeability tests where used to complete the identification of the soil and to obtain the geotechnical parameters.

3.3.2.1. Foundation soil geotechnical data

The base foundation of the embankment is composed of five soft soils: Darkish clay, Yellowish clay, Blackish clay, Blackish sand and Greyish clay.

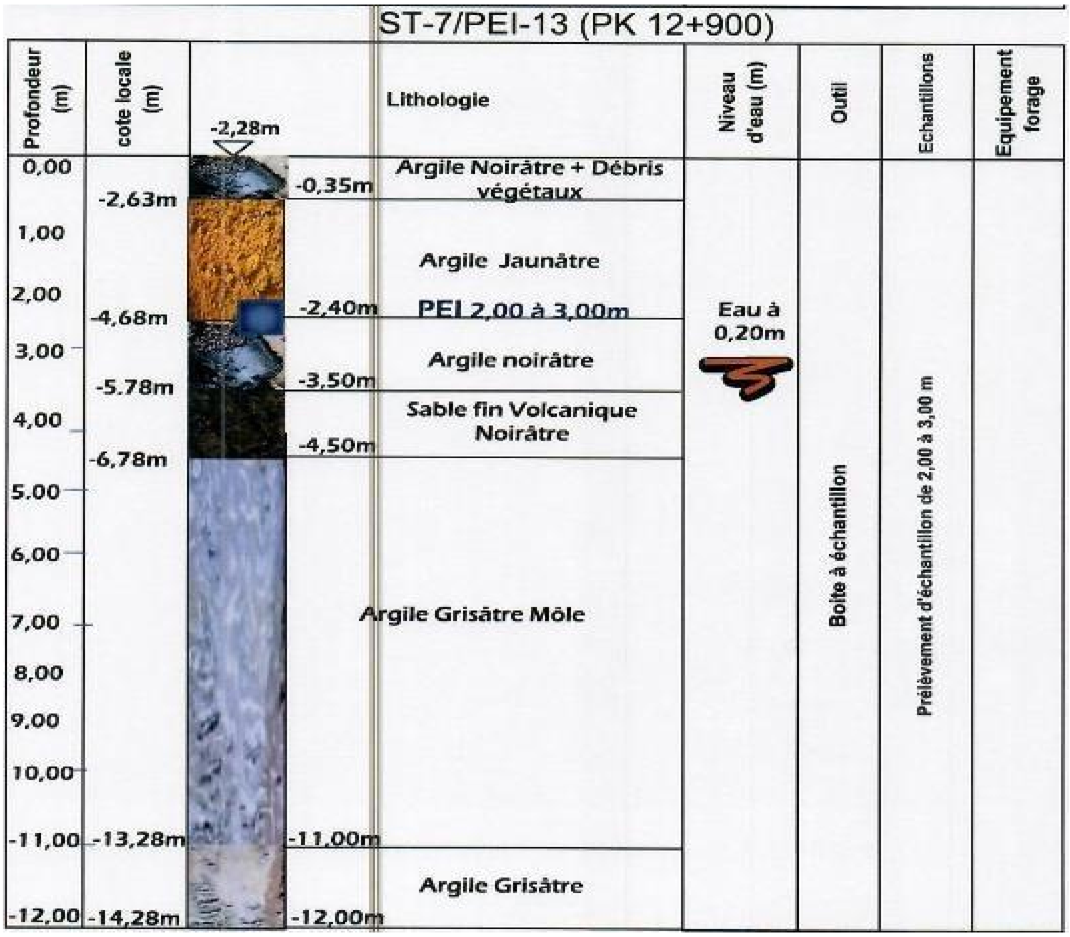

Figure 3.8: CPT test at PK 12+900 m

The results of this CPT test help to establish the stratigraphy of the soil presented in Table 3.1 which present the thickness and depth of each soil layer.

Table 3.1: Soil Stratigraphy (Project Documents)

Soil layers	Depth (m)	Thickness (m)
Darkish clay	0	0.35
Yellowish clay	0.35	2.05
Blackish clay	2.40	1.10
Blackish sand	3.50	1.00
Greyish clay	4.5	7.50
	Total thickness	12.00

The Table 3.2 below presents the geotechnical parameters of each layer of the foundation soil.

Table 3.2: Foundation soil parameters (Project Documents)

Soil layers	Darkish clay	Yellowish clay	Blackish clay	Blackish sand	Greyish clay
γ_{sat} (kN/m^3)	15.25	14.77	16.25	17.27	15.68
γ_{dry} (kN/m^3)	10.07	8.16	11.07	12.23	9.20
Φ' (°)	14.4	22.8	14.4	24.2	4.01
Ψ (°)	-	-	-	-	-
E (kPa)	3491.4	4234.3	3491.4	4531.4	2822.9
ν	-	-	-	-	-
c_u (kPa)	19	19.8	19	33.1	25.3
σ_p (kPa)	39.821	29.7	39.821	59.32	21.95
e_0	1.376	1.236	1.376	0.954	1.741
C_c	0.28896	0.22091	0.28896	0.19752	0.39393
C_r or C_s	0.1201	0.0906	0.1201	0.0639	0.23184
C_α	0.008669	0.00663	0.008669	0.00593	0.011812
K_h (m/day)	0.001	0.01	0.002	0.002	0.002
K_v (m/day)	0.001	0.01	0.002	0.002	0.002
E_{oed} (kPa)	4700	5700	4700	6100	3800
C_v (m^2/s)	0.014	0.036	0.014	0.029	0.009
K_0	-	-	-	-	-

3.3.2.2. Embankment soil geotechnical data

The geotechnical data of the fill materials used for the embankment are presented in the next table:

Table 3.3: Foundation soil parameters (Project Documents)

Soil layers	Pozzolana soil (Fill embankment)	Reddish clay (Fill embankment)
H (m)	1.5	4.5
γ_{sat} (kN/m^3)	14.10	18.61
γ_{dry} (kN/m^3)	13.01	16.68
Φ' (°)	38	30
Ψ (°)	0	0
E (kPa)	10 E+3	10.5 E+4
ν	0.3	0.3
c_u (kPa)	0.5	10
e_0	-	-
K_h (m/day)	10	0.001
K_v (m/day)	10	0.001
K_0	-	-

3.3.3. Settlement plates parameters

The settlement plates are instruments used to follow the evolution of the settlement.

3.3.3.1. Embankment construction

The embankment was modelled using staged construction in three stages based on the number of stages executed by the enterprise on site to have a good basis for comparison of results:

- Phase 1: The first layer of 1.5 m constituted essentially by pozzolana was constructed in 07 days, and then was allowed to consolidate for 60 days;

- Phase 2: The second layer of 3 m constituted by reddish clay was constructed in 21 days and was allowed to consolidate for 60 days;

- Phase 3: Finally, the last layer of 1.5 m constituted also by reddish clay was built in 14 days and the consolidation end time was assessed until the minimum pore pressure of 1 kPa.

The settlement plates were implanted during the first phase of construction, on the pozzolana layer as it can be seen on figure 3.9.

Figure 3.9: Field instrumentation with settlement plates on the pozzolana layer

3.3.3.2. Location of the settlement masse

The plates were placed along the axis of the road every 25m and alternatively on both side (left and rigth) of the road as shown in figure 3.10 and in Table 3.4.

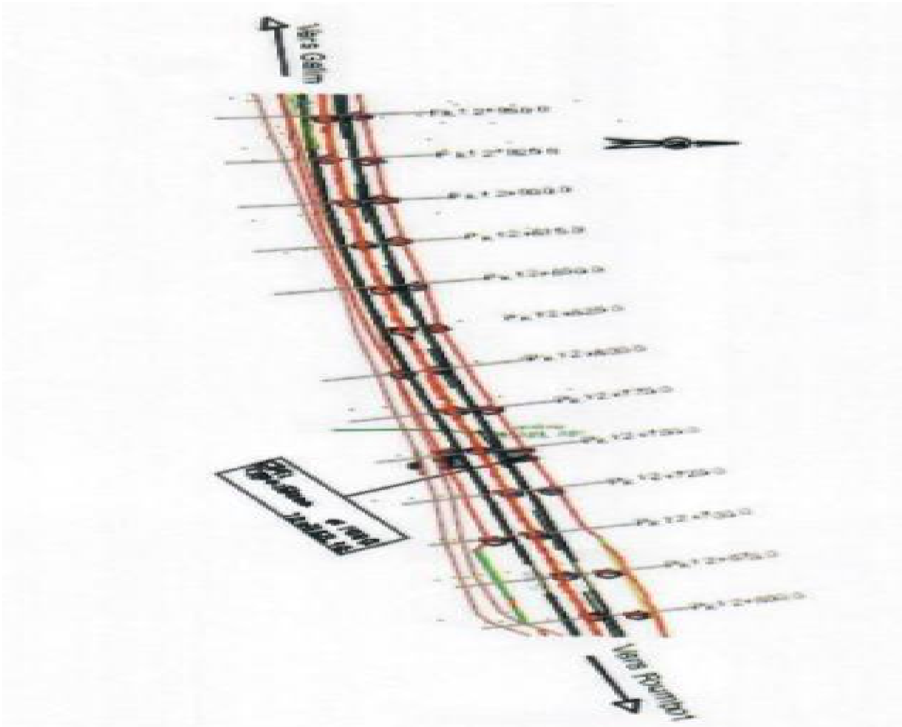

Figure 3.10: Site plan of the settlement plates (Project document)

Table 3.4: Location of the installed plates (Project document)

N° masse	Profile	Side
Masse 1	PK 12+650	X (axe)
Masse 2	PK 12+650	Right (R)
Masse 3	PK 12+675	X (axe)
Masse 4	PK 12+675	R
Masse 5	PK 12+700	X (axe)
Masse 6	PK 12+700	Left (L)
Masse 7	PK 12+725	X (axe)
Masse 8	PK 12+725	R
Masse 9	PK 12+750	X (axe)
Masse 10	PK 12+750	L
Masse 11	PK 12+775	X (axe)
Masse 12	PK 12+775	R
Masse 13	PK 12+800	X (axe)
Masse 14	PK 12+800	L
Masse 15	PK 12+825	X (axe)
Masse 16	PK 12+825	R
Masse 17	PK 12+850	X (axe)

Masse 18	PK 12+850	L
Masse 19	PK 12+875	X (axe)
Masse 20	PK 12+875	R
Masse 21	PK 12+900	X (axe)
Masse 22	PK 12+900	L
Masse 23	PK 12+925	X (axe)
Masse 24	PK 12+925	R
Masse 25	PK 12+950	X (axe)

3.3.3.3. Principle

The preparatory work consisted of assembling the elements of the settlement plates and preparing the bottom of the excavation for the placement of the plates at zone of the study area concerned.

The plates used were made of metal plates (1000 mm x 1000 mm x 1.5 mm), a rod HA25, of 1000 mm length, with a protection tube of diameter 32 mm and 1000 mm long. The rod and the protection tube were welded perpendicular to the metal plate according to the scheme below:

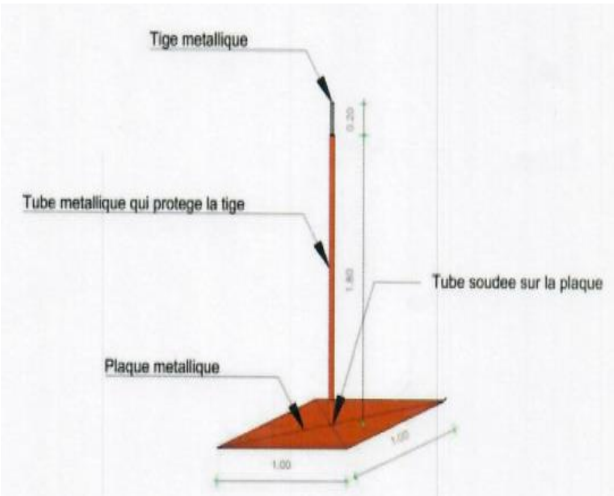

Figure 3.11: Principle of setting up a settlement plate

The flatness of the platform was checked by the topographic team. After laying the plates, a topographic survey of the end of the rod was carried out for each plate. The latter made it possible to have initial level of each settlement plate.

3.3.3.4. Follow-up of the settlement plates

According to the well-defined topographical references, a survey of the rod was carried out by the team of topographers in order to assess the settlement and carry out a follow-up of consolidation of the soil. The rods were lengthened during the rise in embankment when the level of the embankment reached the height of the rod concerned.

During the embankment ascent which was done in several sequences, a survey of the top of the rod was carried out as follows:

- Rod head readings were taken at regular time intervals and on date;
- Follow-up of measurements during the ascent of the embankment;
- The progress of the embankment works has been rigorously monitored and achieved in order to validate the start of the works for the implementation of the pavement layers and to ensure the good progress of the consolidation in the end;
- The plates were implanted on the axis of the roadway as well as on the left and right sides of the profiles. Also, for continuous monitoring, the head of the plates were protected by metal tubes 1000 mm long and 32 mm in diameter. The tube was covered by a flap which served as access for taking measurements on the head of the plates.

3.4. Results from the settlement plates records

In the case of this study, the work will be done with the results from masses 21 and 22 because they are the ones located on the chosen profile.

3.4.1. Topographic data of the PK 12+900 m

Topographic surveying was done weekly from the 11 September 2020 to the 27 march 2021 in the zone between the PK 12+650 to PK 12+950 of the section Foumbot-Galim. The profile of interest is the PK 12+900 where masse 21 and 22 were located. The obtained topographic data are shown below.

3.4.1.1. Masse 21 (PK 12+900 – X)

The follow-up of the masse 21 located on the axis of the PK 12+900 gave the results in Table 3.5:

Table 3.5: Settlement records of masse 21 (Project document)

Ref	Dates	Height of rod records (m)	Cumulated settlement (cm)
1	11/09/2020	1091,175	0
2	30/09/2020	1091,141	3,4
3	03/10/2020	1091,139	3,6
4	22/10/2020	1091,13	4,5
5	05/11/2020	1091,108	6,7
6	30/11/2020	1090,992	18,3
7	05/12/2020	1090,978	19,7
8	22/12/2020	1090,957	21,8
9	04/01/2021	1090,941	23,4
10	18/01/2021	1090,884	29,1
11	01/02/2021	1090,875	30
12	26/02/2021	1090,848	32,7
13	02/03/2021		
14	27/03/2021		

3.4.1.2. Masse 22 (PK 12+900 – L)

The follow-up of the of the masse 22 located on the left side of the PK 12+900 gave the results in Table 3.6.

Table 3.6: Settlement records of masse 22 (Project document)

Ref	Dates	height of rod records (m)	cumulated settlement(cm)
1	11/09/2020	1090,988	0
2	30/09/2020	1090,955	3,3
3	03/10/2020	1090,955	3,3
4	22/10/2020	1090,944	4,4
5	05/11/2020	1090,915	7,3
6	30/11/2020	1090,816	17,2
7	05/12/2020	1090,802	18,6
8	22/12/2020	1090,78	20,8
9	04/01/2021	1090,769	21,9
10	18/01/2021	1090,719	26,9
11	01/02/2021	1090,716	27,2
12	26/02/2021		

13	02/03/2021		Consolidation achieved
14	27/03/2021		

3.4.1.3. Settlement curves

The curves of Figure 3.12 permit to appreciate the evolution of the settlements of the masses 21 and 22 at PK 12+900.

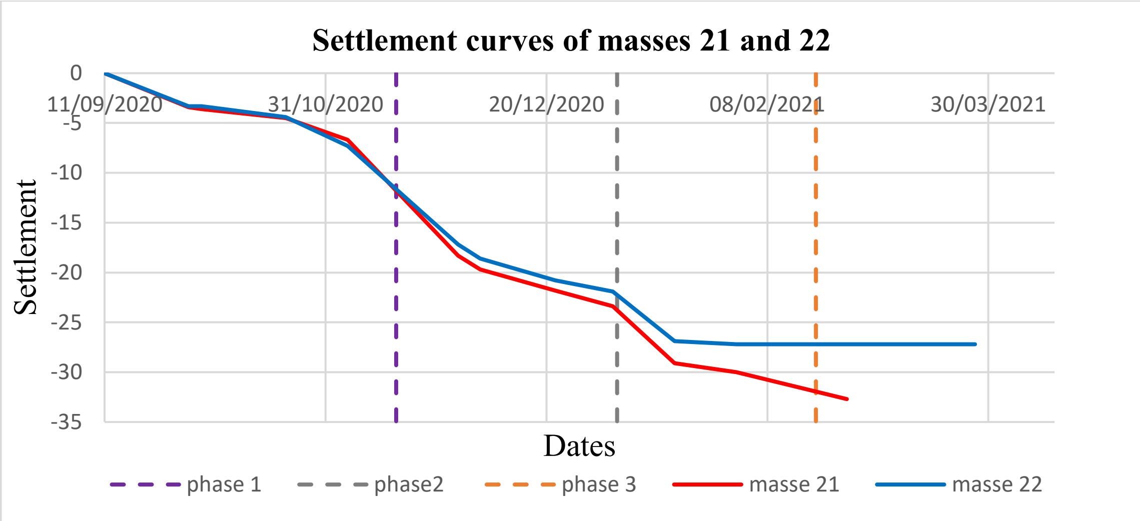

Figure 3.12: Settlement curves of masse 21 and 22 (phase 1, phase 2 and phase 3 being each stage of construction)

Phases 1, 2 and 3 represent the steps of construction.

3.4.2. Other data obtained

From the results obtained after the instrumentation of the embankment with the settlement plates, the following data have been also be obtained.

Table 3.7: Other data obtained from the embankment instrumentation with settlement plates (Project document)

N° of masse	**Masse 21 (PK 12+ 900-X)**	**Masse 22 (PK 12+ 900-G)**
Average settlement value (cm)	16.10	13.72
Penultimate settlement value (cm)	30.00	26.90

Last recorded settlement value (cm)	2.70	0.30
Cumulative total settlement (cm)	32.70	27.20
Monthly settlement rate (cm/month)	0.42	0.05
Monthly tolerated speed limit (cm/month)	0.08	0.08
Prescribed consolidation time (month)	6.5	6.5
Conclusion	Settlement in progress	Consolidation achieved

3.5. PLAXIS simulation results

As mentioned in chapter 1, one way to predict the amount of settlement of an embankment on soft soil is to do a numerical simulation. The numerical simulation consists in doing the simulation of the geometry behaviour using the FEM software PLAXIS through a good choice of input, calculation data and a good analysis of the output information and curves.

3.5.1. Modelling procedure

For the numerical simulation of the initial conditions by PLAXIS, the work in the input program have consisted to draw the stratigraphy of the foundation soil and the embankment using the data from the project documents.

After the drawing of the model, the materials setting was done for each layer of the foundation soil and the embankment, the material model adopted for each layer of the foundation soil (darkish clay, yellowish clay, blackish clay, blackish sand, greyish clay) was the Soft Soil model, the Soft Soil Creep model and Hardening Soil model successively with an undrained behaviour. The SSC and HS models were chosen since they are considered to be, in engineering practice, suitable models for predicting settlement in soft soils. By using the SSC and HS it was possible to compare predictions with and without creep. Drained condition was adopted for the reddish clay (fill embankment) and the Pozzolana soil (fill embankment) with the Mohr-Coulomb behaviour. This was accomplished on the total length of the model despite of the symmetry formation of it.

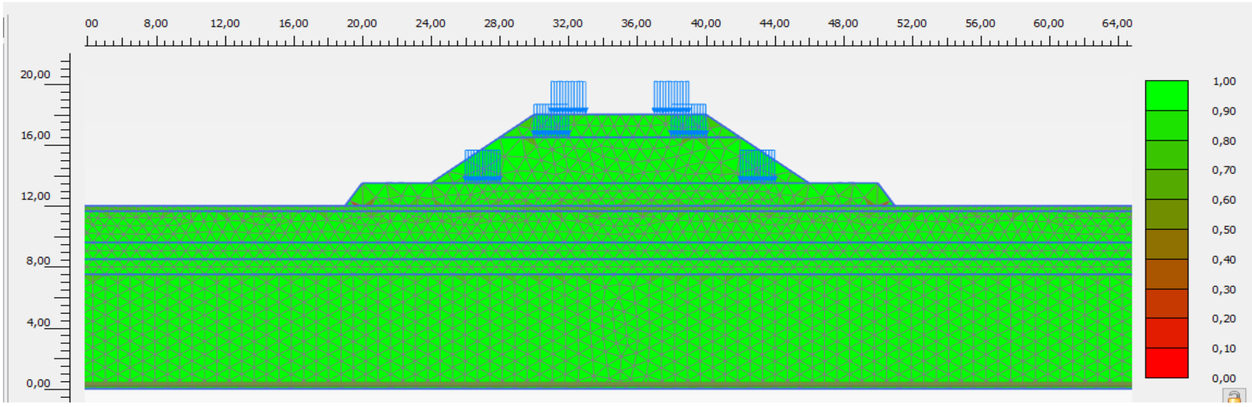

Figure 3.13: Meshing system of the embankment (PLAXIS V20)

Then, the loads of construction engines have been added in order to be in the real conditions of work. The embankment was loaded with a 120 kPa load over a width of 2 m corresponding to the compaction engine loads and its width respectively. This load was replaced by 10 kPa during the interstage consolidation periods (this load stands for the load applied by the vehicles on the embankment during the interstage consolidation period). This load was applied on both senses of the road with the position chosen for the case of maximum deformations. The water table was the defined at 0.2m under the embankment base as given by the geotechnical reports. The plain strain consideration has been selected for the simulation. The finite element mesh was generated automatically with 15-nodes elements as shown in Figure 3.14. In order to do a good analysis, some particular points were chosen, to allow the evaluation of the displacements throughout the construction.

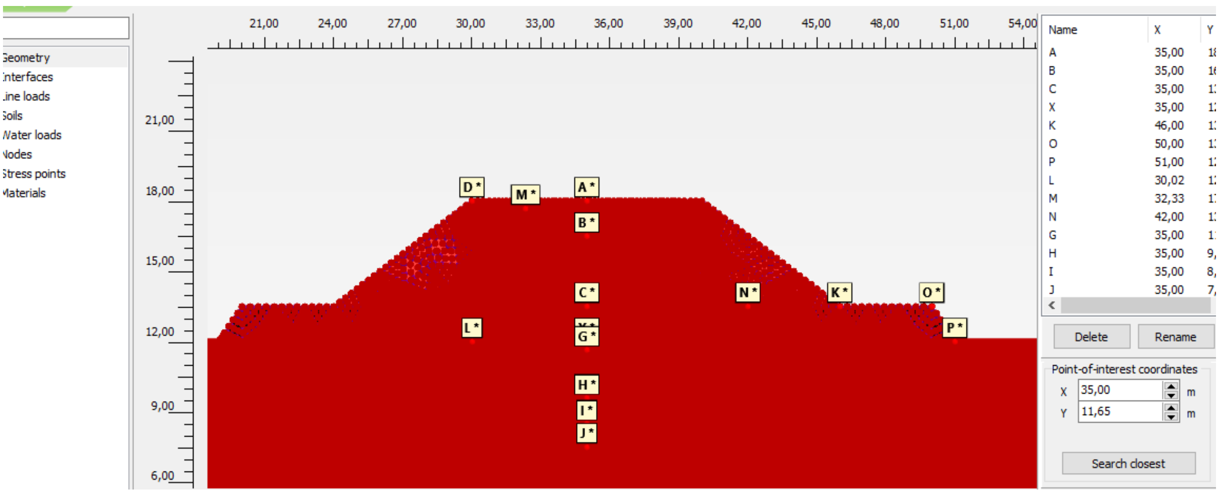

Figure 3.14: Points location in FEM analysis (PLAXIS V20)

The model of the soil and embankment stratigraphy is presented in Figure 3.15 and the calculation steps of construction embankment are shown in Figure 3.16.

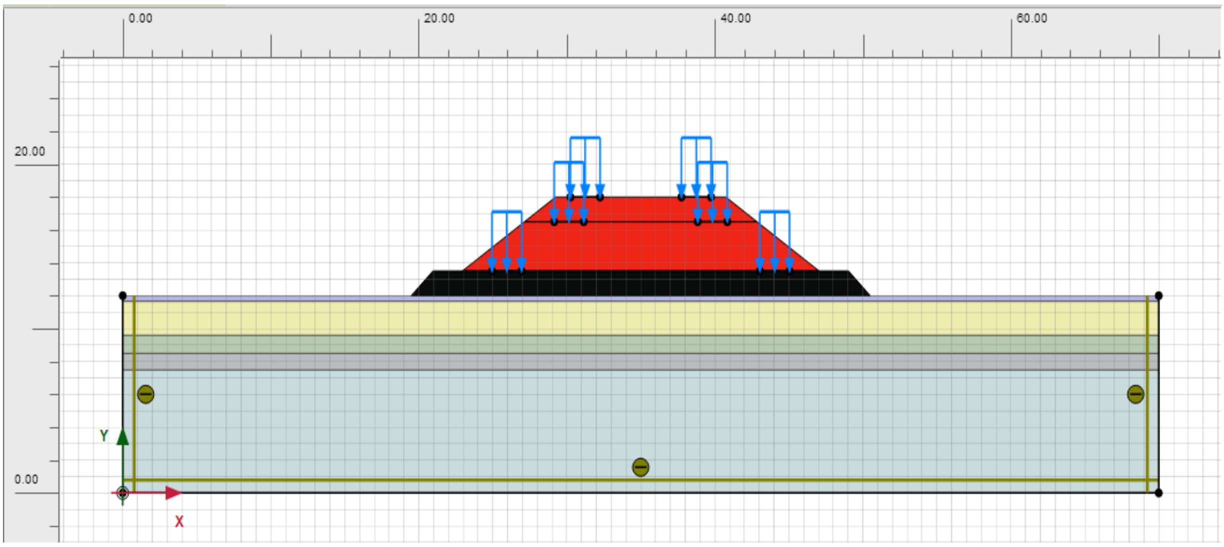

Figure 3.15: Stratigraphy of foundation and embankment soil (PLAXIS V20)

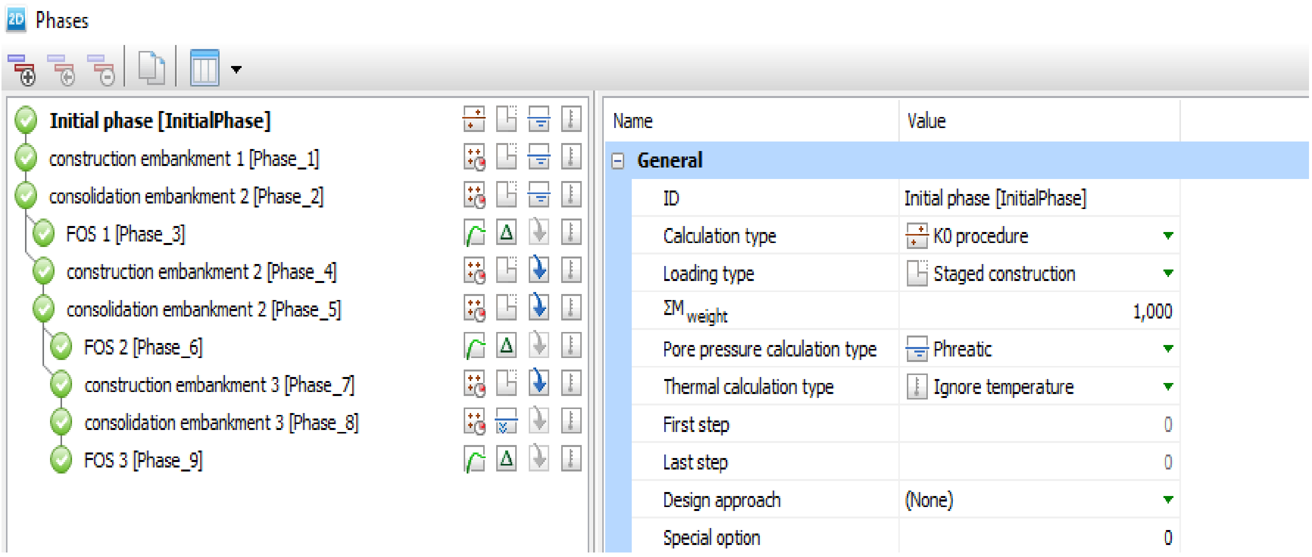

Figure 3.16: Calculation steps of the embankment (PLAXIS V20)

When all this was done, the calculation program was ran followed by the running of the output and curve programs to assess the amount of settlement obtained.

3.5.2. Presentation of the results obtained

PLAXIS estimated many information about the model amongst which the amount of settlements. For this study different material models will be considered to find the best one to predict the settlement that will occur in real life. The Soft Soil Creep and Hardening Soil material models was successively used to characterise each layer of the foundation soil. For each model, the amount of settlement varies as it will be shown in the next lines.

3.5.2.1. Settlement prediction

The prediction was done using different materials models.

a) Soft Soil model

The deformed Mesh obtained at consolidation end time using the Soft Soil model is shown in Figure 3.17.

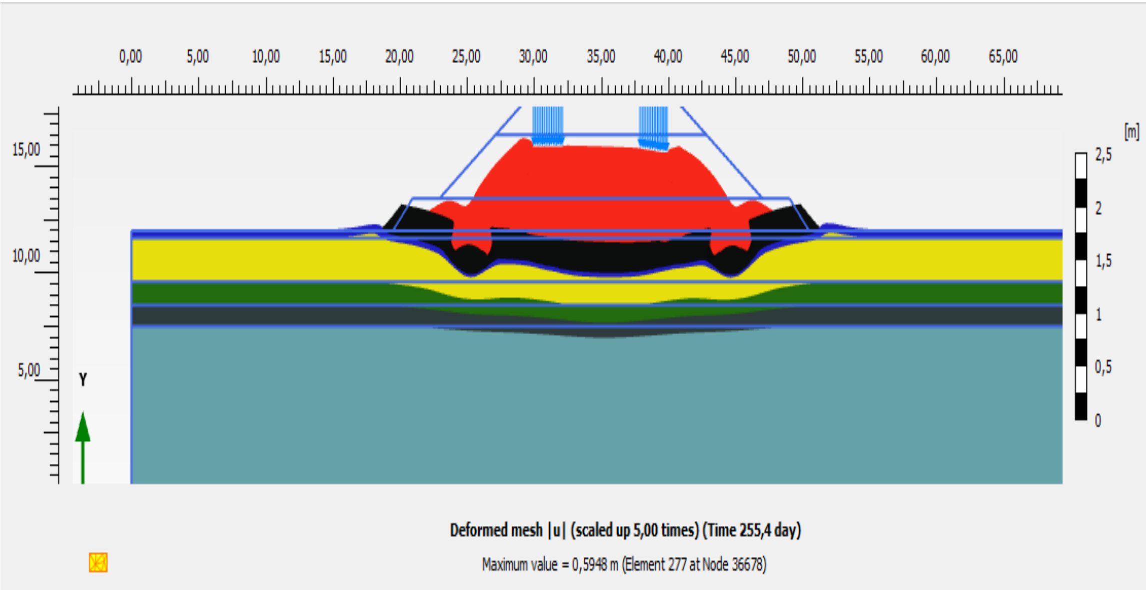

Figure 3.17: Deformed mesh with Soft Soil model (PLAXIS V20)

Figure 3.18 illustrates the distribution of vertical displacement of the embankment predicted using the SS model at the consolidation end time. The vertical displacement of the original ground surface at the consolidation end time was greatest (57.47 cm at point of coordinates (26.95 ; 13.5)) located 8.05 m from the center of the embankment, and was 17.96 cm greater than that below the center. The settlement at the head of the embankment were similar at the center and near the edge of the embankment and rapidly decreased down from almost zero from the edge to the toe.

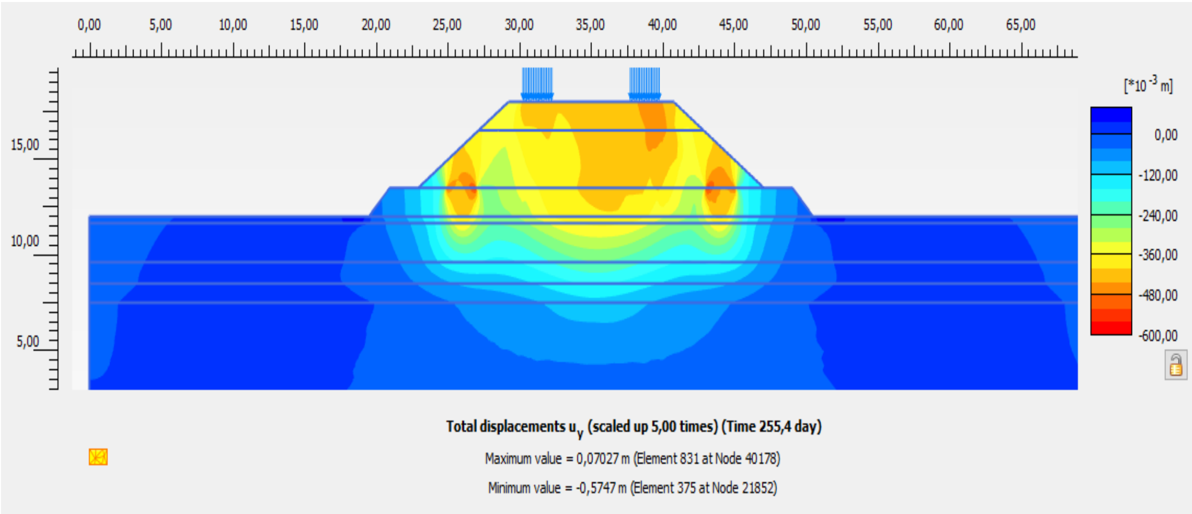

Figure 3.18: Shading of the vertical displacement with Soft soil model (PLAXIS V20)

The curve bellow shows the evolution of the settlement at the two surveyed points. After 168 days (recording time of the settlement plate at the axis n°21), the value of settlement obtained with the simulation is 35.45 cm for the point located on the axis (point X) and 24.47 cm for the point located on the left side (point L). After this 168 days, it can be noted that the settlement is still going on as it can be seen on Figure 3.19.

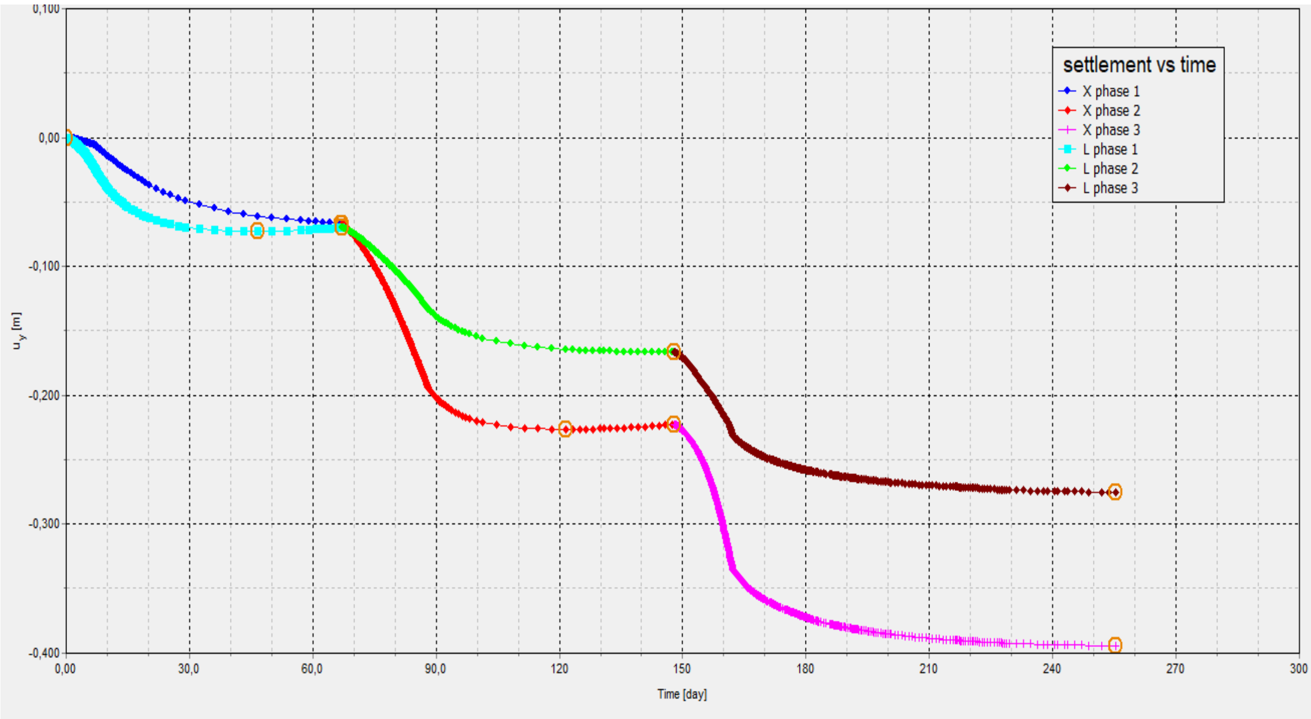

Figure 3.19: Settlement versus time at point X and L with Soft Soil Creep model (PLAXIS V20)

b) Soft Soil Creep model

The deformed mesh obtained at consolidation end time using the Soft Soil Creep model is shown in Figure 3.20.

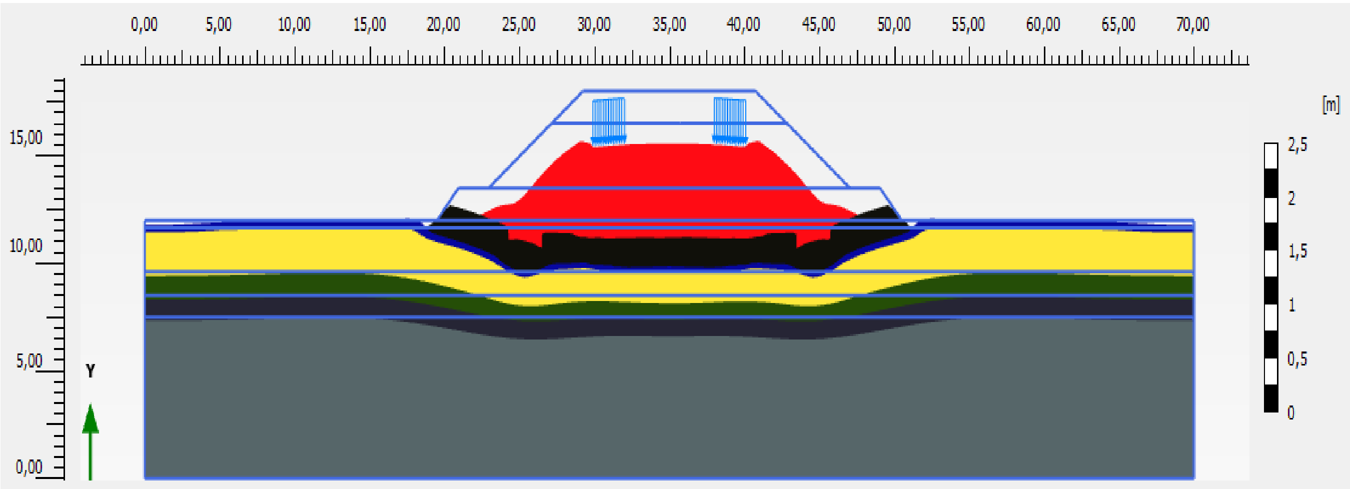

Figure 3.20: Deformed mesh with Soft Soil Creep model

Figure 3.21 illustrates the distribution of vertical displacement of the embankment predicted using the SS model at the consolidation end time. The vertical displacement of the original ground surface at the consolidation end time was greatest (55.76 cm at point of coordinates (43.05 ; 13.5)) located 8.05 m from the center of the embankment, and was 12.9 cm greater than that below the center. The settlement at the head of the embankment were similar at the center and near the edge of the embankment and rapidly decreased down from almost zero from the edge to the toe.

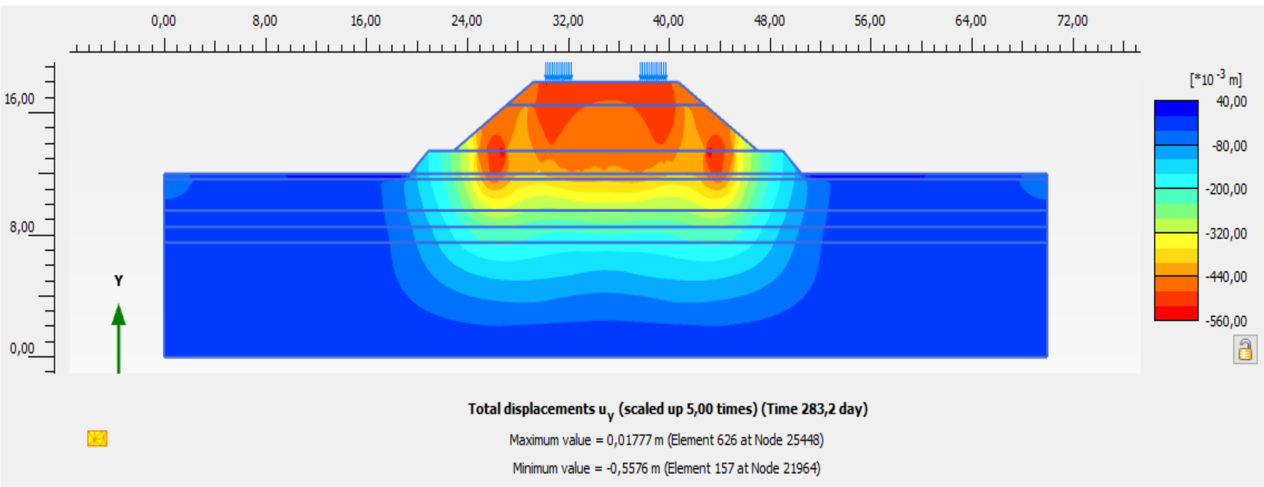

Figure 3.21: Shading of the vertical displacement with Soft soil Creep model (PLAXIS V20)

The curve bellow shows the evolution of the settlement at the two surveyed points. After 168 days (recording time of the settlement plate at the axis n°21), the value of settlement obtained with the simulation is 38.95 cm for the point located on the axis (point X) and 35.22 cm for the point located on the left side (point L). After this 168 days, it can be noted that the settlement is still going on as it can be seen on Figure 3.22.

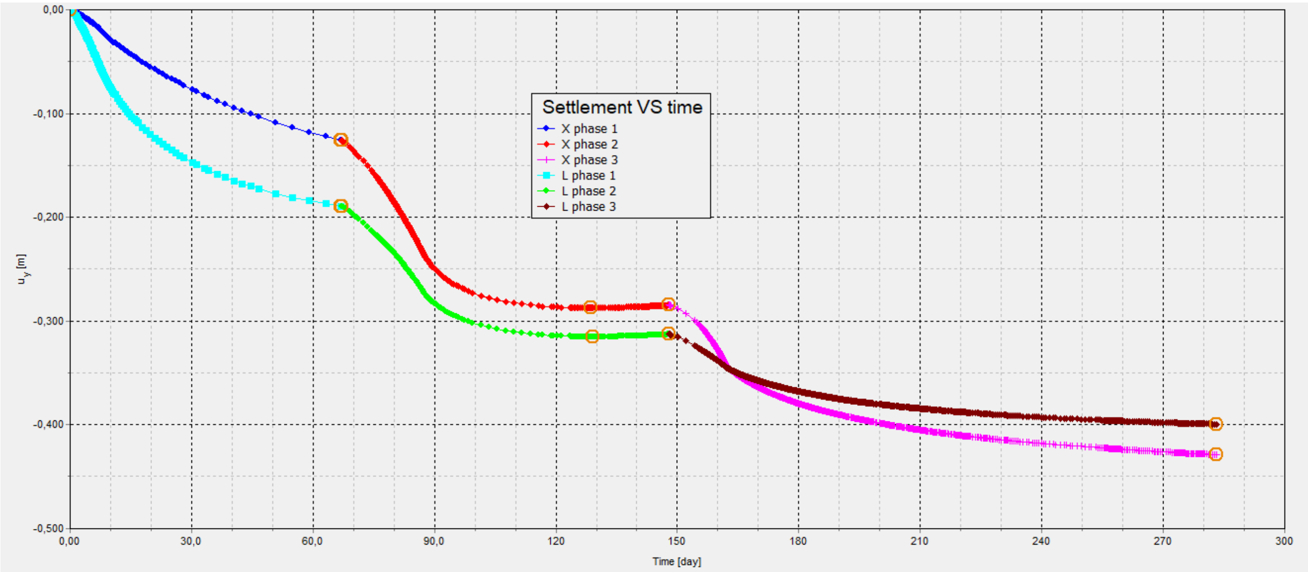

Figure 3.22: Settlement versus time at point X and L with Soft Soil Creep model (PLAXIS)

c) Hardening Soil model

The deformed Mesh obtained at the end of consolidation using the Hardening Soil model is shown in Figure 3.23.

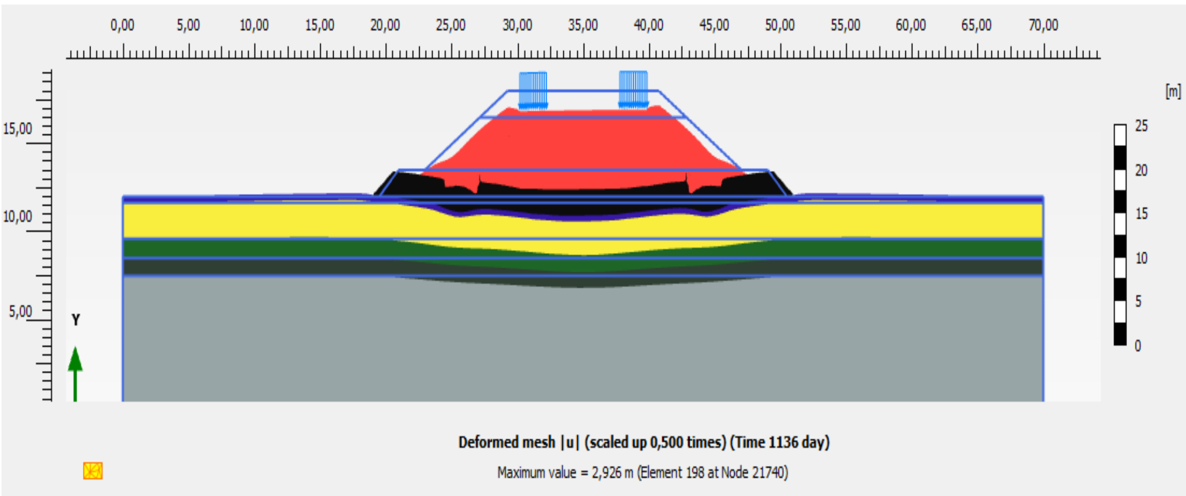

Figure 3.23: Deformed mesh with Hardening Soil model (PLAXIS V20)

Figure 3.24 shows that the same comment as with the SSC model can be made. But it can be noted a faster decrease from the edge to the toe of the embankment of the settlement to almost the zero value and a longer time for the consolidation to end. Also, the maximum value of settlement with the HS model is 2.914 m at the point of coordinates (43.05 ; 13.5) .

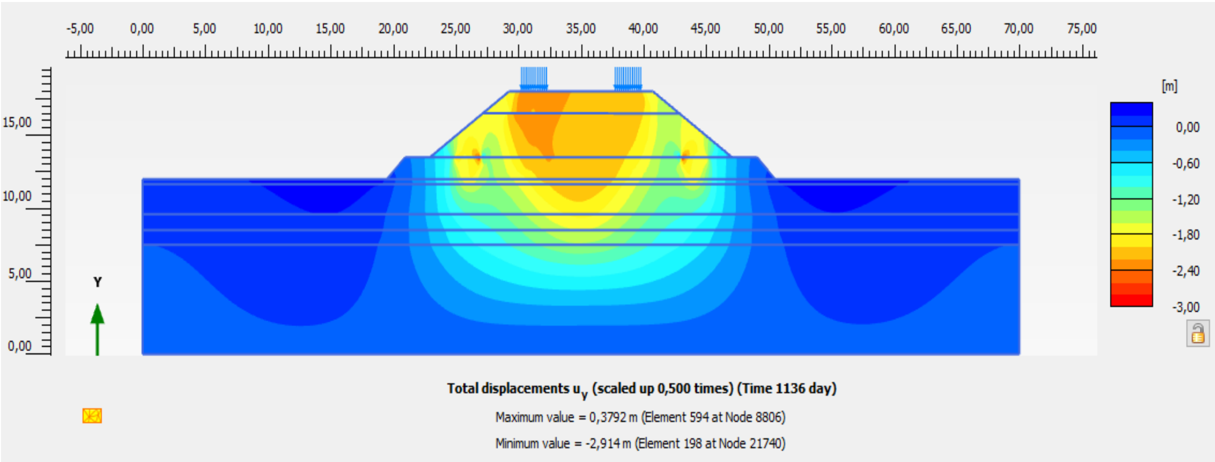

Figure 3.24: Shading of the vertical displacement with Hardening Soil model (PLAXIS V20)

The curve bellow shows the evolution of the settlement at the two surveyed points. After 168 days, the value of settlement obtained with the simulation is 148 cm for the point located on the axis and 98.8 cm for the point on the left side. After these 168 days, it can be noted that the settlement is still going on.

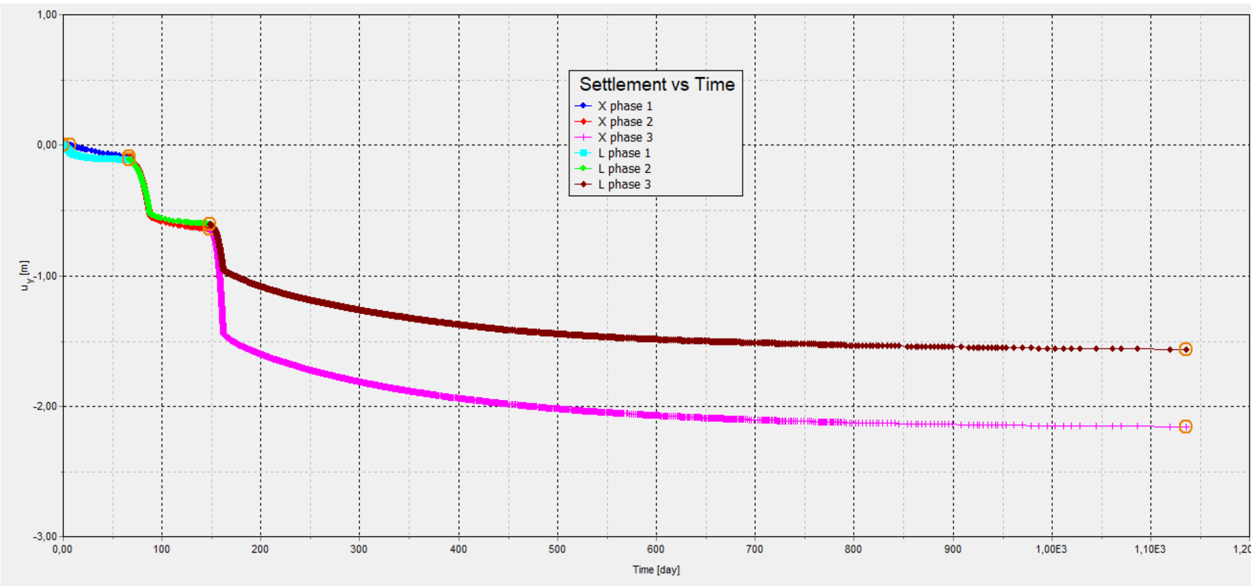

Figure 3.25: Settlement versus time at point X and L with Hardening Soil model (PLAXIS)

3.5.2.2. Predictions of pore pressures

Figures 3.26, 3.28 and 3.30 illustrate the distribution of excess pore pressures at the end of consolidation time, predicted using the SS model, the SSC model and the HS model respectively. The excess pore pressure was highest at the base and below the centre of the embankment, and declined in a horizontal direction.

Figures 3.27, 3.29 and 3.31 show the simulated pore pressure as a function of time at the two studied points X and L obtained using both SS model, SSC model and HS model. The pore pressures increased simultaneously on the loading stages. The pore pressure increased after each loading (phase of construction).

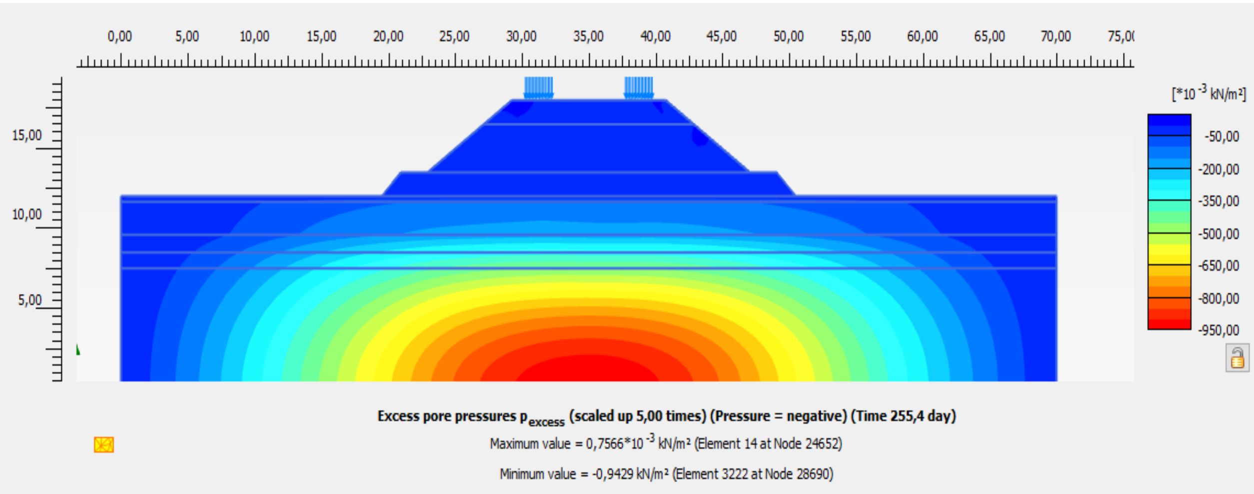

Figure 3.26: Distribution of excess pore pressures at the end of consolidation predicted using the SS model

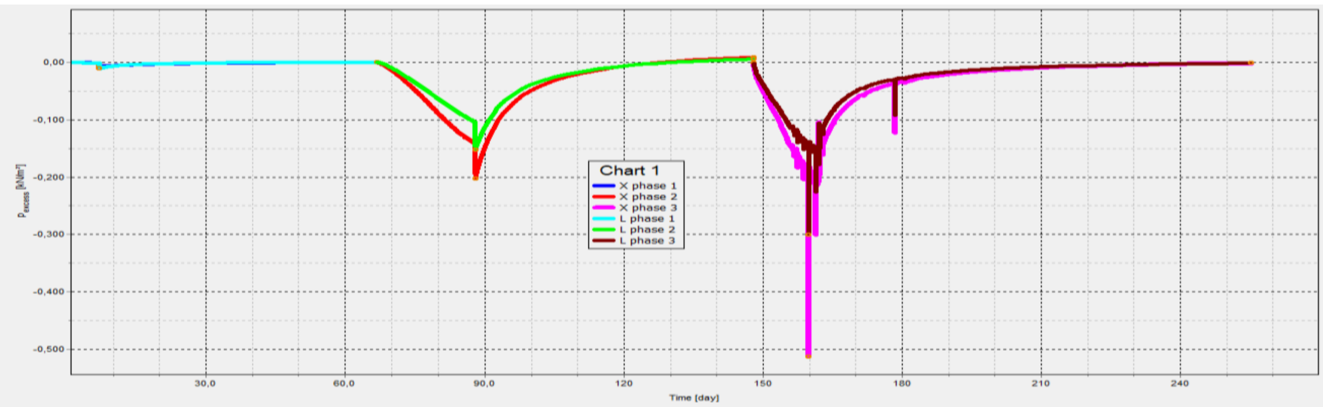

Figure 3.27: Simulated excess pore pressures as a function of time at points X and L using the SS model

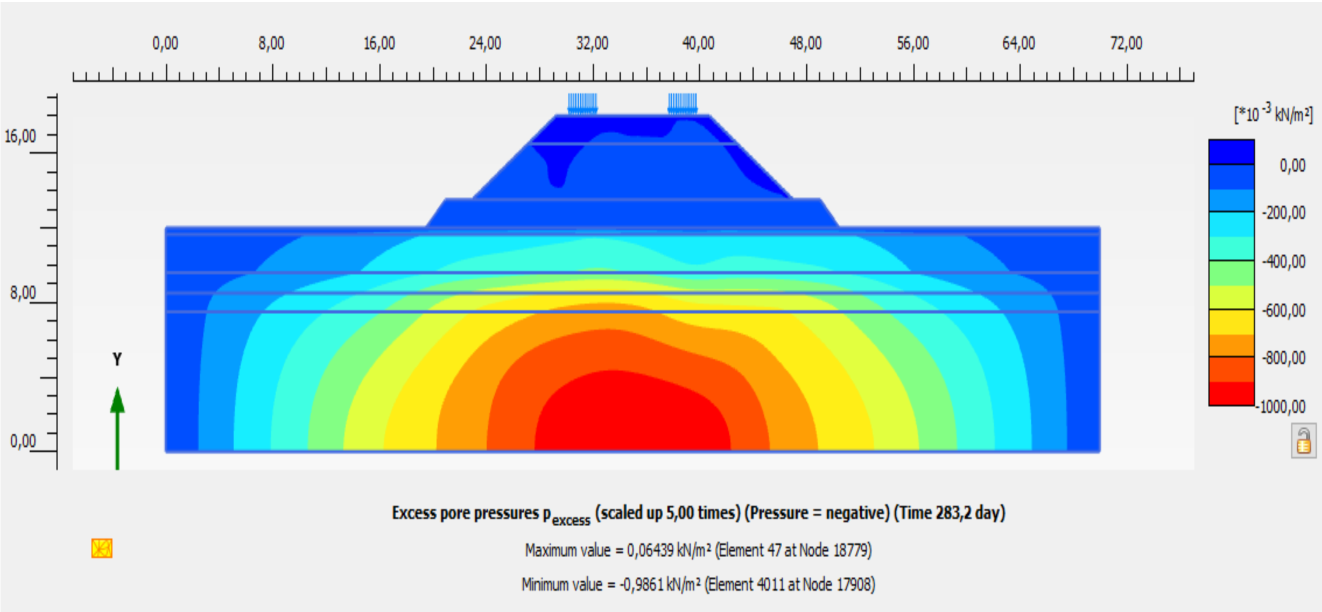

Figure 3.28: Distribution of excess pore pressures at the end of consolidation predicted using the SSC model

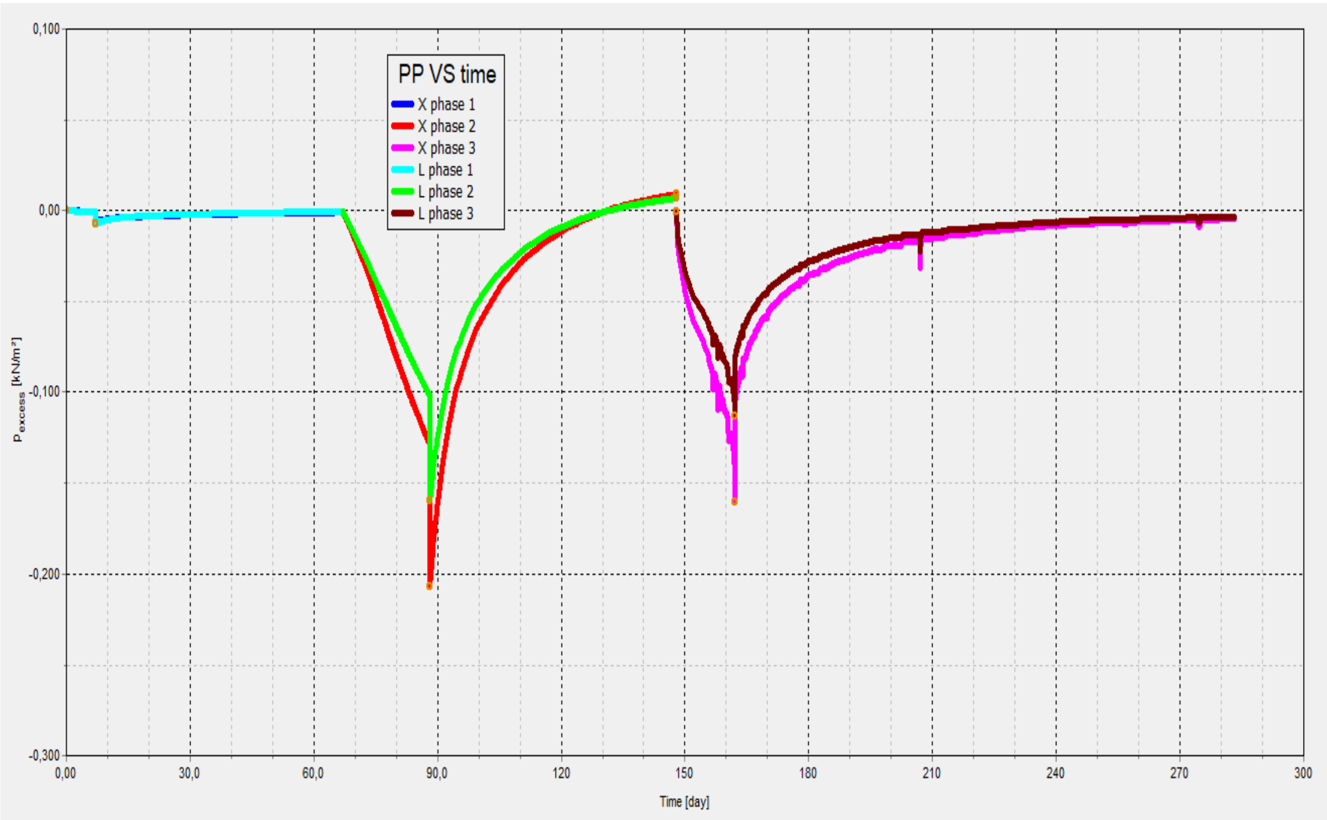

Figure 3.29: Simulated excess pore pressures as a function of time at points X and L using the SS model

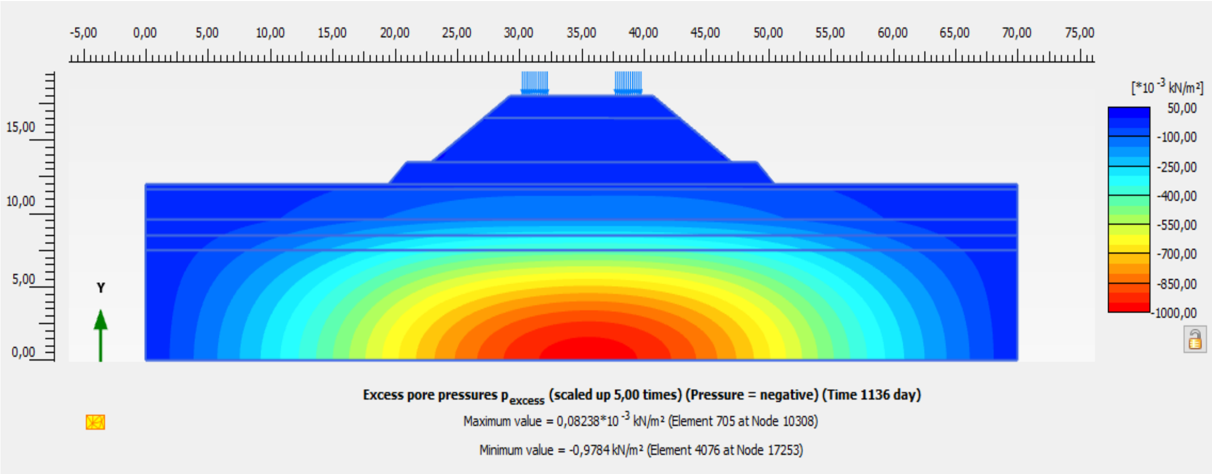

Figure 3.30: Distribution of excess pore pressures at the end of consolidation predicted using the HS model

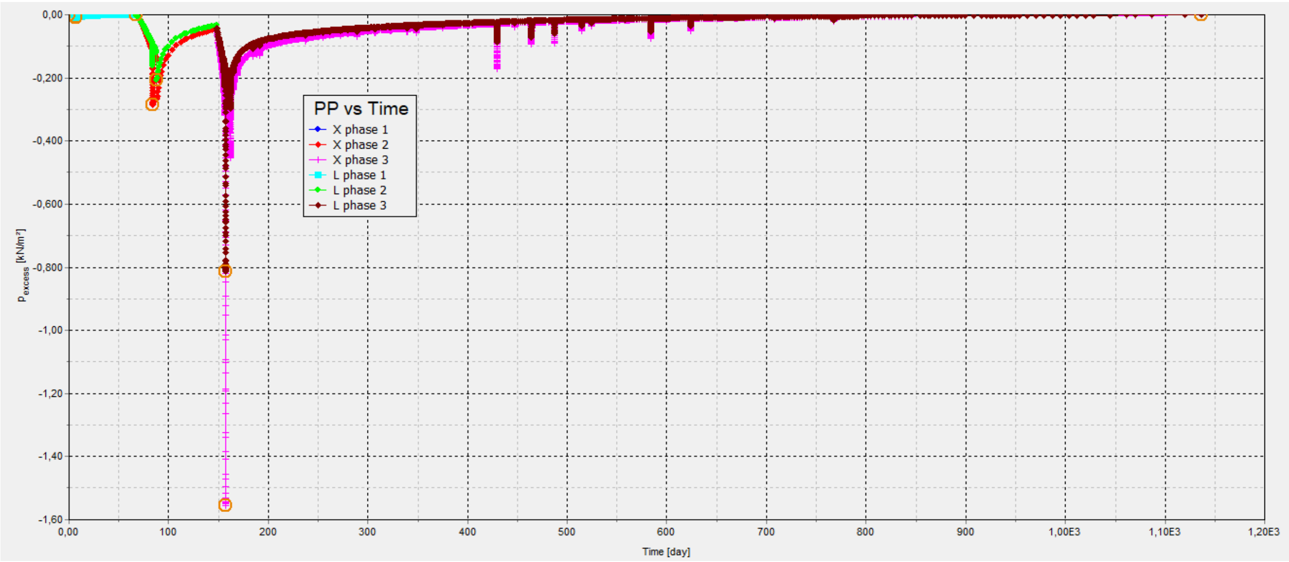

Figure 3.31: Simulated excess pore pressures as a function of time at points X and L using the HS model

3.6. Interpretation of the results obtained

From the results obtained, the following interpretation can be done on the prediction of soil behaviour.

3.6.1. Settlements

In figures 3.32, 3.33, 3.34 and 3.35, the predicted and measured settlement (total settlement) are presented as function of time in the same diagram and as function of logarithm of time in another one at the original ground surface, on the axis and left side respectively. The predicted values are for the SS model, the SSC model and the HS model for plain strain assumption. The total settlements predicted by the SS model are in many points, lower than the ones recorded by the settlement plates.

On the other hand, the total settlement after the 168 days of surveying was predicted by the SSC model 35.45 cm on the axis and 24.47 cm on the left side, values which slightly close than the one recorded on the field.

The HS model on the start gave values very close to the ones recorded on field but just for few days and then overestimate the amount of total settlement the discrepancies been 115.3 cm on the axis and 71.6 cm on the left side after 168 days.

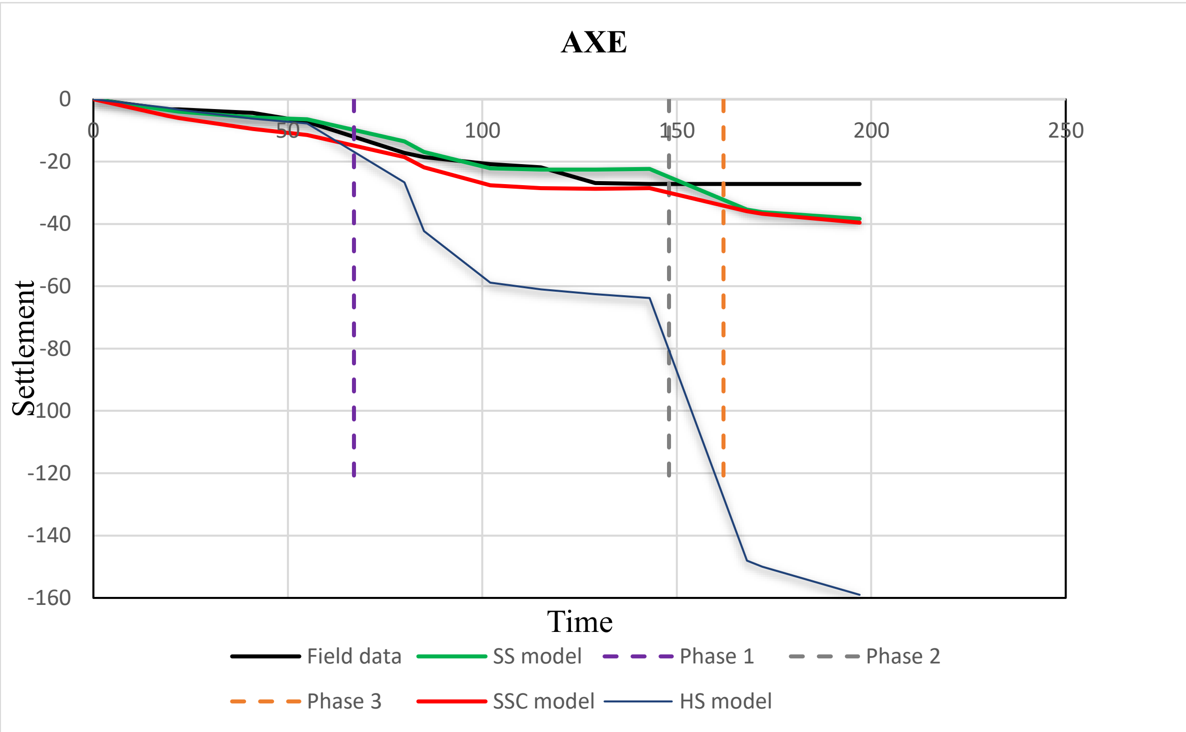

Figure 3.32: Measured and predicted settlements on the axis of the embankment with different models

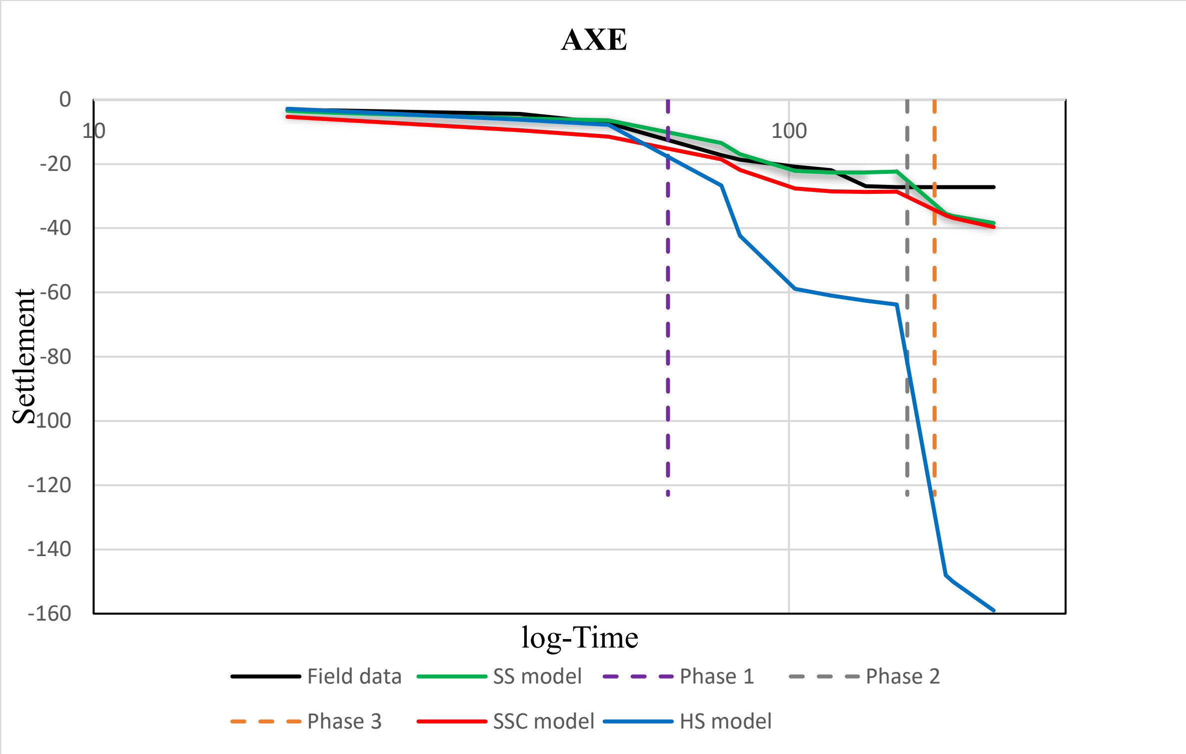

Figure 3.33: Measured and predicted settlements on the axis of the embankment with different models with logarithmic scale

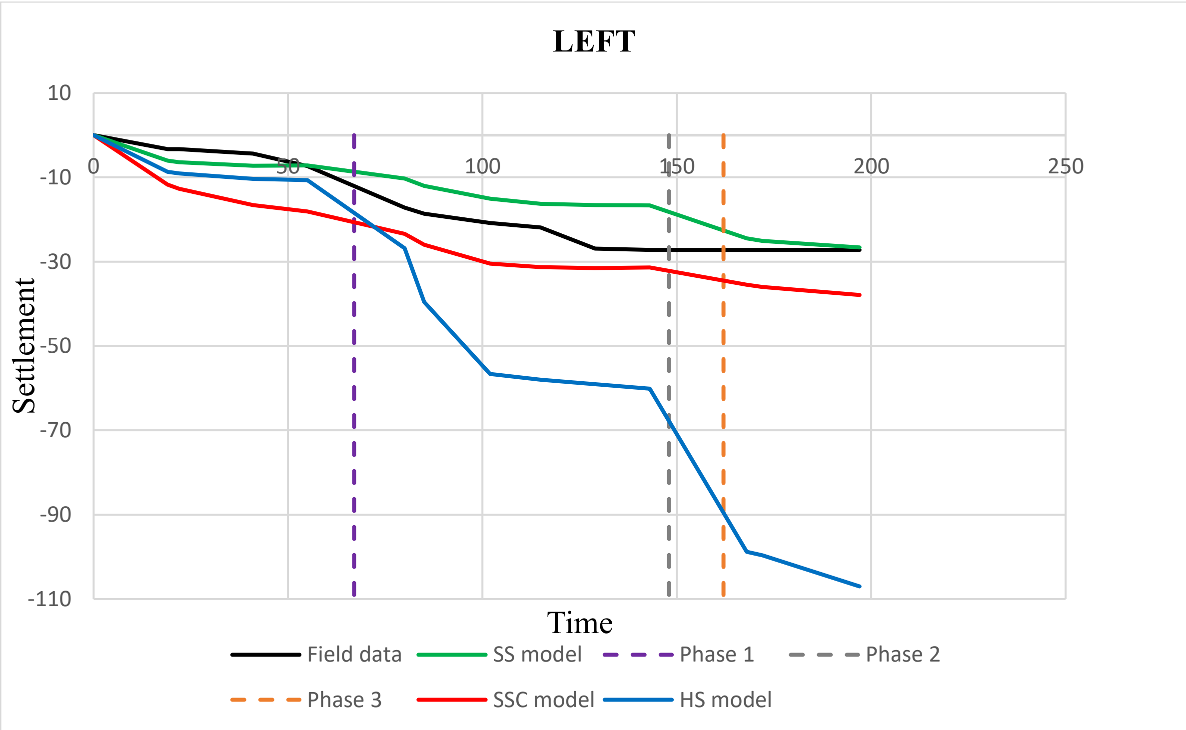

Figure 3.34: Measured and predicted settlements on the left side of the embankment with different models

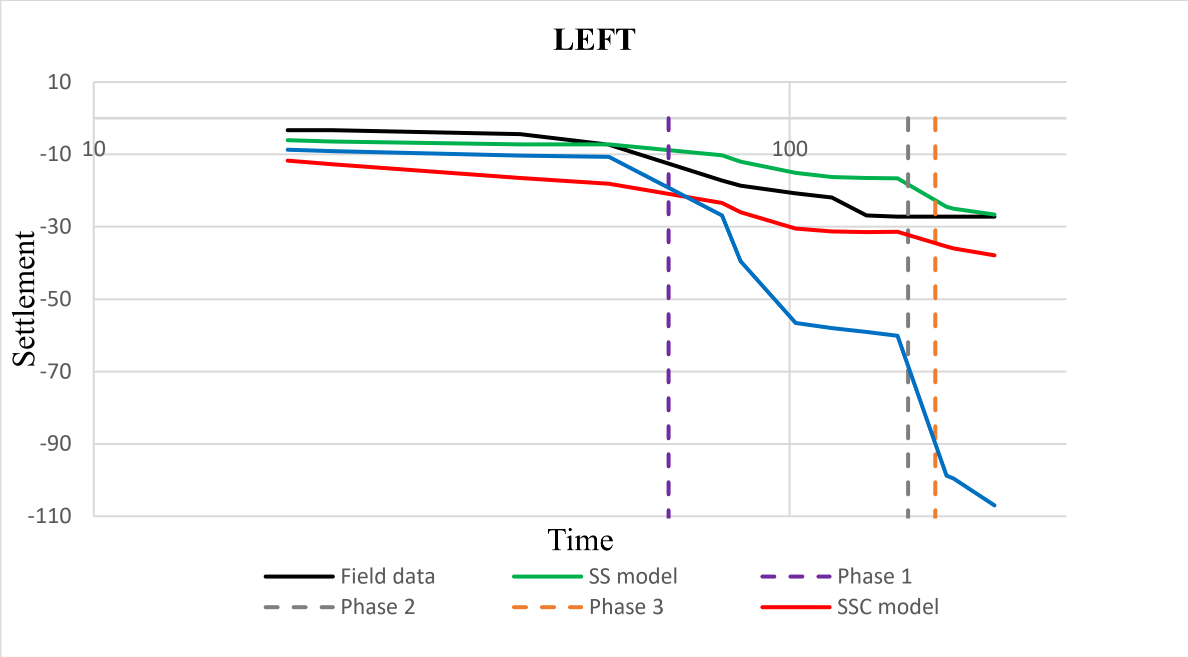

Figure 3.35: Measured and predicted settlements on the left side of the embankment with different models with logarithmic scale

The settlement-time relationship is qualitatively better predicted by the SSC model than with the SS model and the HS model which respectively underestimates and greatly overestimates the settlements (see table 3.8). The predictions in this study suggest that creep should be included to better match the in situ measured settlements.

Table 3.8: Measured and predicted values of total settlement after the 168 days

	Measured in situ	Predicted with Soft Soil model	Predicted with Soft Soil Creep model	Predicted with Hardening Soil model
Value of total settlement on the Axis (cm)	32.7	35.45	35.97	148
Value of total settlement on the left side (cm)	27.2	24.47	35.48	98.8
Consolidation end time (days)	~ 195	255.4	283.2	1136

As shown by Figure 3.32 and **Table *3.8*** it can be seen that the settlement and the consolidation time of an embankment can be predicted using a numerical model. But obtaining values close to reality require a good choice of inputs and particularly the materials sets. According to the terms of the project, the maximum time allowed for consolidation was 6.5 months (around 195 days).

- The Soft Soil model gave a consolidation end time close to the one obtained from field measurement but underestimates the amount settlement obtained at the end of the consolidation. This is due to the fact that is does not take in account the creep which occur during the secondary consolidation.
- The Soft Soil Creep model gave values of total settlement and consolidation end time slightly higher than those collected on the field but presented the closest behaviour compare to the real one.
- The Hardening Soil model highly overestimated both total settlement and consolidation end time probably because it does not account for softening due to soil dilatancy and de-bonding effects.

It is important to note that the monitoring of settlements of the backfill instrumentalized by the settlement plates was done from September to March. During this period, there is a transition from the rainy season to the dry season. The embankment being built in a marshy area, the rainfall will have a significant impact on the evolution of the consolidation. but natural changes are not taken into account during numerical modelling. Similarly, although the compaction energy has been taken into account, the load due to the various traffic has not been fully considered. These parameters could justify the difference that exists between the data recorded in the field and the results obtained after the numerical analysis.

3.6.2. Consolidation end time

The consolidation end time is the time needed to reach a minimum value of excess pore water pressure ($P \leq 1kPa$ in this case). It varies depending on the behaviour of the material chosen.

- For the Soft Soil model, the consolidation ended 93.4 days (about 3.1 months) after the end of the construction. The overall consolidation time is 120 + 93.4 = 213.4 days (~ 7.1 months).

- For the Soft Soil Creep model, the consolidation ended 121.2 days (about 4 months) after the end of the construction. The overall consolidation time is 120 + 121.2 = 241.2 days (~ 8.0 months).
- For the Hardening Soil model, the consolidation ended 974 days (about 2.7 years) after the end of the construction. The overall consolidation time is 120 + 974 = 1094 days (~ 3.0 years).

It can also be noted that the consolidation end-time with the SS model is lowest than those with the other models. it can be seen that the soil behaviour has a substantial influence on the consolidation time prediction.

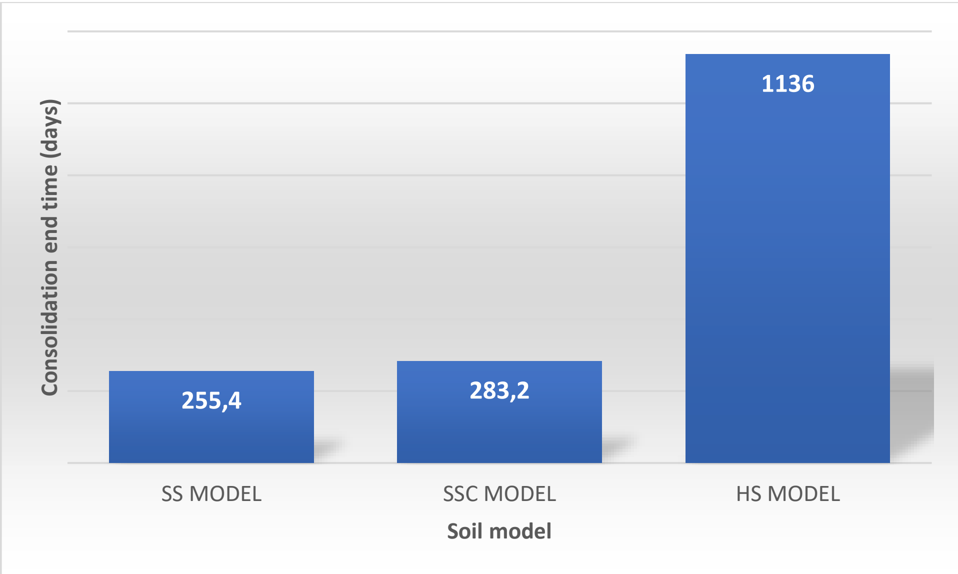

3.6.3. Pore pressures

The figures 3.36 and 3.37 show that excess pore water pressures attain the maximum amount after the construction stage of each step for embankment fill. It will then reduce progressively for each step during the consolidation period but at the end of construction of the last stage, it will reduce with time until it becomes minimum (1 *kPa*) at consolidation end time.

The highest excess pore water pressures for the embankment is reached during construction of the third stage for SS model and HS model and during construction of the second phase for the SSC model due to the consideration of the creep effect of the SS model.

Another remark is that excess pore water pressure increases with increase in depth due to stress increase. Points located above the water table are just very slightly submit to excess pore water pressure. The maximum negative excess Pore Pressure is 38.88 kN/m^2 for SS model, 59.08 kN/m^2 for SSC model and 65.39 kN/m^2 for HS model. Figures 3.36 and 3.37 show the variation of excess pore water pressure with time at point X and L for each model.

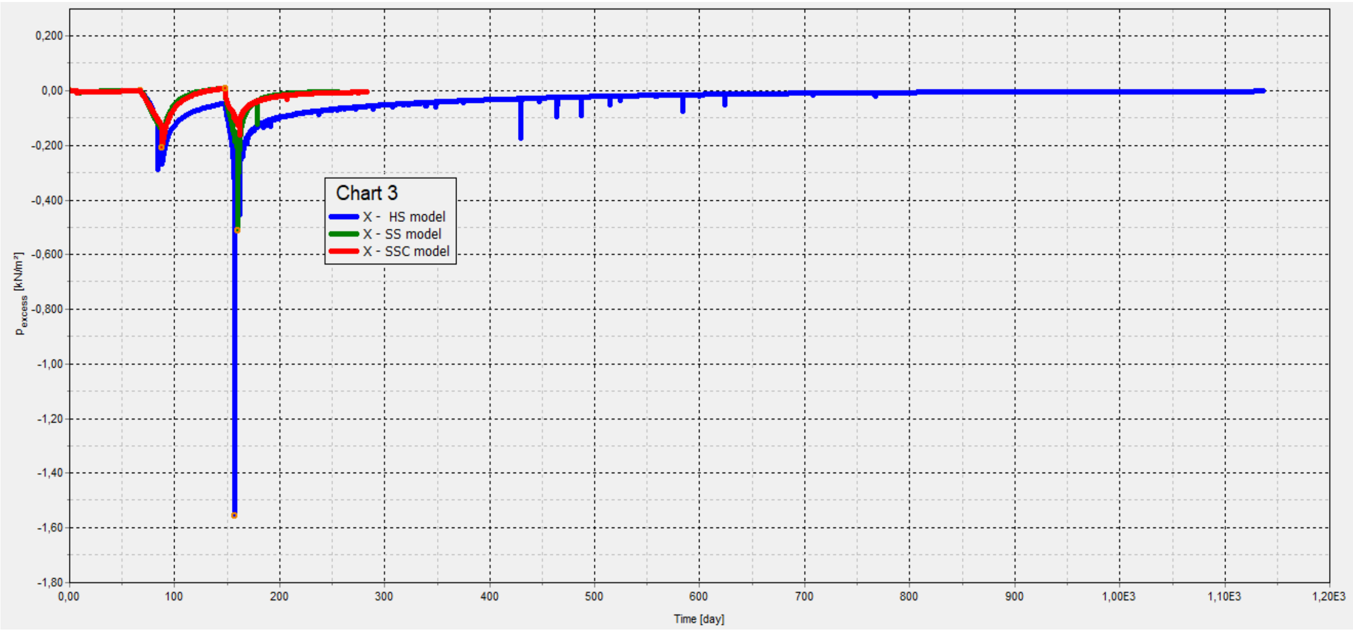

Figure 3.36: Predicted excess pore pressure versus time at point X

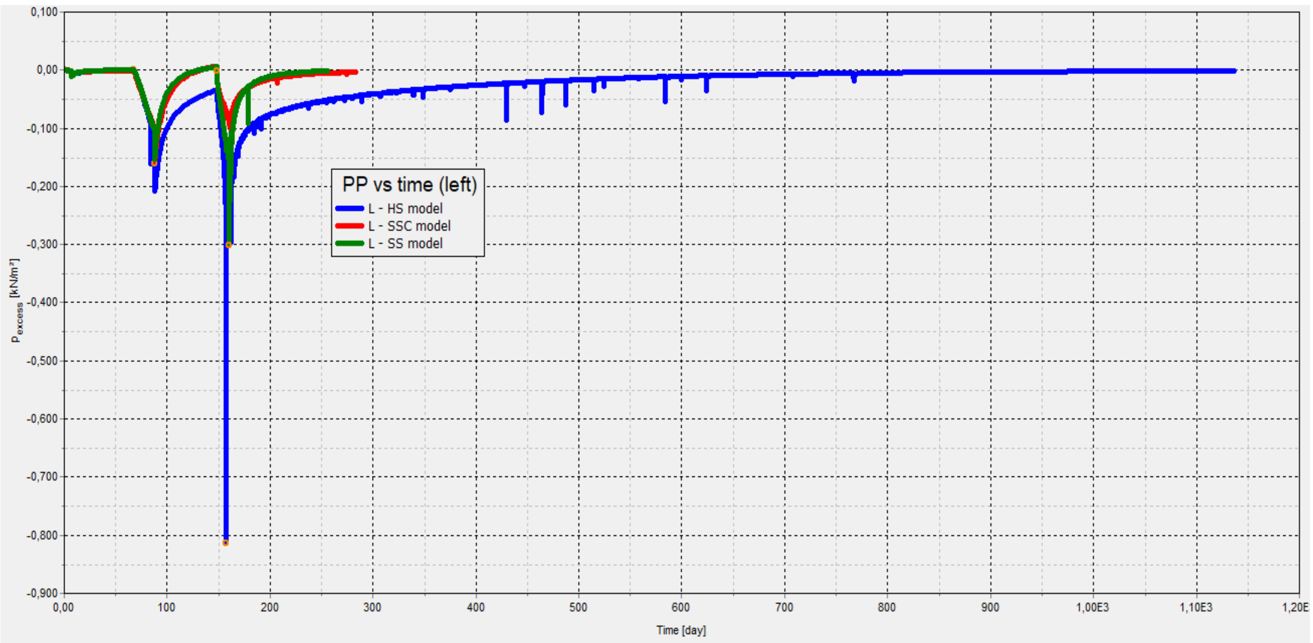

Figure 3.37: Predicted excess pore pressure versus time at point L

3.6.3. Factor of safety

The safety factor analysis was launched at the end of the consolidation phase of each stage of construction. The safety factor at the end of the consolidation is 1.142 for the SS model, 1.138 for the SSC model and 1.136 for the HS model.

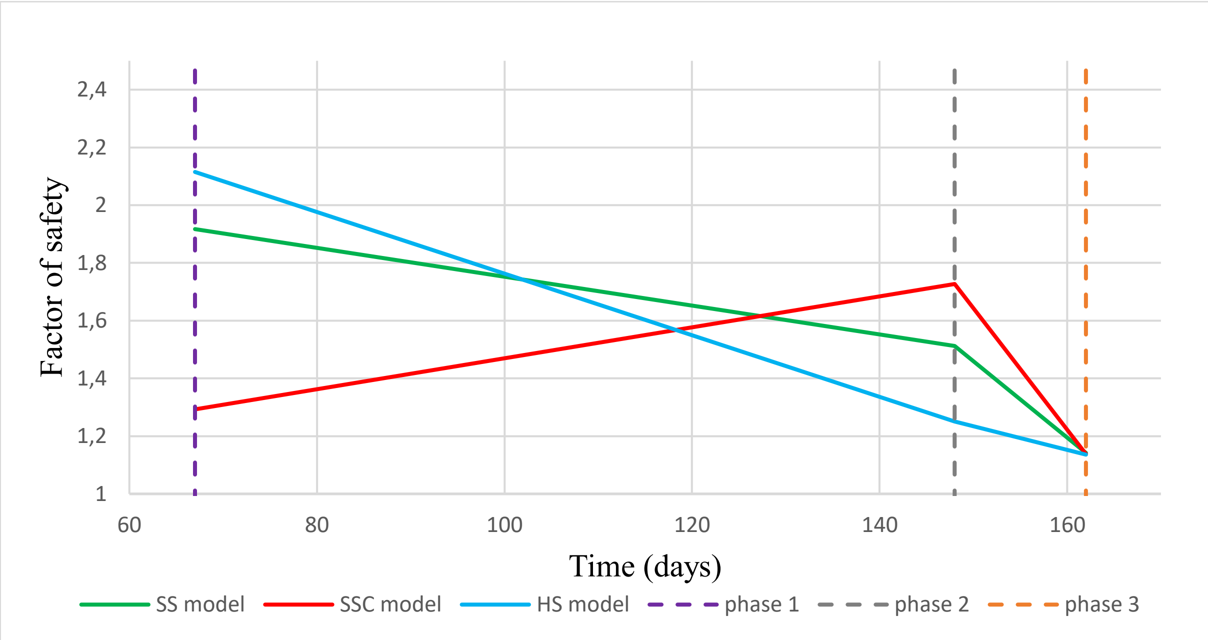

Figure 3.38: Variation of Safety factors Vs time for the different models

The safety factors (FOS) decreases as the phases of construction, this can be explained from the principle of the PHI/C reduction method which reduce the shear strength parameters *tan φ* (friction angle) and *c* (cohesion) up to the first points of failure. Another explanation is that during the embankment rise, the forces acting on the soil increase causing a need in more resistance of the soil. The FOS values converge approximatively to the same value because they are independent from the soil model.

The FOS to be considered is that at the end of the consolidation process.

Conclusion

The main objective of this chapter was to present the results obtained from the field instrumentation with settlement plates and the simulation using the software PLAXIS, then compare the results and do an interpretation. In a first part, the project was presented followed by a description of the study area and the needed data. Then the results from the settlement plates instrumentation and those from the simulation were shown. The simulation was done using successively the Soft Soil model, the Soft Soil Creep model and the Hardening Soil model as material models and then chose the best one to simulate the behaviour of soft soils. Based on the results of field measurements and numerical predictions of settlements, the SSC model predicted relatively well the measured total settlements for the follow up time comparatively to the SS model and HS model. The HS model, on the beginning presented a very good settlement-time relation but for a very short time. If the creep deformations were excluded, the SS model underestimated the settlement so it is useful to incorporate creep for modelling the stress-strain-time behaviour of soft soils. The analysis of the excess pore pressure shows that it is also an important parameter to take in consideration when predicting soil behaviour.

GENERAL CONCLUSION

The main objective of this thesis entitled "comparative analysis of predicted and measured settlement of an embankment on soft soil along the Foumbot-Bamendjing-Galim road" was to show the capability to predict the duration of consolidation and the amount of settlement at the end of consolidation of an embankment on soft soil using a numerical simulation. It was question here to do a comparison between the measurements done in-situ and the results obtained from a numerical simulation with the Finite Element software PLAXIS 2D using different material models.

To achieve this goal, a general review was done on soft soils properties, behaviour of embankment on soft soil, field instrumentation to measure settlement and numerical method to predict settlements followed by a presentation of the methodology used to achieve this study. The last part was about the results and their interpretations.

The approach adopted was to predict the total settlement and the consolidation end time of the embankment using a numerical modelling with the software PLAXIS 2D and setting the inputs with different material models notably the Soft Soil model, the Soft Soil Creep model and the Hardening Soil model. The results obtained were compare with the measurements done in-situ and it was seen that, using the right soil model depending on the soil characteristics. This enable to do the following conclusions:

- ❖ Total settlement and consolidation end time of an embankment can be predicted using numerical modelling;
- ❖ The relevance of the results depends on a good choice of inputs and the choice of the material model which will reproduce the real behaviour of the soil;
- ❖ The total settlement recorded on the field was 32.7 cm on the axis and 27.2 cm on the left side at the end of the settlement which was allowed to be 6.5 months. The simulation with the Soft Soil model underestimates the settlement (37.21 cm on the axis and 27.12 cm on the left side) but with a good prediction of the consolidation end

time (around 7 months) contrarily to the Hardening Soil model which highly overestimated both the amount of settlement and the consolidation time (158 cm on the axis and 97.8 cm left side with consolidation end time of 3.1 years). However, the Soft Soil Creep model predicted values a bit higher than those obtained on the field (38.95 cm on the axis and 36 cm on the left side) with a consolidation end time of 8.2 months.

- ❖ The pore pressure increase was almost instantaneous after loading and greatly depend on the model chosen.

It was important to note that, the only use of settlement as the base element to choose a material model was not enough. Others criteria as pore pressures are crucial in the study of the behaviour of a material.

In order to improve the results of this research and ensure the continuity of this study, the following perspectives can be formulated:

- ❖ Study the trend overtime and at different depth and not just settlement at the ground surface at a few times in order to assess the performance of the model used;
- ❖ Conduct the study also considering the evolution of the pore pressure;
- ❖ Perform more precise geotechnical tests in order to be able to have more precise values with simulation and study the more advanced soil models.

REFERENCES

BOOKS AND ARTICLES

[1] Asaoka, A., (1978). Observation procedure of settlement prediction. Soils and Foundations, Vol. 18, No. 4, (pp. 87-101).

[2] Budhu, M. (2011). Soil Mechanics and Foundation 3rd ed. Arizona: John Wiley & Sons, Inc.

[3] Collin, J. G., Leshchinsky, D., and Hung, C.-J. J., (2005), Soil Slope and Embankment Design–Reference Manual, (Publication No. FHWA NHI-05-123), National Highway Institute, Federal Highway Administration, U.S. Department of Transportation, Washington D.C.

[4] Craig, R. F. (2004). Craig's soil mechanics 7th ed. New York: Spon Press.

[5] Das, B. M. (1994). consolidation and settlement in clay. In B. M. Das, Principles of Geotechnical Engineering (p. 10). Boston : PWS Publisher.

[6] Mitchell, J. K., & Soga, K. (2005). *Fundamentals of Soil Behavior* (3rd edition, Vol. 4, Issue 4). John Wiley & Sons, Inc.

[7] Frans Barends (May 2011). Soft soil geotechnic content, context and application.

[8] Ian Smith, (2014) Element of soil mechanics.

[9] Japanese Society of soils mechanics and Foundation Engineering (1978). Observational procedure of settlement prediction, vol 18 No 4

[10] Joseph E. Bowles, RE., S.E (1997), Foundation Analysis and Design, 5th ed.

[11] Kamon, M and Bergado, D.T. (1991) Ground Improvement Techniques. Proc. 9th Asian Regional Conf. Soil Mech. Fond. Eng'g'., Bangkok, Thailand, 2 P. 526-546

[12] NAVFAC, 1971, Design Manual: Soil Mechanics, Foundations, and Earth Structures, DM-7.

[13] Prof. Krishna Reddy, Engineering Properties of Soils Based on Laboratory Testing, UIC

[14] Qianwen Wand Et al. Research progress on solidification of soft muddy soils.

[15] Miśkiewicz, M., Meronk, B., Brzozowski, T., Wilde, K. (2017). Monitoring system of road embankment

[16] PLAXIS Manuals Edition V20

[17] R. Lancellotta, (1995). GEOTECHNICAL ENGINEERING, Editeur Balkema

[18] Balasubramaniam, A. S., & Brenner, R. P. (1981). Consolidation and settlement of soft clay. In *Developments in Geotechnical Engineering* (Vol. 20, Issue C, pp. 479–566). Elsevier Scientific Publishing Company, Amsterdam.

[19] Robert Holtz, Ahmad Baroutaji (2016). Construction materials: soil and natural materials.

[20] Sina Kazemian, et al. (2011), A State of art review of peat: Geotechnical engineering perspective

[21] Taylor D.W. Fondamentals in Soils Mechanics.

[22] Terzaghi, K. (1943). Theoretical Soils Mechanics. Newyork: John Wiley & Sons.

[23] V.N. S Murthy (2002) Geotechnical Engineering, Principles and practice of soil mechanics and Foundation Engineering

The course of Geotechnics at the National advanced school of public works by Dr. Lorenzo BREZZI in the academic year 2018/2019

The course of Foundation at the National advanced school of public works by Prof. Eng. Simonetta COLA in the academic year 2020/2021

WEBSITE

[24] https://blog.virtuosity.com/the-soft-soil-and-soft-soil-creep-model

[25]http://docs.itascacg.com/3dec700/common/models/camclay/doc/modelcamclay.htlm?node525

[26] https://www.constructioncivil.com/embankment-meaning-construction-quality-control/

APPENDIX

Appendix 1: Uniform C_α/C_c ratio

Material	C_α/C_c ratio
Inorganic material	0.025 – 0.065
Clay	0.025 – 0.085
Silt	0.030 – 0.075
peat	0.030 – 0.085

Appendix 2: Predicted and measured values of settlement during the follow-up time

Time (Days)	Field		SS		SSC		HS	
	Axe	Left	Axe	Left	Axe	Left	Axe	Left
0	0	0	0	0	0	0	0	0
19	-3,4	-3,3	-3,44	-6,07	-5,31	-11,72	-2,8	-8,7
22	-3,6	-3,3	-3,96	-6,44	-6,05	-12,68	-3,4	-9,08
41	-4,5	-4,4	-5,83	-7,24	-9,53	-16,55	-6,21	-10,35
55	-6,7	-7,3	-6,4	-7,2	-11,44	-18,07	-7,75	-10,65
80	-18,3	-17,2	-13,5	-10,25	-18,55	-23,41	-26,7	-26,85
85	-19,7	-18,6	-16,93	-12,02	-21,84	-25,99	-42,3	-39,55
102	-21,8	-20,8	-22,15	-15,06	-27,62	-30,48	-58,83	-56,6
115	-23,4	-21,9	-22,6	-16,29	-28,5	-31,3	-60,96	-58
129	-29,1	-26,9	-22,6	-16,55	-28,71	-31,5	62,6	-59,05
143	-30	-27,2	-22,36	-16,64	-28,56	-31,37	-63,79	-60,1
168	-32,7	-27,2	-35,45	-24,47	-35,97	-35,48	-148	-98,8
172		-27,2	-36,2	-25,04	-36,75	-35,99	-150	-99,6
197		-27,2	-38,38	-26,62	-39,6	-37,89	-159	-107

Appendix 3: Settlement (measured and predicted using SS model) vs Time curve in point X

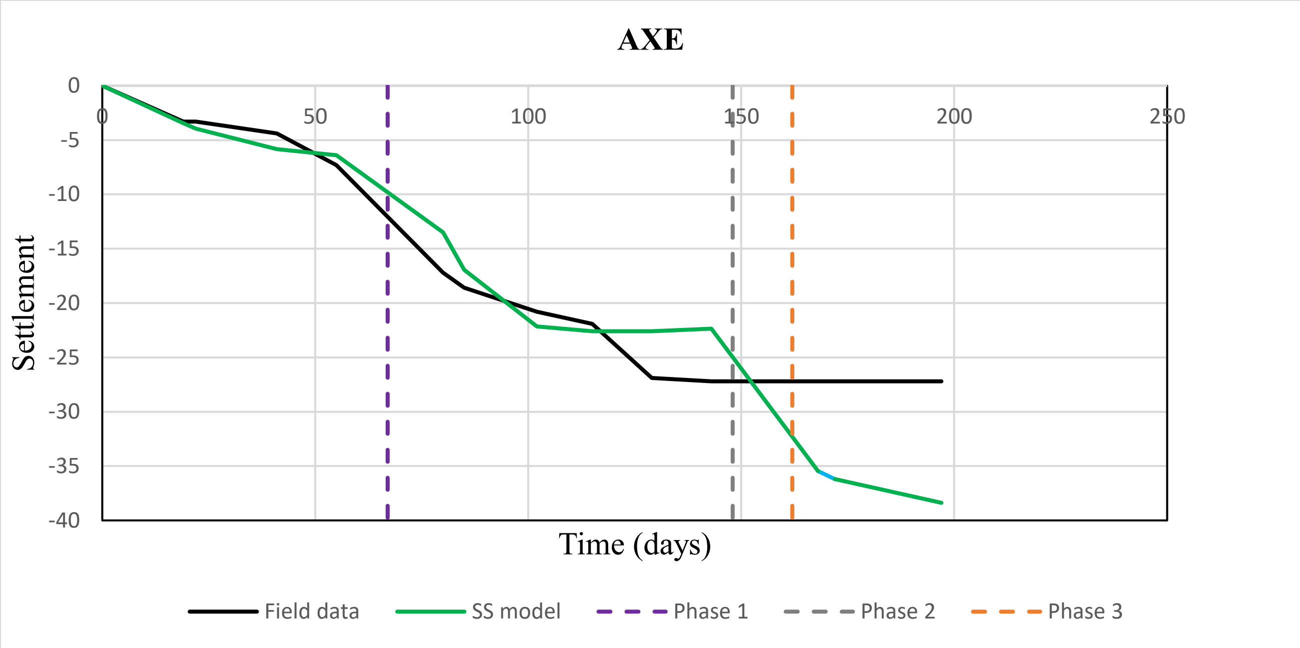

Appendix 4: Settlement (measured and predicted using SS model) vs log-Time curve in point X

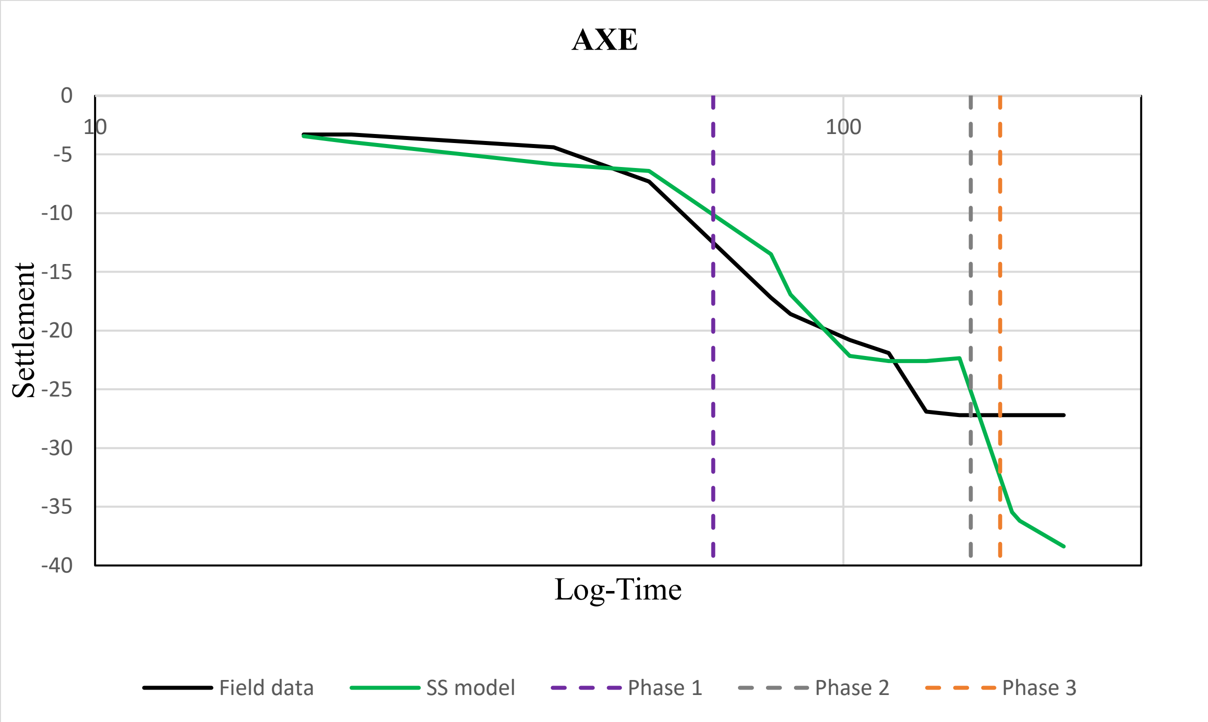

Appendix 5: Settlement (measured and predicted using SS model) vs Time curve in point L

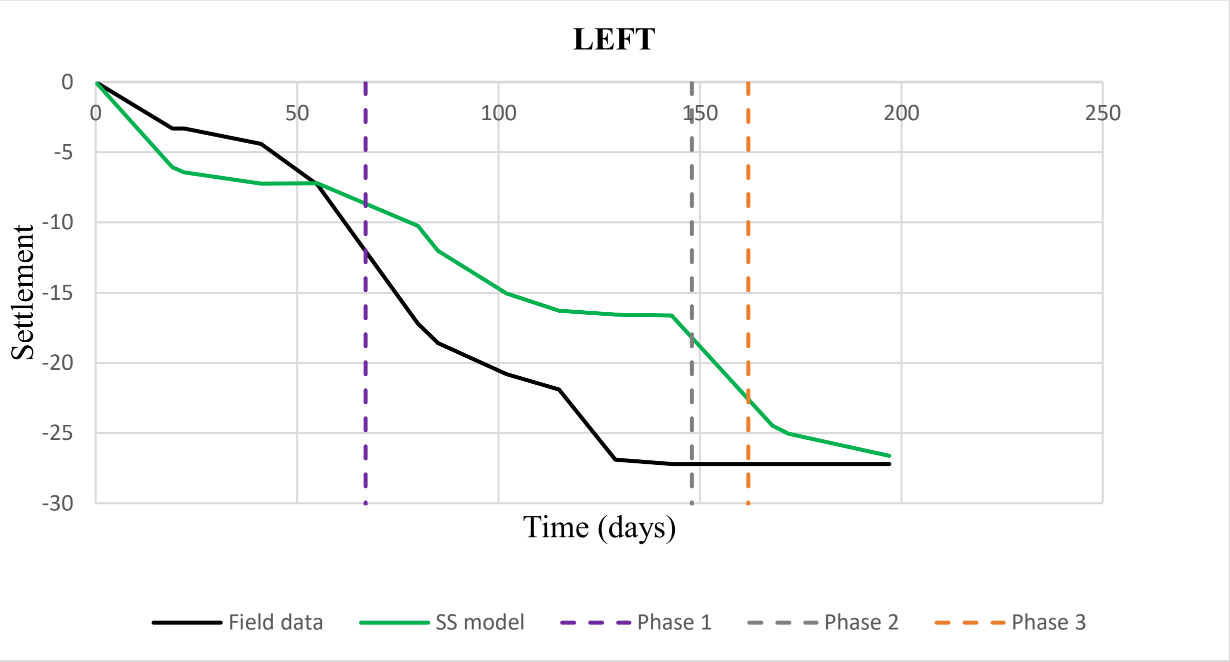

Appendix 6: Settlement (measured and predicted using SS model) vs log-Time curve in point L

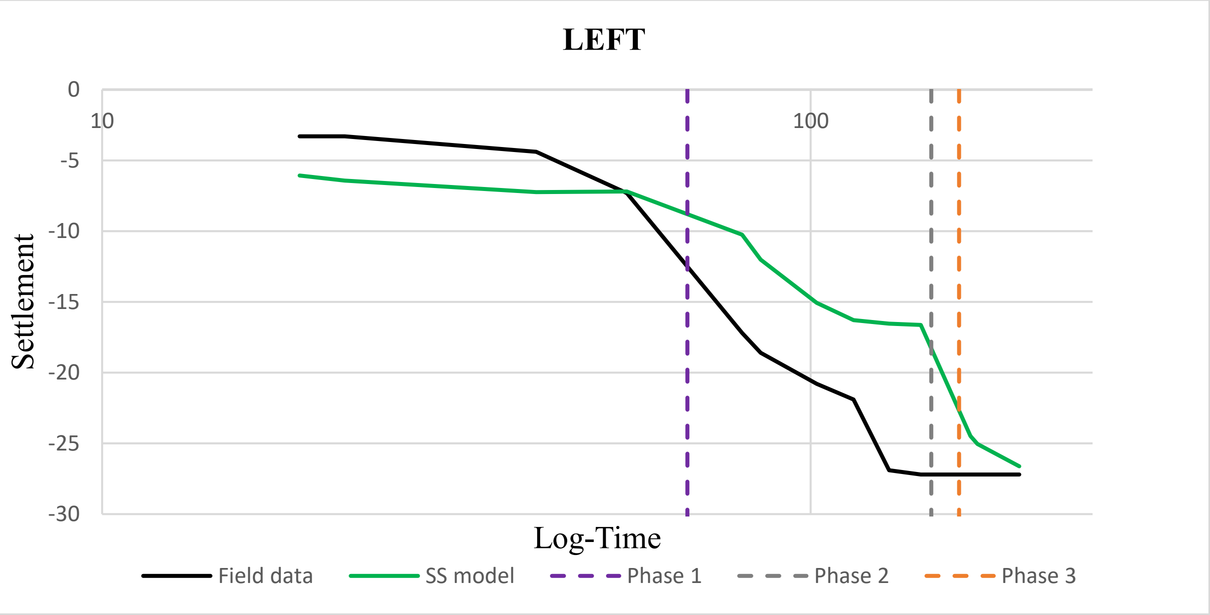

Appendix 7: Settlement (measured and predicted using SSC model) vs Time curve in point X

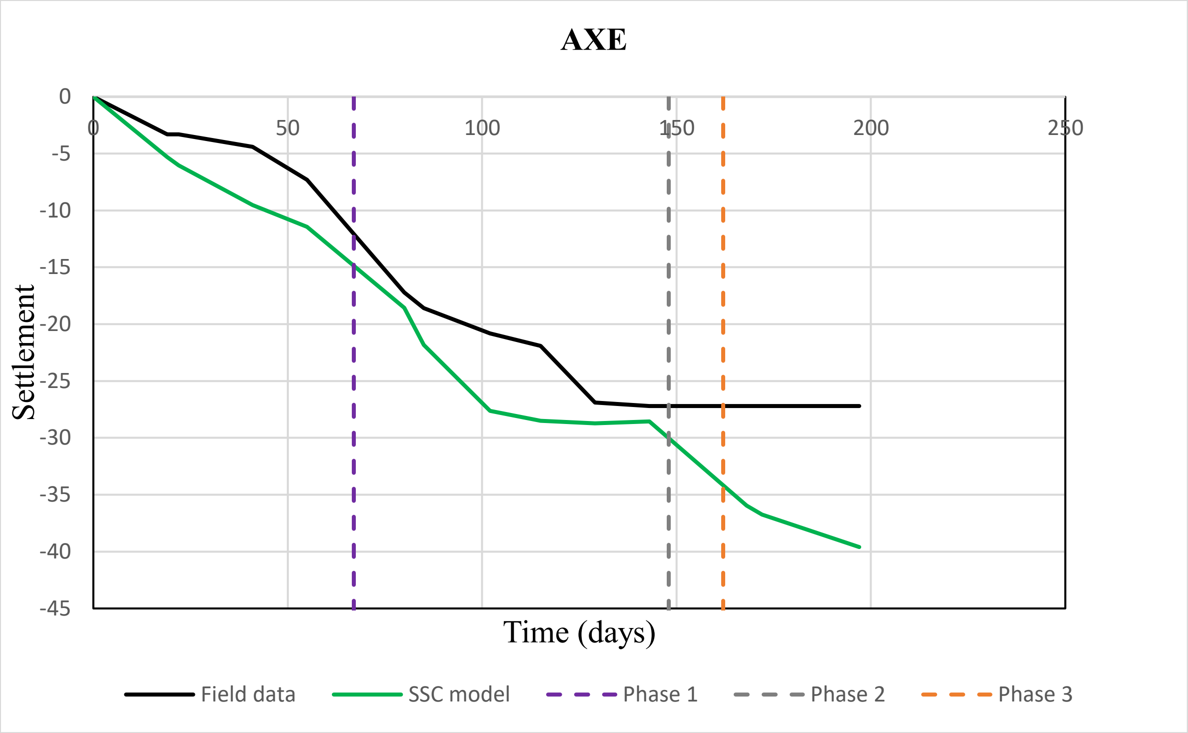

Appendix 8: Settlement (measured and predicted using SSC model) vs log-Time curve in point X

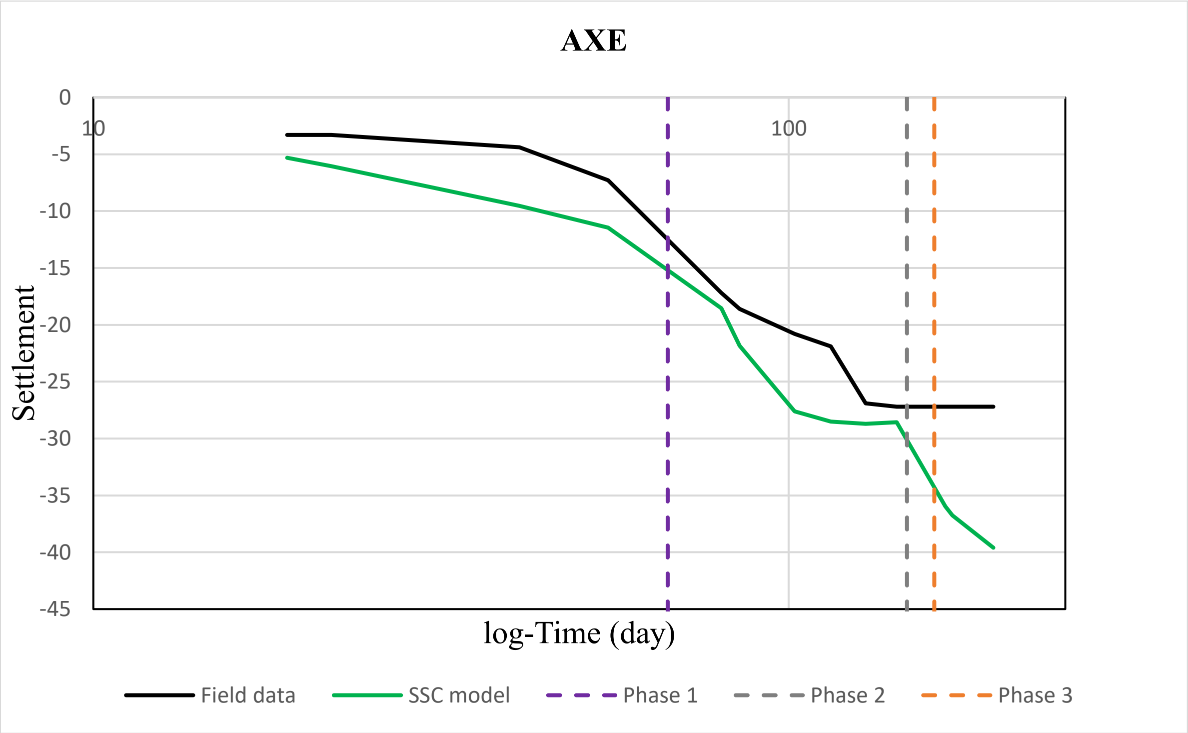

Appendix 9: Settlement (measured and predicted using SSC model) vs Time curve in point L

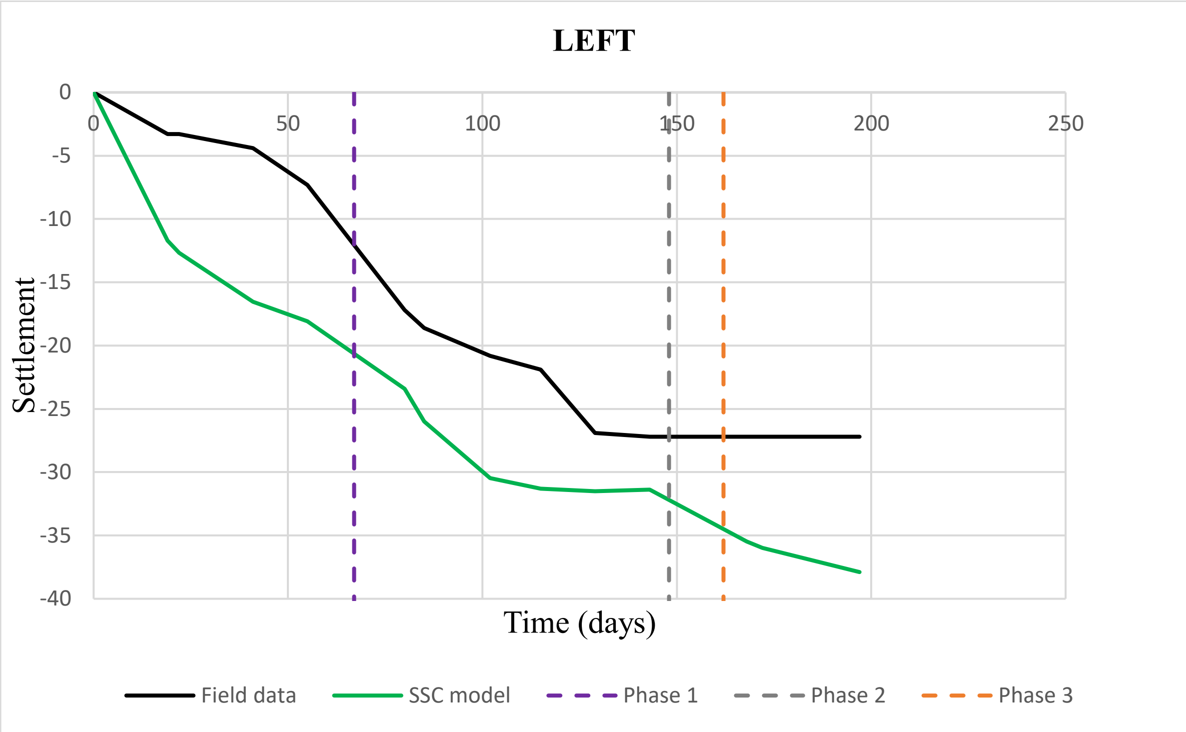

Appendix 10: Settlement (measured and predicted using SSC model) vs log-Time curve in point L

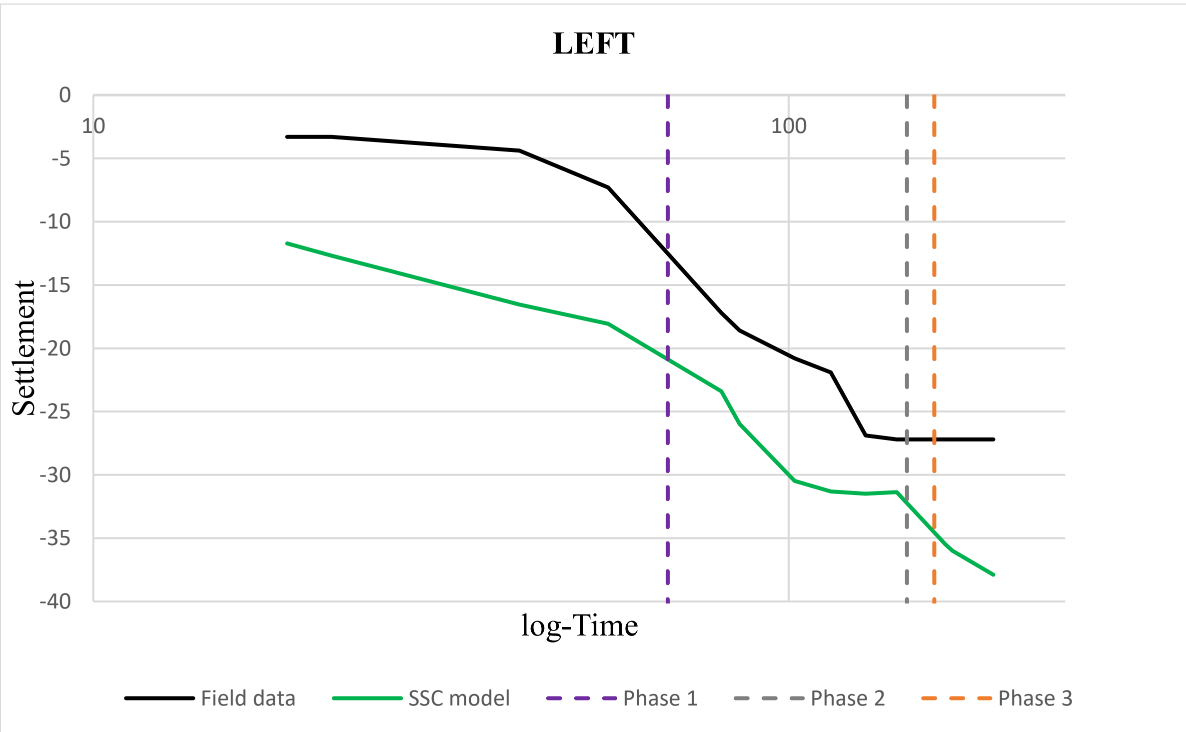

Appendix 11: Settlement (measured and predicted using HS model) vs Time curve in point X

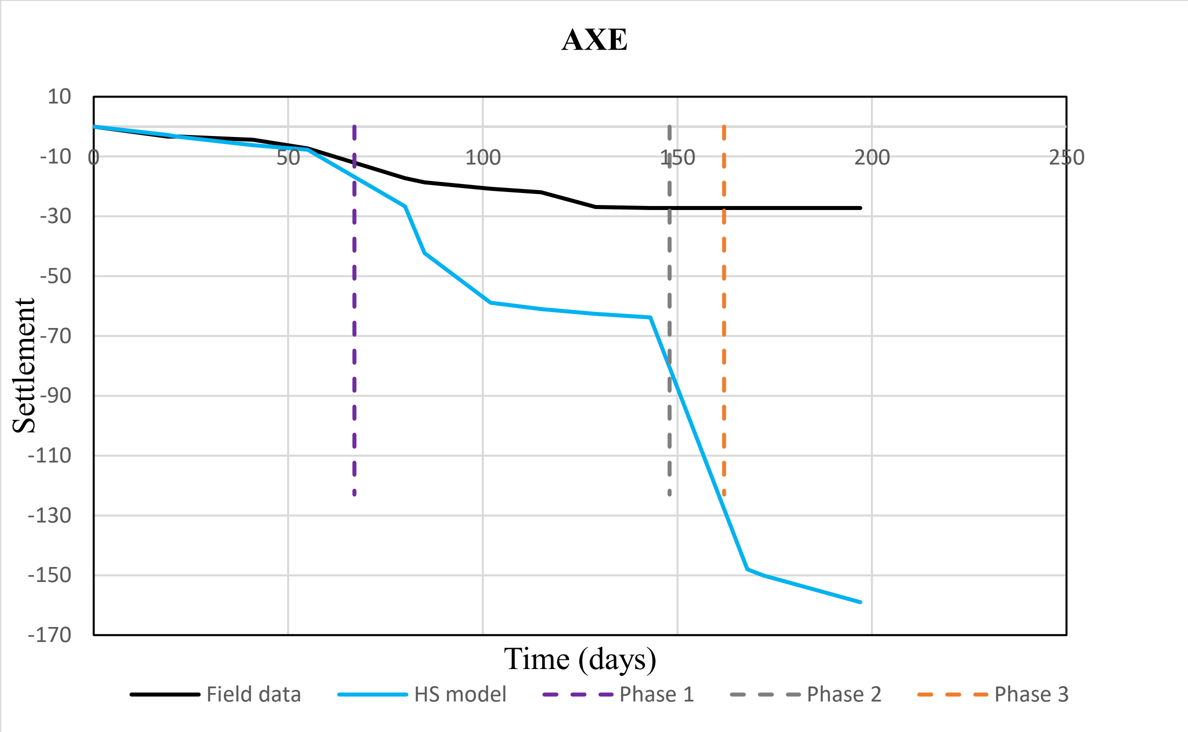

Appendix 12: Settlement (measured and predicted using HS model) vs log-Time curve in point X

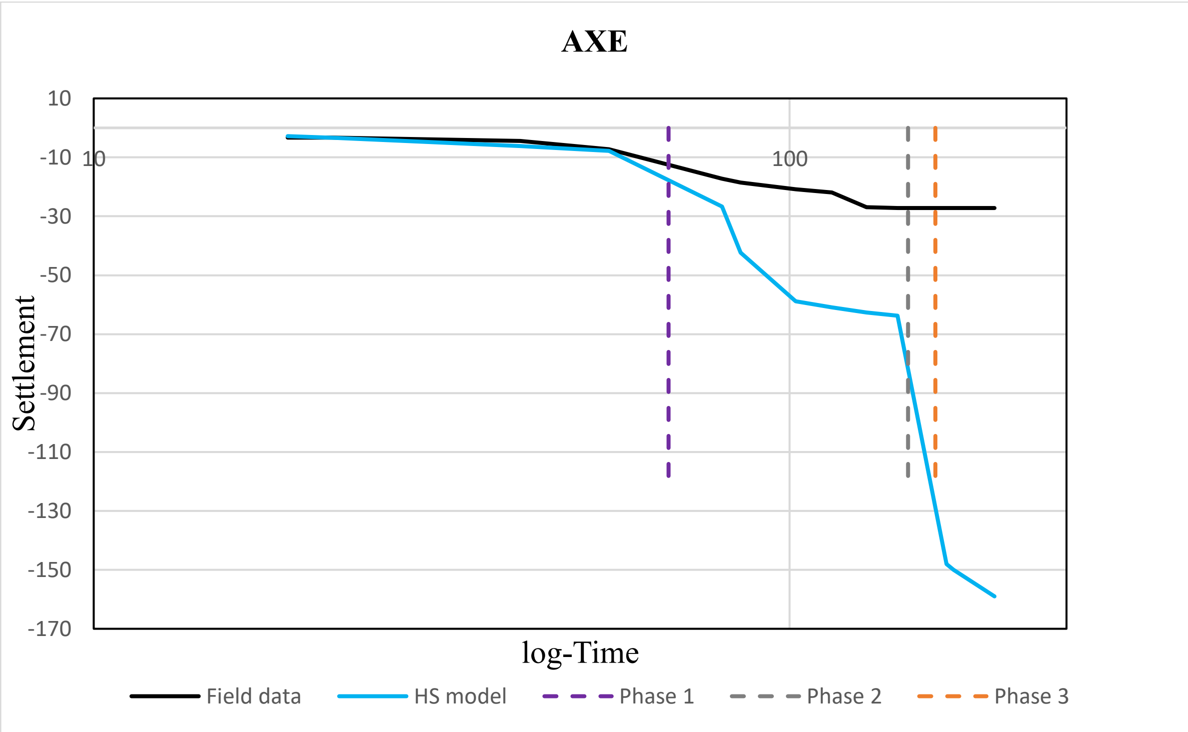

Appendix 13: Settlement (measured and predicted using HS model) vs Time curve in point L

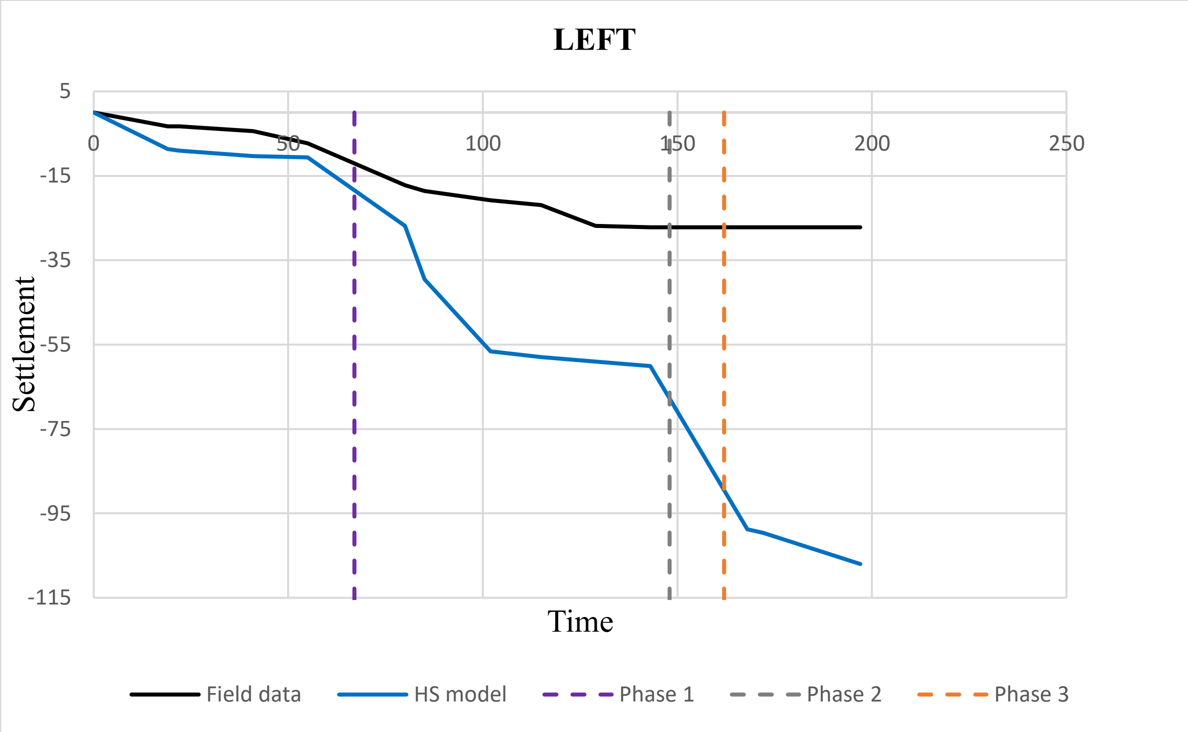

Appendix 14: Settlement (measured and predicted using HS model) vs log-Time curve in point L

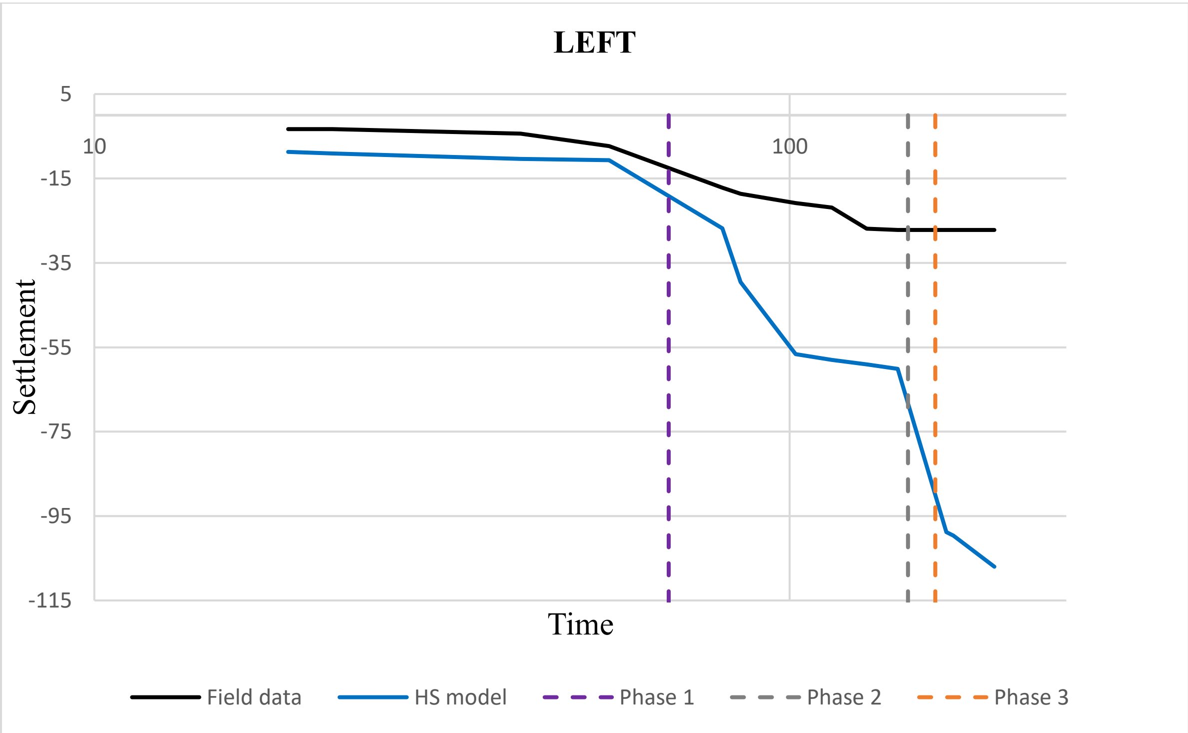

Appendix 15: Longitudinal profile PK 12+650m to PK 12+650m.

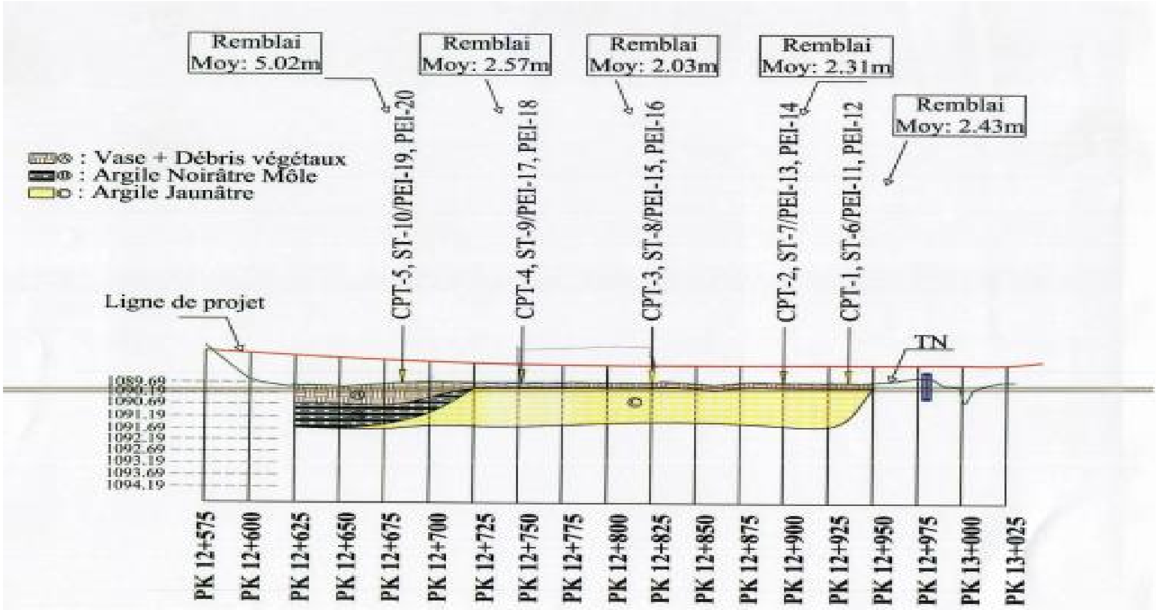

Appendix 16: Results of the oedometer test

Essai oedométrique - XP P94-090-1 / Consolidation ASTM D2435

	23/10/2019	Project	Zone marécageuse du Pk 12+900 (Tronçon Foumbot - Bamendjin)	
Boring, Sample No	6			
Depth	2.00 - 3.00 m	Mould	Oedometer	
Soil description	Argile [Noirâtre (PEI_13)	S, cm²	38.5	E_{oedo} [MPa]
Final weight of water, Pef	35.1	h_s	0.924	4.7
Spécific, gravity γS	2.249	Initial void ratio e_0	1.376	a_v (1/Mpa)
Dry material, Ps	80	Ho, mm	21.96	0.43492
Final moisture content, Wf	43.9%	Initial moisture content, Wi		46.8%
Dates	Pressure, kg/cm²	Settlement H(cm)	Ho-H	e
12-oct.-19	0.100	0.106	2.091	1.262
13-oct.-19	0.300	0.144	2.052	1.205
13-oct.-19	0.500	0.183	2.013	1.178
14-oct.-19	1.000	0.230	1.966	1.127
15-oct.-19	2.000	0.294	1.902	1.058
16-oct.-19	1.000	0.292	1.905	1.061
17-oct.-19	0.500	0.288	1.908	1.064
18-oct.-19	0.100	0.284	1.913	1.069
19-oct.-19	0.500	0.288	1.908	1.064
18-oct.-19	1.000	0.291	1.906	1.062
19-oct.-19	2.000	0.300	1.897	1.052
20-oct.-19	4.000	0.380	1.816	0.965
21-oct.-19	0.100	0.360	1.836	0.987
22-oct.-19				
Compression Index Cc	**0.289**	Swelling Index Cs	**0.12011**	Perméability Kv (cm/s)
Preconsolidation pressure σ_p, Kg/cm²	**0.398**	Consolidation coefficient Cv, cm²/s	**1.6336E-03**	**2.68E-06**

Appendix 17: Sieve analysis test results

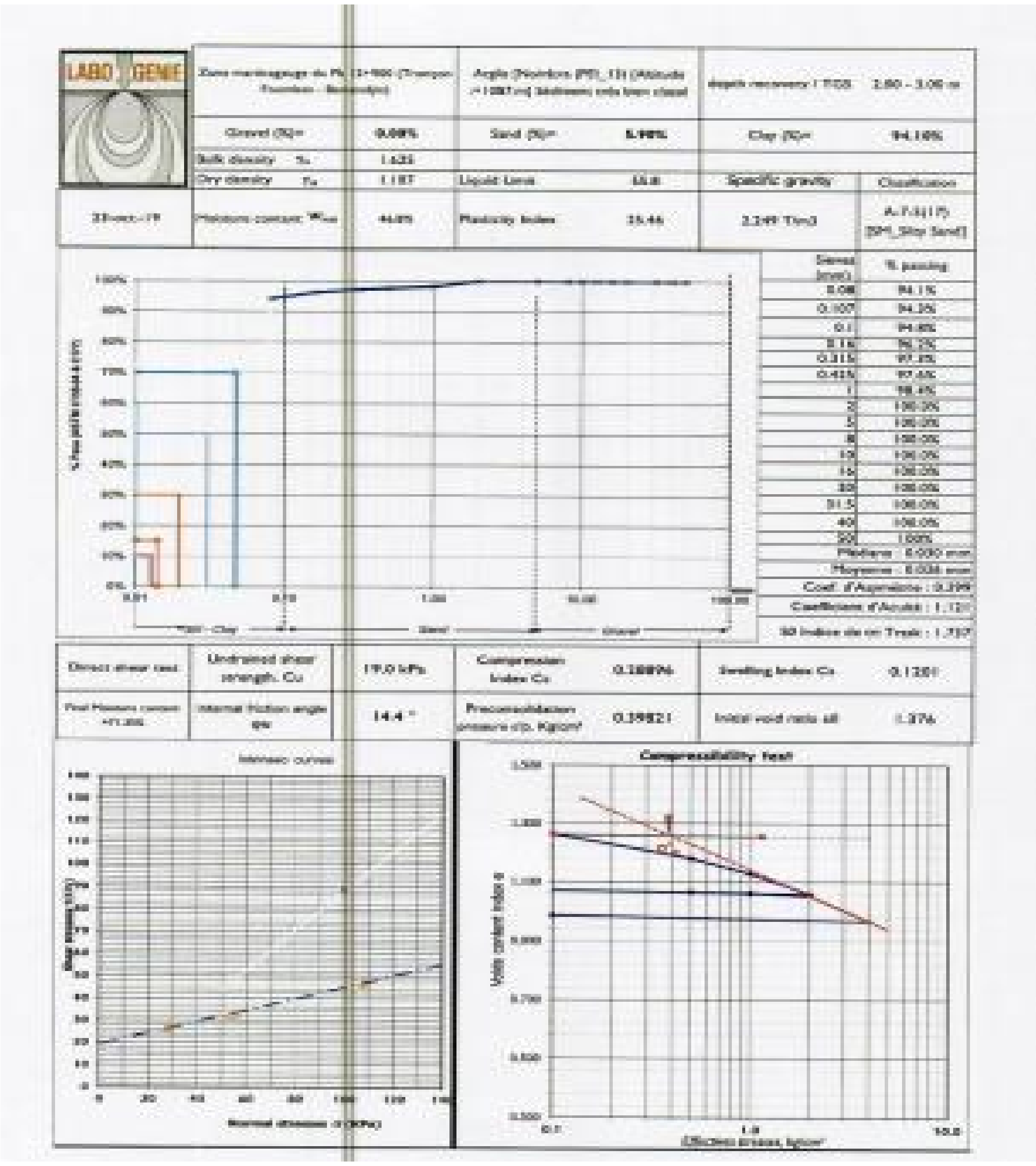

Appendix 18: Compressibility test results

LABO GENIE

COMPRESSIBILITY TEST

Equipment apparatus OEDOMETER

CV TEST - TAYLOR METHOD

Step from 1 to 2 kg/cm²

Zone marécageuge du Pk 12+900 (Tronçon Foumbot - Bamendjin) - Argile [Noirâtre (PEI_13) - 2.00 - 3.00 m

23/10/19

Time (mn)	Settlement (mm)	√ T
0.0500	1.890	0.22
0.25	1.910	0.50
0.5	1.934	0.71
1	1.964	1.00
2	2.010	1.41
4	2.060	2.00
8	2.096	2.83
15	2.140	3.87
30	2.178	5.48
60	2.220	7.75
120	2.250	10.95
240	2.266	15.49
1440	2.300	37.95
Ho, cm	**1.966**	
T90 (mm)	**8.363**	
S90 (mm)	**2.127**	**Cv, cm²/s**
Sc (mm)	**1.857**	**1.63E-03**

Appendix 19: Direct shear test result

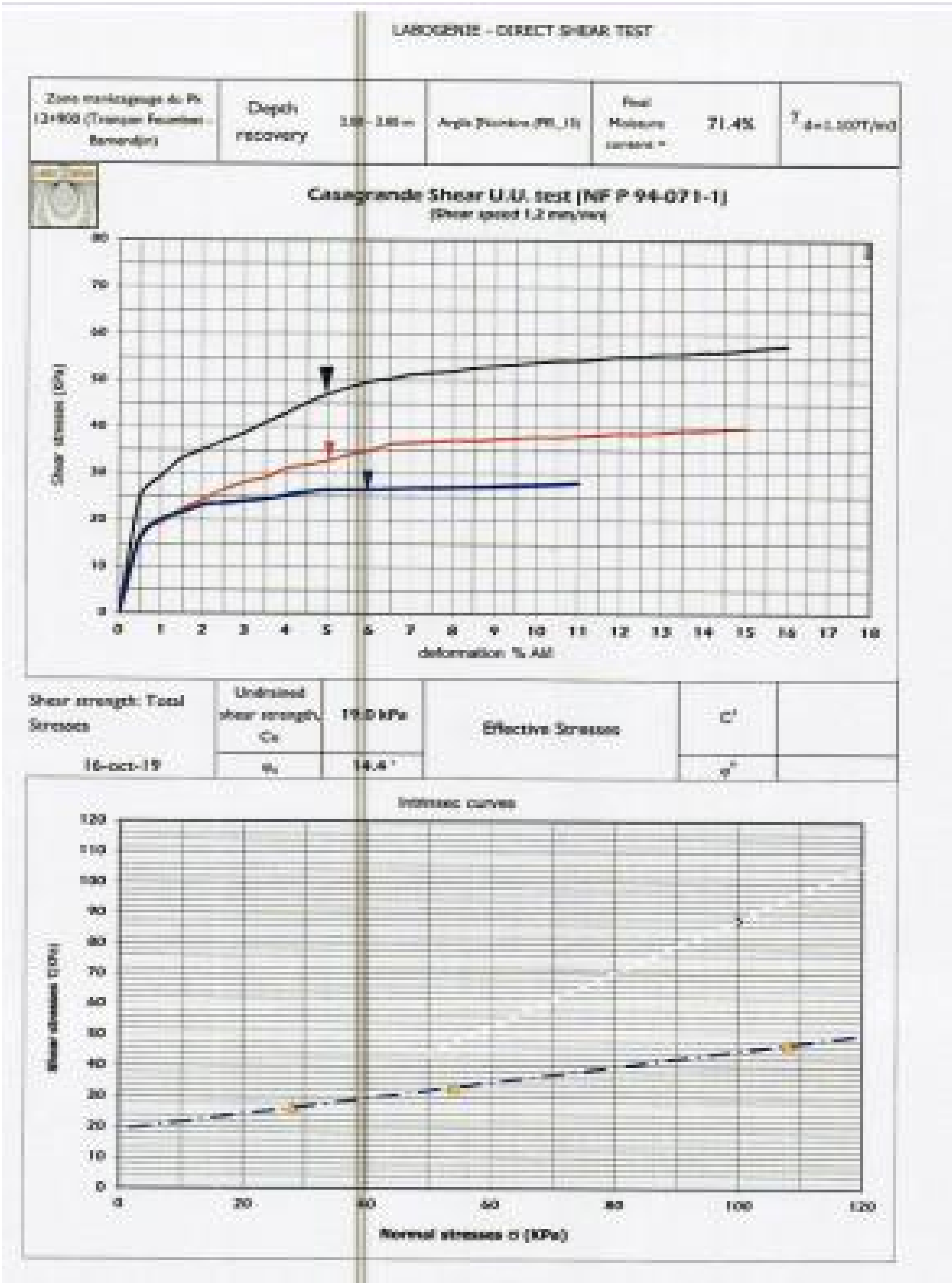

Appendix 20: Permeability test result

Permeability Test on Fine Soils ASTM ASTM D 5856 (Falling Head) / AASHTO T-88

Test No.

Date of Test 14/10/19

Location of Sample	Zone marécageuse du Pk 12+900 [Tronçon Foumbot - Bamendjin]	Date of sampling	11/10/19
		Date of lab conditioning	15/10/19
Boring : (PEI_13)	Sample	Depth recovery	2.00 - 3.00 m

Description of Soil: Argile (Noirâtre (PEI_13)

Equipment Used : Oedometer fitted with : two porous disk + Manometer outlets
Variable-Head Filter Tubes;Manometers Tubes, Balance
Miscellaneous Apparatus : Thermometer, clock with sweep second hand, etc.

Détermination des poids unitaires

Diameter, D, cm	7.00	Bulk Sample Weigth, g	115.10
Section, A, cm²	38.485	Weight of dry sample, g	80.00
Lenght, L, cm	1.90	Bulk density, kN/m³	15.74
Tube inlet Area, a cm²	0.33183	Grains density, kN/m³	22.49
		Apply pressure, kPa	100.000
		Moisture content (air-dried)	43.88%
Filler passing under 80-µm (No. 200) Sieve	94.10%	Dry Unit Weigth, kN/m³	10.94
		Void ratio, e	1.056

PERMEABILITY TEST

Depth recovery (m)	Apply pressure, kPa	Manometers Tube H_0	Manometers Tube H_1	Log (H_0/H_1)	a/A	t s	Temperature, °C	Permeability k cm/s
2.00 - 3.00 m	100.0	1000	500	0.301029996	0.00862245	3600	28.5	2.68E-06